ENERGY LABORATORY

MASSACHUSETTS INSTITUTE OF TECHNOLOGY

TREATMENT OF PHYSICAL AND NUMERICAL DIFFUSION IN FLUID DYNAMIC SIMULATIONS

by
Kang Yul Huh and Michael W. Golay

Energy Laboratory Report No. MIT-EL-83-011

August 1983

TREATMENT OF PHYSICAL AND NUMERICAL DIFFUSION IN FLUID DYNAMIC SIMULATIONS

by

Kang Yul Huh

and

Michael W. Golay

Energy Laboratory and

Department of Nuclear Engineering

Massachusetts Institute of Technology

Cambridge, MA 02139

MIT-EL-83-011

August 1983

Sponsored by:

Boston Edison Co.
Duke Power Co.
Northeast Utilities Service Corp.
Public Service Electric and Gas Co. of New Jersey

ABSTRACT

TREATMENT OF PHYSICAL AND NUMERICAL DIFFUSION

IN FLUID DYNAMIC SIMULATIONS

by

Kang Y. Huh and Michael W. Golay

A computer code is developed to predict the behavior of the hydrogen gas in the containment after a loss-of-coolant accident. The conservation equations for the four components, i.e., air, hydrogen, steam and water, are set up and solved numerically by decoupling the continuity and momentum equations from the energy, mass diffusion and turbulence equations. The homogeneous mixture form is used for the momentum and energy equations and the steam and liquid droplets are assumed to be in the saturation state.

There are two diffusion processes, molecular and turbulent, which should be modelled in different ways. Molecular diffusion is modelled by Wilke's formula for the multi-component gas diffusion, where the diffusion constants are dependent on the relative concentrations. Turbulent diffusion is basically modelled by the k-ε model with modifications for low Reynolds number flow effects. Numerical diffusion is eliminated by a corrective scheme which is based on accurate prediction of cross-flow diffusion. The corrective scheme in a fully explicit treatment is both conservative and stable, therefore can be used in long transient calculations. The corrective scheme allows relatively large mesh sizes without introducing the false diffusion and the time step size of the same order of magnitude as the Courant limit may be used.

ACKNOWLEDGEMENTS

This research was conducted under the sponsorship of Boston Edison Co., Duke Power Co., Northeast Utilities Service Corp. and Public Service Electric and Gas Co. of New Jersey. The authors gratefully acknowledge this support. The authors thank all those who assisted them during this research especially Dr. Vincent P. Manno, Mr. B.K. Riggs, Ms. Rachel Morton and Prof. Andrei Schor. The work was expertly typed by Mr. Ted Brand and Ms. Eva Hakala.

TABLE OF CONTENTS

LIST OF FIGURES

LIST OF TABLES

NOMENCLATURE

Letter	Definition
A	Area
c_p	Specific heat at constant pressure
c_v	Specific heat at constant volume
C_x, C_y	Courant numbers in x and y directions
D	(1) Dimension (2) Diffusion constant (3) Divergence (4) Discriminant of a quadratic equation
D_{ah}	Binary mixture diffusion constant between air and hydrogen
D_{as}	Binary mixture diffusion constant between air and steam
D_{hs}	Binary mixture diffusion constant between hydrogen and steam
D_x, D_y, D_z	Cross-flow diffusion constants in x,y and z directions
d_x, d_y	Diffusion numbers in x and y directions
e	Internal energy
f	Function of
$\vec{f}$	Body force vector per unit mass
$\vec{f}_d$	Drag force vector per unit mass
g	Gravity
Gr	Grashof number
h	Enthalpy Heat transfer coefficient
I	Imaginary unit, $\sqrt{-1}$
Im	Imaginary
k	(1) Turbulent kinetic energy (2) Thermal conductivity (3) Ratio of specific heats, c_p/c_v
ℓ	Length
M	Mass Molecular weight
Nu	Nusselt number
P	Peclet number
Pe	Effective Peclet number
p	(1) Pressure (2) $\dfrac{\frac{u}{\Delta x}}{\frac{u}{\Delta x} + \frac{v}{\Delta y}}$ or $\dfrac{\frac{u}{\Delta x}}{\frac{u}{\Delta x} + \frac{v}{\Delta y} + \frac{w}{\Delta z}}$
Pr	Prandtl number
Q	Heat source

Letter	Definition
R	Universal gas constant
Re	Reynolds number
Re	Real
R_t	Turbulence Reynolds number
R_x	Reynolds number in x direction
S	Source
Sc	Schmidt number
T	Temperature
t	(1) Time (2) Parameter of a quadratic equation in Von Neumann analysis
Δt	Time step size
u	x-direction velocity
v	y-direction velocity
$\vec{v}$	Velocity vector
w	z-direction velocity
Δx	x-direction mesh spacing
y	Mole fraction in multicomponent gas
Δy	y-direction mesh spacing
Δz	z-direction mesh spacing

Greek

α	Thermal diffusivity or diffusion constant
α_1, α_2	Parameters used in Von Neumann analysis
β	Thermal volumetric expansion coefficient
δ_{ij}	Kronecker delta
ε	Turbulent dissipation rate
ρ	Density
ν	Kinematic viscosity
μ	Viscosity
Φ	(1) Phase change (2) Any general conserved quantity
θ	Velocity direction, $\tan^{-1} \frac{v}{u}$
θ_1	Mesh configuration, $\tan^{-1} \frac{\Delta y}{\Delta x}$
ζ	(1) Vorticity (2) Amplification factor in Von Neumann analysis
τ	Time constant of heat transfer
$\overleftrightarrow{\sigma}$	Traction tensor due to viscosity
Σ	Summation

Superscript

n	Time step n

<u>Subscript</u>

cell	Cell
cf	Cross-flow diffusion
DM	De Vahl Davis and Mallinson's
f	Fluid
g	Gas
i=1	Air
2	Hydrogen
3	Steam
4	Liquid Droplets
L	Left hand side
ℓ	Liquid
m	Molecular
mix	Multicomponent gas mixture
new	New time step
ob	Obstacle
old	Old time step
R	Right hand side
t	Turbulent
total	Total calculation domain
US	Upstream

CHAPTER 1

INTRODUCTION

One of the major concerns in the Three Mile Island (TMI) accident was hydrogen gas accumulation in the containment. Some remedies have been proposed to deal with such problems. However, it is necessary to understand the fluid dynamic phenomena in the containment in order to justify those remedies.

From the hydrogen transport point of view, the response of the containment during an accident can be divided into two stages, the fast blowdown stage and the slow mixing stage. The distinct feature of the second stage is a much longer time scale in comparison with the first blowdown stage. The research work reported here is primarily concerned with the formulation and validation of the physical models and numerical schemes in the second slow mixing stage.

Some simplifying assumptions are made concerning the thermodynamic state in the slow mixing stage. The four components, hydrogen, air, steam and liquid droplets are assumed to be in thermodynamic equilibrium and the relative humidity is assumed to be 100%, although it may be less than 100% when there is no liquid component present.

The governing conservation equations are decoupled in order to simplify the solution procedure. The error due to decoupling is negligible in a slow transient where the state change over one time step is small. In the first step the continuity and momentum equations are decoupled from the energy and other scalar transport equations and solved by the Simplified Marker and Cell (SMAC) method in order to obtain the flow field. In the second step the energy and mass diffusion equations without phase change and turbulence equations are solved using the flow field obtained in the first step. Finally, the phase change is taken into consideration to maintain 100% relative humidity.

Convection and diffusion are the central issues in physical modelling efforts of hydrogen transport. Convection is assumed to occur as a homogeneous mixture, resulting in the same convection velocity for the four components. Diffusion occurs by two independent mechanisms, molecular and turbulent, and the total diffusion constant is the sum of the diffusion constants of those two mechanisms.

The molecular diffusion constant is predicted by Wilke's formula [73] for multi-component diffusion and Chapman-Enskog formula [5] for binary diffusion. The diffusion constant of each component in multi-component gas depends on the mole fraction of that component.

The turbulent diffusion constant is predicted by the k-ε model [45]. The turbulent kinetic energy, k, and turbulent dissipation rate, ε, are determined by their own transport equations. The turbulent kinematic viscosity, which is the diffusion constant for momentum transport can be calculated directly from k and ε. The turbulent Prandtl and Schmidt numbers are assumed to be equal to one.

The leading issue in numerical modelling of convection and diffusion is to minimize the error that occurs in the numerical solution procedures. Since the error usually appears as an additional diffusion, the term, numerical diffusion, has been used to describe the numerical error in general. The numerical diffusion has two different sources, truncation error diffusion and cross-flow diffusion. Truncation error diffusion is a one dimensional profile error and cross-flow diffusion is a multi-dimensional operator error [68] of the finite difference equation. Truncation error diffusion occurs in the flow direction while cross-flow diffusion occurs primarily in the direction normal to the flow. The effective diffusion constants of the two errors are of the same order of magnitude, however the latter turns out to be the dominant error source in most convection dominant problems. This is because the gradient of the scalar quantity under consideration is small in the flow direction in comparison with that in the direction normal to the flow. Therefore, the major obstacle in accurate numerical modelling of convection and diffusion has been the cross-flow diffusion error which arises in donor cell treatment of the convection term in multi-dimensional problems.

There has been much debate on the numerical diffusion and many schemes have been suggested for the past two decades. However, a recent review paper on this topic [65] shows that there is no scheme universally acceptable consistent with using reasonable mesh spacings and computation times. This situation is partly due to misunderstanding of the sources of numerical diffusion and also partly due to use of inappropriate approaches for its elimination.

The schemes presently being used can be divided into two categories, skew differencing and corrective schemes. Raithby's [53] and S. Chang's methods [16] are examples of skew differencing schemes and Huh's corrective scheme and tensor viscosity method [25] are examples of corrective schemes. The corrective scheme is inherently better than the skew differencing scheme in that it is conservative and does not affect the simple solution procedure. The conservative property is essential in a long transient problem like the hydrogen transport in the containment. The corrective scheme can be implemented with any of the explicit, ADI and implicit schemes, although with different stability conditions. The stability conditions for each of the aforementioned schemes can be obtained by a Von Neumann analysis and turns out to be consistent with numerical experiments.

Two implementation strategies for the corrective scheme, mesh point and mesh interface implementations, have been tested for recirculating flow problems. The mesh interface implementation has always given physically reasonable solutions and may be used extensively for all diffusion-convection problems.

The suggested physical models and numerical schemes have been used to simulate the LOCA experiments performed in Battelle-Frankfurt [44] and HEDL (Hanford Engineering Development Laboratory) [6]. Ref. [49] includes all the simulation results compared with experimental data.

CHAPTER 2

PROBLEM STATEMENT AND SOLUTION SCHEME

2.1 Problem Statement

Once a loss-of-coolant accident (LOCA) occurs in a Light Water Reactor (LWR), a large amount of steam and water will come into the containment in the fast blowdown stage increasing the containment pressure. After a while the slow mixing stage follows the initial blowdown stage and continues for an extended period of time. The major safety concern is that of keeping the containment pressure below a certain level to prevent a large scale leakage of radioactive materials.

In addition to the pressure increase due to the primary coolant, hydrogen generation gave a serious concern about the integrity of the containment in the TMI-2 accident. The hydrogen is generated by radiolysis and chemical reaction between water and zirconium in the cladding and may react explosively with oxygen in the air. Thereafter, the hydrogen has received much attention in the safety analysis of nuclear power plants. There have been some mitigation procedures suggested, e.g., containment inerting, installation of ignition devices, use of flame suppressants and enhanced venting capability, for dealing with this problem. In order to justify the design of any mitigation system, it is essential to understand the fluid dynamic phenomena in the containment.

Since a numerical method is suitable for this purpose, a good computational tool has been required to predict the hydrogen concentration distribution. The most difficult aspects of this analysis are the complicated geometry and chaotic post-LOCA conditions, e.g., thermal nonequilibrium, laminar and turbulent flows, phase change and heat transfer between the gas components and wall, etc. Therefore, some simplifying assumptions should be made to use the numerical procedure without impairing the acceptable solution accuracy.

2.2 Governing Equations

The governing conservation equations are set up to describe the post-LOCA fluid dynamics in the containment. The physical implications of the conservation equations will be given with their basic assumptions and limitations.

Continuity: $$\nabla\cdot\vec{v} = 0 \tag{2.1}$$

Momentum: $$\rho[\frac{\partial\vec{v}}{\partial t} + \nabla\cdot\vec{v}\vec{v}] = -\nabla p + \rho g\vec{f} + \vec{f}_d + \nabla\cdot\vec{\sigma} \tag{2.2}$$

Energy: $$\rho[\frac{\partial e}{\partial t} + \nabla\cdot\vec{v}h] = \nabla\cdot k\nabla T + e_{fg}\Phi_\ell \tag{2.3}$$

Mass diffusion: $$\frac{\partial\rho_i}{\partial t} + \nabla\cdot\vec{v}\rho_i = \nabla\cdot D_i\nabla\rho_i + \Phi_i \tag{2.4}$$

Turbulence kinetic energy: $$\frac{Dk}{Dt} = \frac{1}{\rho}\frac{\partial}{\partial x_k}[\frac{\mu_t}{\sigma_k}\frac{\partial k}{\partial x_k}] + \frac{\mu_t}{\rho}(\frac{\partial u_i}{\partial x_k} + \frac{\partial u_k}{\partial x_i})\frac{\partial u_i}{\partial x_k} - \varepsilon + \beta g_k\frac{\nu_t}{Pr_t}\frac{\partial T}{\partial x_k} \tag{2.5}$$

Turbulence dissipation rate: $$\frac{D\varepsilon}{Dt} = \frac{1}{\rho}\frac{\partial}{\partial x_k}[\frac{\mu_t}{\sigma_\varepsilon}\frac{\partial\varepsilon}{\partial x_k}] + C_1\frac{\mu_t}{\rho}\cdot\frac{\varepsilon}{k}(\frac{\partial u_i}{\partial x_k} + \frac{\partial u_k}{\partial x_i})\frac{\partial u_i}{\partial x_k} - C_2\frac{\varepsilon^2}{k} + \frac{\varepsilon}{k}\beta g_k\frac{\nu_t}{Pr_t}\frac{\partial T}{\partial x_k} \tag{2.6}$$

Equation of state: $$p = f_p(\rho_i, T) \tag{2.7}$$

Constitutive equations:

$$\Phi_i = f_\Phi(\rho_i, T) \tag{2.8}$$

$$\vec{\vec{\sigma}} = f_\sigma(\vec{v}) \tag{2.9}$$

$$D_i = D_{im} + D_{it} \tag{2.10}$$

$$\nu = \nu_m + \nu_t \tag{2.11}$$

$$k = k_m + k_t \tag{2.12}$$

$$D_{im} = f_D(\rho_i, T) \tag{2.13}$$

$$\nu_m = f_\nu(\rho_i, T) \tag{2.14}$$

$$k_m = f_k(\rho_i, T) \tag{2.15}$$

$$D_t = \nu_t \tag{2.16}$$

$$k_t = \nu_t \tag{2.17}$$

$$\nu_t = C_\mu k^2/\varepsilon \tag{2.18}$$

$$\rho = \Sigma\rho_i \tag{2.19}$$

Note that

1. The subscript i denotes the four components as

follows:

i=1 air,

i=2 H_2,

i=3 steam,

i=4 liquid droplet.

2. The turbulence equations are written in terms of the Cartesian components in tensor notation.

3. The phase change occurs between steam and liquid droplets and the diffusion constant of liquid droplets is equal to zero.

$$\Phi_1 = \Phi_2 = 0 \tag{2.20}$$

$$\Phi_3 + \Phi_4 = 0 \tag{2.21}$$

$$D_4 = 0 \tag{2.22}$$

There are eleven conservation equations, one continuity, three momentum, one energy, four mass diffusion and two turbulence equations with ten primary unknowns, u, v, w, ρ_i (4), T, k, ε for a three dimensional case. Therefore, there is one more equation than is required.

2.2.1 Continuity and Mass Diffusion Equations

The continuity equation is redundant with the four mass diffusion equations and there is an inconsistency between them. The mass diffusion equations are summed up for the four components, i=1-4.

$$\frac{\partial}{\partial t}(\Sigma\rho_i) + \nabla\cdot\vec{v}(\Sigma\rho_i) = \Sigma(\nabla\cdot D_i\nabla\rho_i) + \Sigma\Phi_i \qquad (2.23)$$

The sum of the phase change terms is equal to zero.

$$\frac{\partial\rho}{\partial t} + \nabla\cdot\vec{v}\rho = \Sigma(\nabla\cdot D_i\nabla\rho_i) \qquad (2.24)$$

Now it can be seen that the continuity equation is valid if and only if the following Eq. 2.25 and Eq. 2.26 are satisfied.

$$\frac{\partial\rho}{\partial t} = 0 \qquad (2.25)$$

$$\nabla\rho_i = 0 \qquad (2.26)$$

It is a reasonable assumption in a turbulent flow regime that the four components have the same diffusion constant. Therefore, Eq. 2.26 can be reduced to the following Eq. 2.27.

$$\nabla\rho = 0 \qquad (2.27)$$

Consequently Eq. 2.1 and Eq. 2.4 are consistent only if the temporal and spatial variations of the total density are very small. Since the concern is only for the slow mixing stage after a LOCA, it is reasonable to assume that Eq. 2.25 and Eq. 2.27 remain valid throughout the transient.

2.2.2 Energy Equation

The energy conservation equation, Eq. 2.3, is also of an approximate nature and the exact form is given in the following.

$$\frac{\partial}{\partial t}(\Sigma\rho_i e_i) + \nabla\cdot[\vec{v}\Sigma\rho_i h_i] = \nabla\cdot k\nabla T \tag{2.28}$$

The temporal term can be divided as follows.

$$\Sigma\rho_i\frac{\partial e_i}{\partial t} + \Sigma e_i\frac{\partial\rho_i}{\partial t} + \nabla\cdot[\vec{v}\Sigma\rho_i h_i] = \nabla\cdot k\nabla T \tag{2.29}$$

The second term on the left hand side of Eq. 2.29 denotes the energy change due to the concentration change in a given control volume. It is clear that the major contribution to this term will come from the latent heat of the phase change.

$$\Sigma e_i\frac{\partial\rho_i}{\partial t} \simeq \Sigma e_i\Phi_i \tag{2.30}$$

Eq.2.30 is substituted in Eq. 2.29 to give the following.

$$\Sigma\rho_i\frac{\partial e_i}{\partial t} + \Sigma e_i\Phi_i + \nabla\cdot[\vec{v}\Sigma\rho_i h_i] = \nabla\cdot k\nabla T \tag{2.31}$$

The thermal equilibrium assumption is incorporated in Eq. 2.31 so that the internal energy and enthalpy can be written in terms of the temperature.

$$(\Sigma\rho_i c_{vi})\frac{\partial T}{\partial t} + \nabla\cdot[\vec{v}T\Sigma\rho_i c_{pi}] + e_{fg}\Phi_g = \nabla\cdot k\nabla T \qquad (2.32)$$

where $\Sigma e_i \Phi_i = e_g\Phi_g + e_\ell \Phi_\ell$

$$= e_{fg}\Phi_g$$

$$e_i = c_{vi}T$$

$$h_i = c_{pi}T$$

Eq. 2.3 and Eq. 2.32 become identical by defining average internal energy and enthalpy as follows.

$$e = \frac{\rho_i e_i}{\rho} = \frac{\rho_i c_{vi} T}{\rho} \qquad (2.33)$$

$$h = \frac{\rho_i h_i}{\rho} = \frac{\rho_i c_{pi} T}{\rho} \qquad (2.34)$$

2.3 Basic Assumptions and Limitations

The governing equations are based on some simplifying assumptions about the physical phenomena in the containment after a LOCA. It is necessary to clarify these assumptions and their limitations for a safe use of the given physical models and solution scheme.

2.3.1 Assumptions

1. The four components all have the same convection velocity. The liquid droplets move with the gas components with no slip.

2. The four components are treated as being nearly incompressible and the phase change rate is moderately small.

3. The turbulent Prandtl and Schmidt numbers are equal to one.

4. The four components are in a state of thermodynamic equilibrium.

5. The relative humidity in the containment is 100%. The relative humidity may be less than 100% when there is no liquid component left.

2.3.2 Limitations

1. The temporal and spatial variations of the total density should be negligibly small because of the incompressibility assumption.

2. The phase change rate should be moderately small because the solution scheme decouples the phase change term from the energy conservation equation.

3. The change of the diffusion constants, ν_t, D_t and k_t over one time step should be small because the turbulence equations are decoupled from the velocity field calculations.

2.4 Solution Scheme

Eq. 2.1-Eq. 2.7 are a coupled set of equations with primary unknowns, u, v, w, p, $\rho_i(4)$, k, ε, T, ϕ_i. Since it is too difficult to solve the whole system of the equations and obtain a consistent solution for all the unknowns, the conservation equations are decoupled into two sets, continuity/momentum equations set and other scalar transport equations set. In the first step the SMAC scheme is used to get the convergent velocity field with zero divergence for every mesh. The SMAC scheme is explained in detail in section 2.5. In the second step, the obtained velocity field is substituted in the scalar transport equations, which are the four mass diffusion equations, energy equation and two turbulence equations. The phase change is assumed to be zero in this step. In the third step phase change is taken into consideration to maintain 100% relative humidity. When there is no liquid component left, the relative humidity may be less than 100%.

The equation of state, Eq. 2.7, is used to update the reference pressure and reference density which is important in calculating the buoyancy force.

2.5 SMAC Scheme and Compressibility

The SMAC (Simplified Marker And Cell) scheme [21] has been used for the incompressible fluid flow with Boussinesq approximation for the buoyancy force. It solves the continuity and momentum equations to get the velocity and pressure field in an iterative way. Since the continuity equation used in the SMAC is an incompressible form, i.e., the divergence of the velocity field vanishes everywhere, the SMAC scheme can be used only for incompressible flow calculations. However, it is possible to modify the SMAC scheme to accommodate a slight compressibility effect, which can arise with net inflow or outflow boundary conditions. The continuity and momentum equations are given in two dimensional Cartesian coordinates in the following.

Continuity: $$\frac{\partial u}{\partial x} + \frac{\partial v}{\partial y} = 0 \tag{2.35}$$

x-direction momentum: $$\frac{\partial u}{\partial t} + u\frac{\partial u}{\partial x} + v\frac{\partial u}{\partial y} = -\frac{1}{\rho}\frac{\partial p}{\partial x} + \nu\left(\frac{\partial^2 u}{\partial x^2} + \frac{\partial^2 u}{\partial y^2}\right) + \rho g_x \tag{2.36}$$

y-direction momentum: $$\frac{\partial v}{\partial t} + u\frac{\partial v}{\partial x} + v\frac{\partial v}{\partial y} = -\frac{1}{\rho}\frac{\partial p}{\partial y} + \nu\left(\frac{\partial^2 v}{\partial x^2} + \frac{\partial^2 v}{\partial y^2}\right) + \rho g_y \tag{2.37}$$

The vorticity conservation equation is derived from Eq. 2.36 and Eq. 2.37 as follows.

$\frac{\partial}{\partial y}$(Eq. 2.36) - $\frac{\partial}{\partial x}$(Eq. 2.37):

$$\frac{\partial \zeta}{\partial t} + u\frac{\partial \zeta}{\partial x} + v\frac{\partial \zeta}{\partial y} = \nu\left(\frac{\partial^2 \zeta}{\partial x^2} + \frac{\partial^2 \zeta}{\partial y^2}\right) \tag{2.38}$$

where

$$\zeta = \frac{\partial u}{\partial y} - \frac{\partial v}{\partial x}$$

The Poisson equation for the pressure field is also derived from Eq. 2.36 and Eq. 2.37 as follows.

$\frac{\partial}{\partial x}$(Eq. 2.36) + $\frac{\partial}{\partial y}$(Eq. 2.37):

$$\nabla^2 p = -\frac{\partial^2}{\partial x^2}(u^2) - \frac{2\partial^2}{\partial x \partial y}(uv) - \frac{\partial^2}{\partial y^2}(v^2) - \frac{\partial D}{\partial t} + \frac{1}{Re}\left(\frac{\partial^2 D}{\partial x^2} + \frac{\partial^2 D}{\partial y^2}\right) \tag{2.39}$$

where

$$D = \frac{\partial u}{\partial x} + \frac{\partial v}{\partial y}$$

The basic idea of the SMAC scheme is to separate each calculational cycle into two parts, the so-called tilde phase and pressure iteration. In the tilde phase the approximate velocity field at time step (n+1) is obtained from Eq. 2.36 and Eq. 2.37 as follows.

$$\frac{u^{n+1}-u^n}{\Delta t} = -\frac{1}{\rho}\frac{\Delta p^{n+1}}{\Delta x} + f^n \tag{2.40}$$

$$\frac{v^{n+1}-v^n}{\Delta t} = -\frac{1}{\rho}\frac{\Delta p^{n+1}}{\Delta y} + g^n \tag{2.41}$$

where f^n and g^n are the explicit quantities at time step n.

Since the pressure field in Eq. 2.40 and Eq. 2.41 are still unknown, a guessed pressure field or the pressure field at time step n is used to start the iteration. The important point is that u^{n+1} and v^{n+1} calculated from Eq. 2.40 and Eq. 2.41 have the right vorticity. The equation of vorticity transport, Eq. 2.38, shows that the vorticity is independent of the pressure field. Therefore, the following relations hold after the tilde phase.

$$\frac{\partial u}{\partial y} - \frac{\partial v}{\partial x} = \zeta \tag{2.42}$$

$$\frac{\partial u}{\partial x} + \frac{\partial v}{\partial y} = D \neq 0 \tag{2.43}$$

It can be seen from Eq. 2.39 that the pressure field is not right due to the fact that the divergence of the velocity field is not equal to zero. Eq. 2.39 may be rewritten as follows.

$$\nabla^2 p = f(u,v) - \frac{\partial D}{\partial t} \tag{2.44}$$

A finite difference form of Eq. 2.44 is given in the following.

$$\frac{p_{i+1j}-2p_{ij}+p_{i-1j}}{\Delta x^2} + \frac{p_{ij+1}-2p_{ij}+p_{ij-1}}{\Delta y^2} = f(u,v) - \frac{D_{ij}^{n+1}-D_{ij}^{n}}{\Delta t} \tag{2.45}$$

The pressure correction formula is obtained by considering the cell (i,j) only and putting D_{ij}^{n+1} equal to zero.

$$-2\delta p\left(\frac{1}{\Delta x^2} + \frac{1}{\Delta y^2}\right) = \frac{D}{\Delta t} \tag{2.46}$$

$$\delta p = -\frac{1}{2}\frac{D}{\Delta t\left(\frac{1}{\Delta x^2} + \frac{1}{\Delta y^2}\right)} \tag{2.47}$$

The pressure correction is given in terms of the residual divergence for every mesh. Once the zero divergence velocity field is obtained, no more correction will be made. The velocity correction formula is derived from Eq. 2.36 and Eq. 2.37 so that it does not change the vorticity implemented in the tilde phase.

$$(\delta u)_L = -\frac{\Delta t \delta p}{\rho \Delta x}$$

$$(\delta u)_R = \frac{\Delta t \delta p}{\rho \Delta x} \tag{2.48}$$

The SMAC scheme can be extended to a slightly compressible fluid flow. The slight compressibility means that the Navier-Stokes equations may be solved safely with the incompressibility assumption, while the continuity equation has the following compressible form.

$$\frac{\partial \rho}{\partial t} + \nabla\cdot(\vec{v}\rho) = 0 \tag{2.49}$$

From Eq. 2.49 the nonzero divergence may be derived as follows.

$$D = \nabla \cdot \vec{v}$$
$$= -\frac{1}{\rho}\frac{\partial \rho}{\partial t} - \frac{\vec{v} \cdot \nabla \rho}{\rho} \qquad (2.50)$$

The two terms on the right hand side of Eq. 2.50 may be given from the previous time information and boundary conditions.

$$\frac{1}{\rho}\frac{\partial \rho}{\partial t} = \frac{1}{\rho^n}\frac{m_{in}/V}{\Delta t} \qquad (2.51)$$

$$\frac{\vec{v} \cdot \nabla \rho}{\rho} = \frac{\vec{v}^n \cdot \nabla \rho^n}{\rho^n} \qquad (2.52)$$

where

m_{in}: total net inflow of mass at the boundary during the time Δt.

V: total volume of the containment.

The associated physical assumption in Eq. 2.51 and Eq. 2.52 is that the pressure perturbation due to the inflow at the boundary propagates throughout the containment instantaneously and the pressure and density increase is uniform over the whole containment.

Now the problem is how to converge to a predetermined nonzero divergence field. This can be done with the following modification of the pressure correction formula of the SMAC scheme.

$$\delta p = \frac{-(D-D_0)}{2\Delta t(\frac{1}{\Delta x^2} + \frac{1}{\Delta y^2})} \tag{2.53}$$

where D_0 is given by Eq. 2.50. The velocity correction formula remains the same as Eq. 2.48.

CHAPTER 3

DIFFUSION MODELLING

The hydrogen, air, steam and liquid components are transported by convection and diffusion in the containment. Convection occurs as a homogeneous mixture resulting in the same convection velocity for the four components. Diffusion occurs by two different mechanisms, molecular and turbulent, which should be modelled independently. The thermal conductivity and viscosity are also diffusion constants in a broader sense for momentum and energy transport. Although turbulent diffusion is greater than molecular diffusion by a few orders of magnitude, proper modelling of the latter is important because the molecular diffusion of hydrogen is significantly greater than those of other gases and also because there may be a laminar flow region in the containment.

3.1 Molecular Diffusion

Molecular diffusion occurs by the collisions of gas molecules. As collisions occur more frequently, the process of diffusion is also increased. Since there may be three gas components, hydrogen, air and steam, in the containment after a LOCA, the diffusion constant of each component is calculated separately by Wilke's formula [73] in Eq. 3.1. It gives the diffusion constant of each component in terms of the binary mixture diffusion constants and mole fraction of that component. The property of air will be replaced with that of nitrogen gas. The resulting diffusion constants are given as follows,

$$D_A = \frac{1-y_C}{\frac{y_B}{D_{AB}} + \frac{y_C}{D_{CB}}} ,$$

$$D_B = \frac{1-y_B}{\frac{y_A}{D_{BA}} + \frac{y_C}{D_{BC}}} ,$$

$$D_C = \frac{1-y_C}{\frac{y_A}{D_{CA}} + \frac{y_B}{D_{CB}}} , \qquad (3.1)$$

where D_i: Diffusion constant of the i-th component

y_i: Mole fraction of the i-th component

D_{ij}: Binary mixture diffusion constant between the i-th and j-th components.

The binary mixture diffusion constants are calculated by the Chapman-Enskog formula, Eq. 3.2.

$$D_{AB} = 0.0018583 \frac{\sqrt{T^3(\frac{1}{M_A} + \frac{1}{M_B})}}{p\sigma_{AB}^2 \Omega_{D,AB}} \qquad (3.2)$$

where

D_{AB}: Binary mixture diffusion constant in [cm^2/sec]

T: Temperature in [°K]

p: Total pressure in [atm]

σ_{AB}: Lennard-Jones parameter in [Å]

M_A, M_B: Molecular weight

$\Omega_{D,AB}$: Dimensionless function of the temperature and intermolecular potential field for one molecule of A and one of B.

The error range of the Chapman-Enskog formula is reported to be about 6-10% [5]. In order to calculate the parameters σ_{AB} and $\Omega_{D,AB}$ in Eq. 3.2, the following relations are required. For non-polar gases σ_{AB} and $\Omega_{D,AB}$ are calculated by Eq. 3.3.

$$\sigma_{AB} = (\sigma_A + \sigma_B)$$

$$\varepsilon_{AB} = \sqrt{\varepsilon_A \cdot \varepsilon_B} \qquad (3.3)$$

For the pair of polar and non-polar gases a correction factor is introduced to account for the polarity.

$$\sigma_{np} = \tfrac{1}{2}(\sigma_n + \sigma_p)\ \xi^{-1/6}$$

$$\varepsilon_{np} = \sqrt{\varepsilon_n \varepsilon_p}\ \xi^2 \qquad (3.4)$$

where the correction factor ξ is given by,

$$\xi = [1+\tfrac{1}{4}\alpha_n^* \ \mu_p^{*2}\sqrt{\frac{\varepsilon_p}{\varepsilon_n}} = [1+\frac{\sqrt{2}}{2}\ \alpha_n^*\ t_p^*\sqrt{\frac{\varepsilon_p}{\varepsilon_n}}\ ]. \qquad (3.5)$$

The parameters in Eq. 3.5 are defined as follows.

$\alpha_n^* = \alpha_n/\sigma_n^3$: Reduced polarizability of the non-polar molecule

$\mu_p^* = \mu_p/\sqrt{\varepsilon_p\sigma_p^3}$: Reduced dipole moment of the polar molecule

$t_p^* = \mu_p^*/\sqrt{8}$

For the steam component the following values will be used.

$t^* = 1.2$

$\varepsilon/\kappa = 380°K$

$\sigma = 2.65$ Å

The polarizability is given for the hydrogen and nitrogen (air) components.

H_2: $\alpha_n = 7.9 \times 10^{-25}$ $[cm^3]$

N_2: $\alpha_n = 17.6 \times 10^{-25}$ $[cm^3]$

The fitting functions for the binary mixture diffusion constants are obtained by the least-square-fit method. The containment pressure is assumed to be 1 atm.

$$D_{ah} = 4.9492 \times 10^{-5}\ T^{1.6947}$$

$$D_{as} = 4.6810 \times 10^{-6}\ T^{1.9035}$$

$$D_{hs} = 2.8916 \times 10^{-5}\ T^{1.8144} \tag{3.6}$$

where

T: [°K]

D: [cm^2/sec]

The viscosity and thermal conductivity can be considered as diffusion constants for momentum and energy transport and calculated similarly as follows [5].

$$\mu_{mix} = \sum_{i=1}^{n} \frac{y_i \mu_i}{\sum_{j=1}^{n} y_j \phi_{ij}} \tag{3.7}$$

$$k_{mix} = \sum_{i=1}^{n} \frac{y_i k_i}{\sum_{j=1}^{n} y_j \phi_{ij}} \tag{3.8}$$

where

$$\phi_{ij} = \frac{1}{\sqrt{8}}\left(1+\frac{M_i}{M_j}\right)^{-\frac{1}{2}}\left[1+\left(\frac{\mu_i}{\mu_j}\right)^{\frac{1}{2}}\left(\frac{M_j}{M_i}\right)^{\frac{1}{4}}\right]^2 \tag{3.9}$$

The viscosity of non-polar gases may be obtained by the following [5].

$$\mu = 2.67 \times 10^{-5}\ \frac{\sqrt{MT}}{\sigma^2 \Omega_\mu} \tag{3.10}$$

where

μ: Viscosity in [poise]

T: Temperature in [°K]

σ: Lennard-Jones parameter in [Å]

Ω_μ: Dimensionless number

The viscosity of steam is,

$$\mu_{steam} = 0.009 \text{ cp} \quad \text{at 1 atm, } 20°C$$

There is another formula suggested for the viscosity of multicomponent gas in the following [5].

$$\mu_{mix} \doteq \sum_{i=1}^{n} \frac{y_i^2}{\dfrac{y_i^2}{\mu_i} + 1.385 \sum\limits_{\substack{k=1 \\ k \neq i}}^{n} y_i y_k \dfrac{RT}{pM_i D_{ik}}} \tag{3.11}$$

There is a useful relationship for the Prandtl number of non-polar polyatomic gases [5].

$$Pr = \frac{c_p}{c_p + 1.25R} \tag{3.12}$$

where c_p is the specific heat per mole at constant pressure.

3.2 Turbulent Diffusion

The diffusion process is greatly enhanced by the turbulence of fluid flow. The effective diffusion constant is therefore the sum of the molecular and turbulent diffusion constants. There are several models suggested for calculating turbulence effects. Presently the best model seems to be the k-ε model originally developed by Launder and Spalding [45]. The k-ε model sets up the transport equations with some empirical constants for the turbulent kinetic energy, k, and turbulent dissipation rate, ε. The turbulent viscosity is given directly in terms of k and ε.

3.2.1 Derivation of Turbulence Equations [15, 29, 34, 45]

The transport equations for the turbulent kinetic energy and turbulent dissipation rate are derived from the continuity, momentum and energy equations by decomposing the variables into mean and fluctuating parts and averaging the resulting equations. For example,

$$u_i = \bar{u}_i + u_i'$$

$$\rho_i = \bar{\rho}_i + \rho_i' \qquad \text{etc.}$$

The effect of turbulence appears as the additional terms due to the product of fluctuations which do not necessarily cancel out. These terms are treated by the eddy viscosity concept of Boussinesq and eddy diffusivity concept which are given in the following.

$$-\overline{u_i' u_j'} = \nu_t \left(\frac{\partial \bar{u}_i}{\partial x_j} + \frac{\partial \bar{u}_j}{\partial x_i}\right) - \frac{2}{3} k \delta_{ij} \tag{3.13}$$

$$-\overline{u_j' \rho_i'} = D_t \frac{\partial \bar{\rho}_i}{\partial x_j} \tag{3.14}$$

$$-\overline{u_j' T'} = \alpha_t \frac{\partial \bar{T}}{\partial x_j} \tag{3.15}$$

The transport equation for $\overline{u_i' u_j'}$ is transformed to the turbulent kinetic energy equation by the contraction, j=i. The turbulent dissipation rate equation can also be derived in a similar way and some assumptions should be made in modelling various terms that appear in the derivation.

3.2.2 k-ε Model

The transport equations for the turbulent kinetic energy and turbulent dissipation rate form the basis of the k-ε model. A two dimensional cylindrical coordinate form of the k-ε model is introduced in Eq. 3.16.

$$\frac{\partial k}{\partial t} + \frac{1}{r}\frac{\partial}{\partial r}(ruk) + \frac{\partial}{\partial z}(wk) = \frac{1}{\rho}\left[\frac{1}{r}\frac{\partial}{\partial r}\left(r\frac{\mu_t}{\sigma_k}\frac{\partial k}{\partial r}\right) + \frac{\partial}{\partial z}\left(\frac{\mu_t}{\sigma_k}\frac{\partial k}{\partial z}\right)\right]$$
$$+ \frac{\mu_t}{\rho}\left[2\left(\frac{\partial u}{\partial r}\right)^2 + 2\left(\frac{\partial w}{\partial z}\right)^2 + \left(\frac{\partial w}{\partial r} + \frac{\partial u}{\partial z}\right)^2\right.$$
$$\left. + 2\frac{u^2}{r^2}\right] - \varepsilon + \beta g\frac{\nu_t}{Pr_t}\frac{\partial T}{\partial z}$$

$$\frac{\partial \varepsilon}{\partial t} + \frac{1}{r}\frac{\partial}{\partial r}(ru\varepsilon) + \frac{\partial}{\partial z}(w\varepsilon) = \frac{1}{\rho}\left[\frac{1}{r}\frac{\partial}{\partial r}\left(r\frac{\mu_t}{\sigma_\varepsilon}\frac{\partial \varepsilon}{\partial r}\right) + \frac{\partial}{\partial z}\left(\frac{\mu_t}{\sigma_\varepsilon}\frac{\partial \varepsilon}{\partial z}\right)\right]$$
$$+ C_1\frac{\mu_t}{\rho}\frac{\varepsilon}{k}\left[2\left(\frac{\partial u}{\partial r}\right)^2 + 2\left(\frac{\partial w}{\partial z}\right)^2\right.$$
$$\left. + \left(\frac{\partial w}{\partial r} + \frac{\partial u}{\partial z}\right)^2 + 2\frac{u^2}{r^2}\right] - C_2\frac{\varepsilon^2}{k}$$
$$+ \frac{\varepsilon}{k}\beta g\frac{\nu_t}{Pr_t}\frac{\partial T}{\partial z} \qquad (3.16)$$

The turbulent viscosity μ_t is given in terms of k and ε in Eq. 3.17.

$$\mu_t = C_\mu \rho k^2/\varepsilon \tag{3.17}$$

The suggested values of the constants are given in the following table.

C_μ	C_1	C_2	σ_k	σ_ε
0.09	1.44	1.92	1.0	1.3

The molecular effects can be included in Eq. 3.16 as follows.

$$\frac{\mu_t}{\sigma_k} \rightarrow \mu_m + \frac{\mu_t}{\sigma_k}$$

$$\frac{\mu_t}{\sigma_\varepsilon} \rightarrow \mu_m + \frac{\mu_t}{\sigma_\varepsilon}$$

The turbulent Prandtl and Schmidt numbers are usually assumed to be equal to one.

3.3 Low Reynolds Number Flow

While both turbulent and laminar flows are possible in the containment after a LOCA depending on the hydrogen generation rate and geometry, it is difficult to determine whether a region under consideration is in a turbulent or laminar flow. Since the k-ε model is applicable to fully turbulent flow, it is required to extend the model to laminar flow regime or to switch to laminar models according to some criterion. The model presently being used is just to use the sum of the molecular and turbulent contributions for every region in the containment. A more refined model is introduced in this section because consistent treatment of laminar and turbulent flows and transition between them may be required in the future modelling efforts.

The following k-ε model is a modified form by Jones and Launder [40, 41].

$$\frac{D}{Dt} = \frac{1}{\rho}\frac{\partial}{\partial x_k}\left[\left(\frac{\mu_t}{\sigma_\varepsilon} + \mu\right)\frac{\partial \varepsilon}{\partial x_k}\right] + C_1 \frac{\mu_t}{\rho}\frac{\varepsilon}{k}\left(\frac{\partial u_i}{\partial x_k} + \frac{\partial u_k}{\partial x_i}\right)\frac{\partial u_i}{\partial x_k} - C_2 \frac{\varepsilon^2}{k}$$

$$- 2.0 \frac{\nu\mu_t}{\rho}\left(\frac{\partial^2 u_i}{\partial x_\ell \partial x_\ell}\right)^2$$

$$\frac{Dk}{Dt} = \frac{1}{\rho}\frac{\partial}{\partial x_k}\left[\left(\frac{\mu_t}{\sigma_k} + \mu\right)\frac{\partial k}{\partial x_k}\right] + \frac{\mu_t}{\rho}\left(\frac{\partial u_i}{\partial x_k} + \frac{\partial u_k}{\partial x_i}\right)\frac{\partial u_i}{\partial x_k} - \varepsilon - 2\nu\left(\frac{\partial k^{1/2}}{\partial x_k}\right)^2 \tag{3.18}$$

In the above equations C_1, σ_k and σ_ε retain the values assigned in the ordinary k-ε model, Eq. 3.16, while C_μ and C_2 are to vary with turbulence Reynolds number, R_t.

$$C_\mu = C_{\mu 0} \exp[-2.5/(1+R_t/50)]$$

$$C_2 = C_{2\,0}\,[1.0 - 0.3 \exp(-R_t^{\,2})] \tag{3.19}$$

where $R_t = \rho k^2/\mu\varepsilon$

The $C_{\mu 0}$ and $C_{2\,0}$ are fully turbulent values of C_μ and C_2. This modified form of the k-ε model was developed to cover all the laminar, transitional and fully turbulent regions. The constants were fitted to the data of a low Re flow in a round pipe to include the effect of laminar wall boundary layer. Although its applicability to a low Reynolds number flow in general is questionable, the model may be used with some confidence if it has the proper limit of laminar regime with the decay of turbulence. It may also be used in the transitional regime by assuming an adequate interpolation between the two extremes. Equation 3.18 shows that k and ε have the same order of magnitude with the decay of turbulence. In other words, both k^2/ε and ε^2/k will go to zero as k and ε go to zero separately. Therefore, the turbulent viscosity μ_t which is proportional to k^2/ε will vanish with the decay of turbulence. In order to have the proper laminar limit, the total diffusion constant should be expressed as the sum of the turbulent and laminar diffusion constants. It may also be reasonable to assume that the turbulent Prandtl and Schmidt numbers are equal to one.

CHAPTER 4

NUMERICAL DIFFUSION

The final numerical solution involves two types of errors which come from physical modelling and numerical solution procedure. The error in physical modelling is an intrinsic error which cannot be eliminated by the solution procedure. The error in numerical solution procedure is the difference between exact and numerical solutions of the governing equation, which usually appears as additional diffusion. It is clarified that there are two sources of numerical diffusion, truncation error diffusion and cross-flow diffusion. This chapter is primarily concerned with how to predict and eliminate these additional false diffusions to get an accurate solution.

4.1 Truncation Error Diffusion

Truncation error diffusion occurs due to the approximate nature of the finite difference formulations. The name of the truncation error originates from the Taylor series expansion where the second and higher order terms are truncated. Although the Taylor series expansion is not a proper way of interpreting a finite difference equation, the name of the truncation error will be retained here. Since the truncation error exists in multidimensional problems in the same way as it exists in one dimensional problems, it can be analyzed in the following one dimensional conservation equation without any loss of generality.

$$\frac{\partial \Phi}{\partial t} + u\frac{\partial \Phi}{\partial x} = \alpha\frac{\partial^2 \Phi}{\partial x^2} + S \tag{4.1}$$

where

Φ: any general conserved quantity

S: source term

The velocity u and diffusion constant α will be assumed constant. Equation 4.1 is integrated in the domain $[x_{i-\frac{1}{2}}, x_{i+\frac{1}{2}}]$ and $[t_n, t_{n+1}]$.

$$\int_{x_{i-\frac{1}{2}}}^{x_{i+\frac{1}{2}}} \int_{t_n}^{t_{n+1}} \frac{\partial \Phi}{\partial t}\, dt\, dx + \int_{x_{i-\frac{1}{2}}}^{x_{i+\frac{1}{2}}} \int_{t_n}^{t_{n+1}} u\frac{\partial \Phi}{\partial x}\, dt\, dx$$

$$= \int_{x_{i-\frac{1}{2}}}^{x_{i+\frac{1}{2}}} \int_{t_n}^{t_{n+1}} \alpha\frac{\partial^2 \Phi}{\partial x^2}\, dt\, dx + S\,\Delta x\,\Delta t \tag{4.2}$$

where

$\Delta t = t_{n+1} - t_n$

$\Delta x = x_{i+\frac{1}{2}} - x_{i-\frac{1}{2}}$

When a function f(x) is continuous, there exists a point x=c in [a,b] such that,

$$\frac{1}{b-a}\int_a^b f(x)\, dx = f(c)\ . \tag{4.3}$$

Using Eq. 4.3, we may transform Eq. 4.2 as follows.

$$\frac{1}{\Delta t}\left[\phi_{i+f}^{n+1} - \phi_{i+f}^{n}\right] + \frac{u}{\Delta x}\left[\phi_{i+\frac{1}{2}}^{n+g} - \phi_{i-\frac{1}{2}}^{n+g}\right]$$

$$= \frac{\alpha}{\Delta x}\left[\left(\frac{\partial \phi}{\partial x}\right)_{i+\frac{1}{2}}^{n+g} - \left(\frac{\partial \phi}{\partial x}\right)_{i-\frac{1}{2}}^{n+g}\right] + S \qquad (4.4)$$

where

$-\frac{1}{2} \leq f \leq \frac{1}{2}$

$0 \leq g \leq 1$

Equation 4.1 may also be reduced to Eq. 4.5. It is fully explicit and the convection term is finitely differenced by the donor scheme.

$$\frac{\phi_i^{n+1} - \phi_i^{n}}{\Delta t} + \frac{u}{\Delta x}(\phi_i^{n} - \phi_{i-1}^{n})$$

$$= \frac{\alpha}{\Delta x^2}(\phi_{i+1}^{n} - 2\phi_i^{n} + \phi_{i-1}^{n}) + S \qquad (4.5)$$

From Eq. 4.4 and 4.5, $(\phi_{i+f}^{n+1})_{EXACT}$ and $(\phi_i^{n+1})_{FD}$ can be obtained as follows.

$$(\phi_i^{n+1})_{FD} = \phi_i^{n} + \Delta t \left[-u\frac{\phi_i^{n} - \phi_{i-1}^{n}}{\Delta x} + \frac{\alpha}{\Delta x^2}(\phi_{i+1}^{n} - 2\phi_i^{n} + \phi_{i-1}^{n}) \right.$$

$$\left. + S \right] \qquad (4.6)$$

$$(\phi_{i+f}^{n+1})_{EXACT} = \phi_{i+f}^{n} + \Delta t \left[-u\frac{\phi_{i+\frac{1}{2}}^{n+g} - \phi_{i-\frac{1}{2}}^{n+g}}{\Delta x} \right.$$

$$\left. + \frac{\alpha}{\Delta x}\left[\left(\frac{\partial \phi}{\partial x}\right)_{i+\frac{1}{2}}^{n+g} - \left(\frac{\partial \phi}{\partial x}\right)_{i-\frac{1}{2}}^{n+g}\right] + S \right] \qquad (4.7)$$

Subtracing Eq. 4.6 from Eq. 4.7, we obtain the error at time step (n+1).

$$(\phi^{n+1}_{i+f})_{EXACT} - (\phi^{n+1}_{i})_{FD} = \phi^{n}_{i+f} - \phi^{n}_{i} + \Delta t \ [-u(\frac{\partial \phi}{\partial x})^{n+g}_{i+a}$$

$$+ u(\frac{\partial \phi}{\partial x})^{n}_{i+b} + \alpha(\frac{\partial^2 \phi}{\partial x^2})^{n+g}_{i+c} - \alpha(\frac{\partial^2 \phi}{\partial x^2})^{n}_{i+d} \ ] \qquad (4.8)$$

where the following relations have already been used.

$$\frac{\phi^{n+g}_{i+\frac{1}{2}} - \phi^{n+g}_{i-\frac{1}{2}}}{\Delta x} = (\frac{\partial \phi}{\partial x})^{n+g}_{i+a} \qquad -\tfrac{1}{2} < a < \tfrac{1}{2}$$

$$\frac{\phi^{n}_{i} - \phi^{n}_{i-1}}{\Delta x} = (\frac{\partial \phi}{\partial x})^{n}_{i+b} \qquad -1 < b < 0$$

$$\frac{1}{\Delta x} \ [(\frac{\partial \phi}{\partial x})^{n+g}_{i+\frac{1}{2}} - (\frac{\partial \phi}{\partial x})^{n+g}_{i-\frac{1}{2}} \ ] = (\frac{\partial^2 \phi}{\partial x^2})^{n+g}_{i+c} \qquad -\tfrac{1}{2} < c < \tfrac{1}{2}$$

$$\frac{\phi^{n}_{i+1} - 2\phi^{n}_{i} + \phi^{n}_{i-1}}{\Delta x^2} = (\frac{\partial^2 \phi}{\partial x^2})^{n}_{i+d} \qquad -1 < d < 1$$

The mean value theorem, Eq. 4.3, is for a one dimensional case. It can be extended to a two dimensional form as follows.

$$f(x+a,y+b) = f(x,y) + (\frac{\partial f}{\partial x})_A a + (\frac{\partial f}{\partial y})_B b \qquad (4.9)$$

where A and B denote some interior points in the domain bounded by [x,x+a] and [y,y+b].

Now Eq. 4.9 reduces Eq. 4.8 to the following form.

$$(\phi_i^{n+1})_{EXACT} - (\phi_i^{n+1})_{FD} = -f\Delta x^2(f_1-f_2)\frac{\partial^2\phi}{\partial x^2} \text{ ------- A}$$

$$-f\Delta x\Delta t\frac{\partial^2\phi}{\partial x\partial t} \text{ ------------ B}$$

$$-u\Delta t\Delta x(a+b)\frac{\partial^2\phi}{\partial x^2} \text{ -------- C}$$

$$+\Delta t^2 g\frac{\partial^2\phi}{\partial t\partial x} \text{ ------------- D}$$

$$+\alpha\Delta x(c-d)\Delta t\frac{\partial^3\phi}{\partial x^3} \text{ -------- E}$$

$$+\alpha g\Delta t^2\frac{\partial^2\phi}{\partial t\partial x} \text{ ----------F} \quad (4.10)$$

The derivatives with respect to time and space in Eq. 4.10 are at some appropriate points in the domain $[x_{i-\frac{1}{2}},x_{i+\frac{1}{2}}]$ and $[t_n,t_{n+1}]$. The terms A, C and E are truncation error diffusion terms while the terms B, D and F are time derivative terms which become negligible for slow transients.

In a stable scheme the error introduced at a certain step decreases in its absolute magnitude in the following steps and most of the error occurs between neighboring time steps. Although the error terms in Eq. 4.10 are based on the assumption of perfect information at time step n, they may represent the errors over many time steps in a stable scheme.

4.1.1 Truncation Error Diffusion in a One Dimensional Problem

The truncation error diffusion in a one dimensional problem is analyzed for a steady-state case with no source. The results may be extended to a general one dimensional problem if the effects of the transient and source terms are not dominant in determining the profile of Φ.

$$u\frac{\partial \Phi}{\partial x} = \alpha\frac{\partial^2 \Phi}{\partial x^2} \tag{4.11}$$

Consider a case in which the domain is divided into N equal meshes and the mesh size is Δx.

0 1 2 3 i-1 1 i+1 N

L

$$\Phi(x=0) = \Phi_0$$

$$\Phi(x=L) = \Phi_N$$

$$N\Delta x = L$$

Two boundary values Φ_0 and Φ_N are given as constant. The analytical solution of Eq. 4.11 is given as,

$$\Phi = C_1 e^{cx} + C_2 \ , \tag{4.12}$$

where $\quad c = u/\alpha \quad ,$

and $\quad C_1 = \dfrac{\Phi_N - \Phi_0}{e^{cL} - 1} \ , \quad C_2 = \dfrac{\Phi_0 e^{cL} - \Phi_N}{e^{cL} - 1} \ .$

Equation 4.11 is finitely differenced using donor cell scheme for the convection term in the following.

$$u\frac{\Phi_i - \Phi_{i-1}}{\Delta x} = \alpha\frac{\Phi_{i+1} - 2\Phi_i + \Phi_{i-1}}{\Delta x^2} \tag{4.13}$$

where the velocity u is positive.

Equation 4.13 can also be solved with the given boundary conditions by reducing it to the following form.

$$P(\Phi_i - \Phi_{i-1}) = \Phi_{i+1} - 2\Phi_i + \Phi_{i-1}$$

where $P = \frac{u\Delta x}{\alpha}$ (4.14)

The parameter P in Eq. 4.14 is the cell Reynolds number or cell Peclet number according to whether the diffusion constant α is the kinematic viscosity or thermal diffusivity. Equation 4.14 may be recast to Eq. 4.15 and solved for Φ_i in subsequent procedures.

$$\Phi_{i+1} - \Phi_i = (P+1)(\Phi_i - \Phi_{i-1}) \tag{4.15}$$

Equation 4.16 is easily obtained from Eq. 4.15.

$$\Phi_{i+1} - \Phi_i = (P+1)^i(\Phi_1 - \Phi_0) \tag{4.16}$$

Then,

$$\Phi_2 - \Phi_1 = (1+P)(\Phi_1 - \Phi_0)$$

$$\Phi_3 - \Phi_2 = (1+P)^2(\Phi_1 - \Phi_0)$$

$$\vdots$$

$$\Phi_N - \Phi_{N-1} = (1+P)^{N-1}(\Phi_1 - \Phi_0)$$

$$\Phi_N - \Phi_1 = (\Phi_1 - \Phi_0)\frac{(1+P)[(1+P)^{N-1} - 1]}{P} \tag{4.17}$$

Φ_1 can be expressed in terms of Φ_0 and Φ_N by Eq. 4.17.

$$\Phi_1 = \frac{\frac{(1+P)^N - (1+P)}{P}\Phi_0 + \Phi_N}{\frac{(1+P)^N - (1+P)}{P} + 1} \tag{4.18}$$

Therefore, $(\Phi_1 - \Phi_0)$ is given as follows.

$$\Phi_1 - \Phi_0 = \frac{P(\Phi_N - \Phi_0)}{(1+P)^N - 1} \tag{4.19}$$

Inserting Eq. 4.19 into Eq. 4.16, we obtain the solution for Φ_i as,

$$\Phi_i = \Phi_0 + \frac{(1+P)^i - 1}{(1+P)^N - 1}(\Phi_N - \Phi_0) \ . \tag{4.20}$$

Now the analytical solution Eq. 4.12 and numerical solution Eq. 4.20 have been obtained without any approximation for Eq. 4.11 and Eq. 4.13. Both the analytical and numerical solutions will be reinserted to the finite difference equation, Eq. 4.13, and the effective diffusion constant for the numerical solution will be obtained. The analytical solution Eq. 4.12 is substituted for Φ_i in Eq. 4.13.

$$\Phi_{i+1} - 2\Phi_i + \Phi_{i-1} = \frac{e^{(i-1)P}}{e^{NP} - 1}(e^P - 1)^2(\Phi_N - \Phi_0) \qquad (4.21)$$

The finite difference solution Eq. 4.20 is also substituted for Φ_i in Eq. 4.13.

$$\Phi_{i+1} - 2\Phi_i + \Phi_{i-1} = \frac{(1+P)^{i-1}P^2}{(1+P)^N - 1}(\Phi_N - \Phi_0) \qquad (4.22)$$

Comparing Eq. 4.21 and Eq. 4.22 we can obtain the effective Peclet number Pe of the finite difference solution in terms of the real Peclet number P as follows.

$$\frac{e^{(i-1)Pe}}{e^{NPe} - 1}(e^{Pe}-1)^2 = \frac{(1+P)^{i-1}P^2}{(1+P)^N - 1} \qquad (4.23)$$

Therefore,

$$Pe = \ln\,(1+P) \qquad (4.24)$$

It is also possible to go through the similar procedures with a central differencing form of the convection term in Eq. 4.25.

$$u\frac{\Phi_{i+1} - \Phi_{i-1}}{2\Delta x} = \frac{\Phi_{i+1} - 2\Phi_i + \Phi_{i-1}}{\frac{2}{\Delta x}} \qquad (4.25)$$

The effective Peclet number for the finite difference solution of Eq. 4.25 can be derived as follows.

$$Pe = \ln\left(\frac{2+P}{2-P}\right) \tag{4.26}$$

where $-2 < P < 2$

The effective diffusion constant De can be readily obtained from the following relation.

$$Pe = \frac{u\Delta x}{De} \tag{4.27}$$

In general, the transient and source terms and the mixed type of boundary conditions will not affect the numerical diffusion appreciably if they are not dominant terms in determining the profile of Φ. Therefore, Eq. 4.24 and Eq. 4.26 may be a good indication of the truncation error diffusion occurring in a general one dimensional problem.

4.1.2 Another Approach For a One Dimensional Truncation Error Diffusion

The truncation error diffusion in a one dimensional problem can be evaluated in a different approach. Although this approach is approximate and overpredicts the truncation error diffusion, it helps understanding the origin of the truncation error diffusion.

As in the previous section the velocity u is assumed to be positive and constant. The convection terms in

Eq. 4.4 and Eq. 4.5 may be approximated as follows.

$$-u\frac{\Phi_i - \Phi_{i-1}}{\Delta x} \cong -u\left(\frac{\partial \Phi}{\partial x}\right)_i \tag{4.28}$$

$$-u\frac{\Phi_{i+\frac{1}{2}} - \Phi_{i-\frac{1}{2}}}{\Delta x} \cong -u\left(\frac{\partial \Phi}{\partial x}\right)_{i+\frac{1}{2}} \tag{4.29}$$

The truncation error diffusion can be quantified by subtracting Eq. 4.29 from Eq. 4.28.

$$-u\left(\frac{\partial \Phi}{\partial x}\right)_i + u\left(\frac{\partial \Phi}{\partial x}\right)_{i+\frac{1}{2}} = \frac{u\Delta x}{2}\left(\frac{\partial^2 \Phi}{\partial x^2}\right)_{i+f} \tag{4.30}$$

where

$$0 \leq f \leq \tfrac{1}{2}$$

Both Eq. 4.28 and Eq. 4.29 hold only when the Peclet number is large, i.e, the convection is dominant over the diffusion. If the Peclet number is small, i.e., the diffusion is dominant over the convection, the profile of Φ will be linear and the truncation error will be reduced to zero. It can be shown that as P goes to zero, Pe also goes to zero resulting in no diffusion error in Eq. 4.24 and Eq. 4.26. Therefore, the truncation error diffusion constant for a convection dominant problem may be given approximately as follows.

$$D_{ND} \cong \frac{u\Delta x}{2} \tag{4.31}$$

4.1.3 Truncation Error Diffusion in a Two Dimensional Problem

There are two sources of numerical diffusion in a two dimensional problem, one is the truncation error diffusion and the other is the cross-flow diffusion. The formulas for the truncation error and cross-flow diffusion constants derived in this chapter reveal that they are approximately of the same order of magnitude. It will be shown that the truncation error diffusion in the direction normal to the flow cancels out and there is only a flow direction component left. Since the gradient of Φ in the flow direction is negligible in a convection dominant problem, the total diffusion quantity of Φ due to the truncation error is not significant in comparison with that due to the cross-flow diffusion.

A steady-state, two dimensional, conservation equation with no source term is given in the following.

$$u\frac{\partial \Phi}{\partial x} + v\frac{\partial \Phi}{\partial y} = \alpha\left(\frac{\partial^2 \Phi}{\partial x^2} + \frac{\partial^2 \Phi}{\partial y^2}\right) \tag{4.32}$$

Equation 4.32 is finitely differenced using donor cell scheme for the convection term.

$$u\frac{\Phi_{ij} - \Phi_{i-1j}}{\Delta x} + v\frac{\Phi_{ij} - \Phi_{ij-1}}{\Delta y} = \alpha\left(\frac{\Phi_{i+1j} - 2\Phi_{ij} + \Phi_{i-1j}}{\Delta x^2} + \frac{\Phi_{ij+1} - 2\Phi_{ij} + \Phi_{ij-1}}{\Delta y^2}\right) \tag{4.33}$$

The approach in section 4.1.2 is applied to Eq. 4.33, then the truncation error of the convection term is given as follows.

$$-u\frac{\Phi_{ij}-\Phi_{i-1j}}{\Delta x} - v\frac{\Phi_{ij}-\Phi_{ij-1}}{\Delta y} + \frac{1}{\Delta x\Delta y}\int_{y_{j-\frac{1}{2}}}^{y_{j+\frac{1}{2}}}\int_{x_{i-\frac{1}{2}}}^{x_{i+\frac{1}{2}}}(u\frac{\partial\Phi}{\partial x})\,dxdy$$

$$+ \frac{1}{\Delta x\Delta y}\int_{y_{j-\frac{1}{2}}}^{y_{j+\frac{1}{2}}}\int_{x_{i-\frac{1}{2}}}^{x_{i+\frac{1}{2}}}(v\frac{\partial\Phi}{\partial y})\,dx\,dy$$

$$= -u(\frac{\partial\Phi}{\partial x})_{ij} - v(\frac{\partial\Phi}{\partial y})_{ij} + u(\frac{\partial\Phi}{\partial x})_{i+\frac{1}{2},j+\frac{1}{2}} + v(\frac{\partial\Phi}{\partial y})_{i+\frac{1}{2},j+\frac{1}{2}}$$

$$= \frac{\Delta x}{2}\,u(\frac{\partial^2\Phi}{\partial x^2}) + \frac{\Delta y}{2}\,u(\frac{\partial^2\Phi}{\partial x\partial y}) + \frac{\Delta x}{2}\,v(\frac{\partial^2\Phi}{\partial x\partial y}) + \frac{\Delta y}{2}\,v(\frac{\partial^2\Phi}{\partial y^2})$$

$$= \frac{1}{2}[u\Delta x\frac{\partial^2\Phi}{\partial x^2} + (u\Delta y+v\Delta x)\frac{\partial^2\Phi}{\partial x\partial y} + v\Delta y\frac{\partial^2\Phi}{\partial y^2}]$$

$$= \frac{U\Delta x}{2}[\cos\theta\frac{\partial^2\Phi}{\partial x^2} + (\cos\theta\,\tan\theta_1 + \sin\theta)\frac{\partial^2\Phi}{\partial x\partial y} + \sin\theta\,\tan\theta_1\frac{\partial^2\Phi}{\partial y^2}] \tag{4.34}$$

where

$$U = \sqrt{u^2+v^2}$$

$$\tan\theta = \Delta y/\Delta x$$

$$\tan\theta_1 = v/u$$

The coordinate (x,y) is transformed to the coordinate (ξ,η) by rotation.

$$\xi = x\cos\theta + y\sin\theta$$

$$\eta = -x\sin\theta + y\cos\theta \tag{4.35}$$

where ξ is the coordinate in the flow direction.

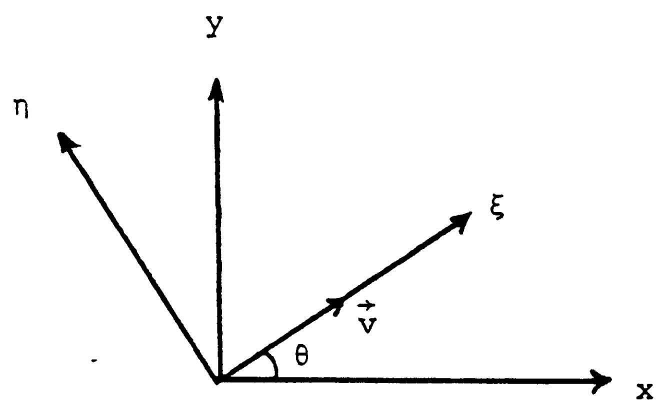

Then Eq. 4.32 is reduced to the following form.

$$U\frac{\partial\Phi}{\partial\xi} = \alpha\left(\frac{\partial^2\Phi}{\partial\xi^2} + \frac{\partial^2\Phi}{\partial\eta^2}\right) \tag{4.36}$$

where $U = \sqrt{u^2+v^2}$

Now Eq. 4.34 will be transformed to the coordinate system (ξ,η) given by Eq. 4.35.

$$(\Delta\Phi) \sim [(\sin\theta\ \tan\theta_1 + \cos\theta)\frac{\partial^2\Phi}{\partial\xi^2} + (-\sin\theta + \cos\theta\tan\theta_1)\frac{\partial^2\Phi}{\partial\xi\partial\eta}$$
$$+ (0)\frac{\partial^2\Phi}{\partial\eta^2}]\frac{U\Delta x}{2} \tag{4.37}$$

Equation 4.37 shows that the diffusion component in the η direction (normal to the flow direction) is zero and the cross differential term also vanishes when θ is equal to θ_1. Therefore, dominant truncation error diffusion occurs only in the flow direction. When θ is equal to 0 or $\pi/2$, the problem is basically one dimensional and the truncation error diffusion occurs in the flow direction as in a one dimensional problem.

4.2 Cross-flow Diffusion

Most of the confusion about the nature of numerical diffusion comes from the fact that there exists an additional source of false diffusion, that will be named here as the cross-flow diffusion. It is entirely different from the truncation error diffusion. Recently this additional false diffusion was explained by Patankar [52] and Stubley et al. [67,68] and it was clarified that this is the dominant source of the error in most multi-dimensional problems. In this section the origin of the cross-flow diffusion will be illustrated and the corresponding diffusion constant will be quantified so that they can be used in the corrective scheme of section 4.3.4.

The cross-flow diffusion comes from the multi-dimensionality of the problem, therefore it exists only in two or three dimensional problems when the flow direction is not aligned with the mesh configuration. The origin of the cross-flow diffusion is illustrated in Fig. 4.1, which shows a single mesh with pure convection. In Fig. 4.1(A), the hot and cold fluid enters the mesh from the left and bottom surfaces at 45° angle. The hot fluid will come out of the top surface and the cold fluid out of the right surface. In the donor cell scheme Fig. 4.1(A) is transformed into

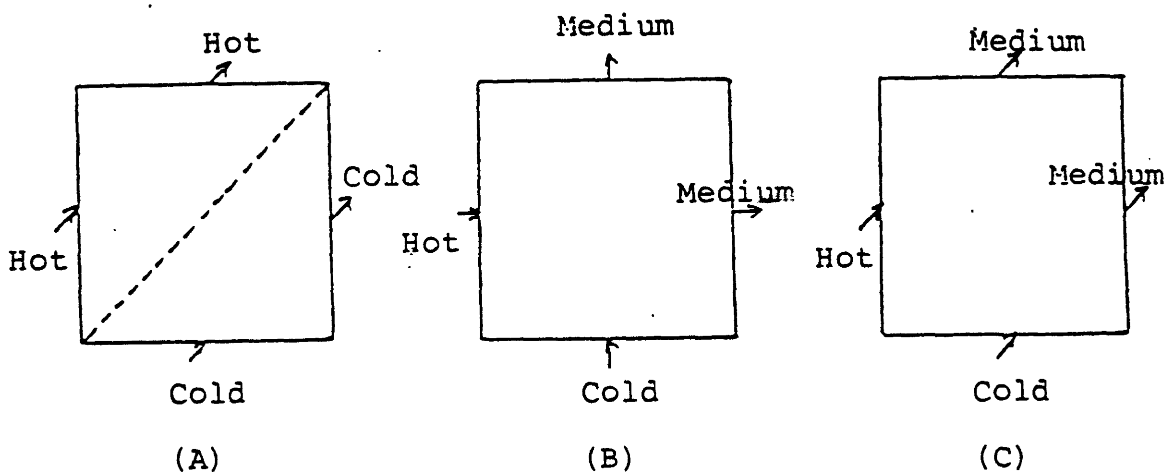

Fig. 4.1. Illustration of the cross-flow diffusion in a single mesh with pure convection

Fig. 4.1(B) where the velocity components normal to the surface are considered. Then homogeneous mixing occurs in the mesh, and intermediate temperature fluid will come out of the top and right surfaces. The numerical results in Fig. 4.1(B) are again interpreted as Fig. 4.1(C) by a program user. Therefore, an appreciable amount of false diffusion occurs in multidimensional donor cell differencing of the convection term.

Another illustration of the cross-flow diffusion is given in Fig. 4.2 which shows a row of meshes aligned in the x-direction. The value of Φ at the point A should reappear at the point X because there is no physical diffusion. In the donor cell scheme it is distributed all along the points A_1, A_2, A_3 . . . and the sum of the values at those points is exactly equal to Φ. This distribution of the value of ϕ causes the cross-flow diffusion.

$$(1-p)\Phi[1+p+p^2+ \ . \ . \ . \ ] = (1-p)\Phi\frac{1}{1-p} = \Phi$$

where

$$p = \frac{\frac{u}{\Delta x}}{\frac{u}{\Delta x} + \frac{v}{\Delta y}}$$

The effective diffusion constant for the cross-flow diffusion will be calculated in the two dimensional Cartesian coordinate in Fig. 4.3. This is a pure convection problem with no physical diffusion. Consider the fluid element CAB which looks like a long one-dimensional rod. The fluid

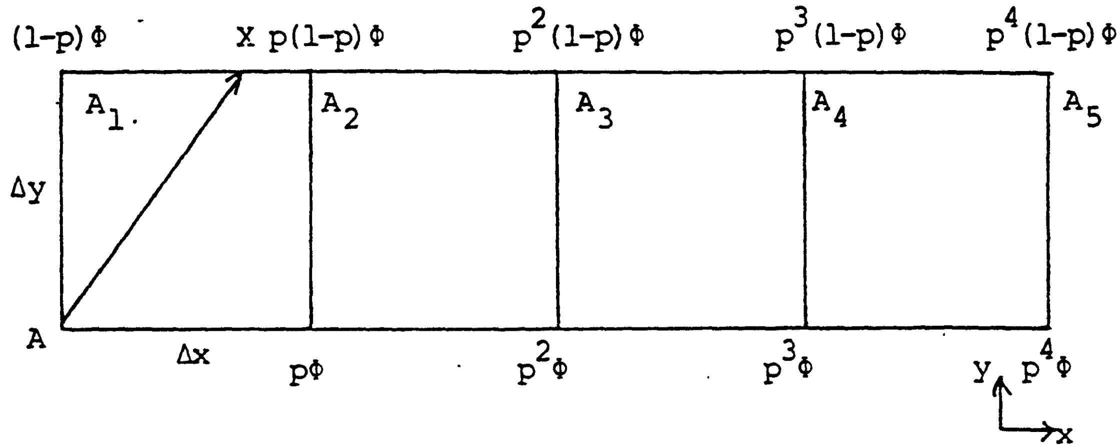

$$\text{where} \quad p = \frac{\frac{u}{\Delta x}}{\frac{u}{\Delta x} + \frac{v}{\Delta y}}$$

Fig. 4.2. Illustration of the cross-flow diffusion in a row of meshes aligned in the x-direction with pure convection

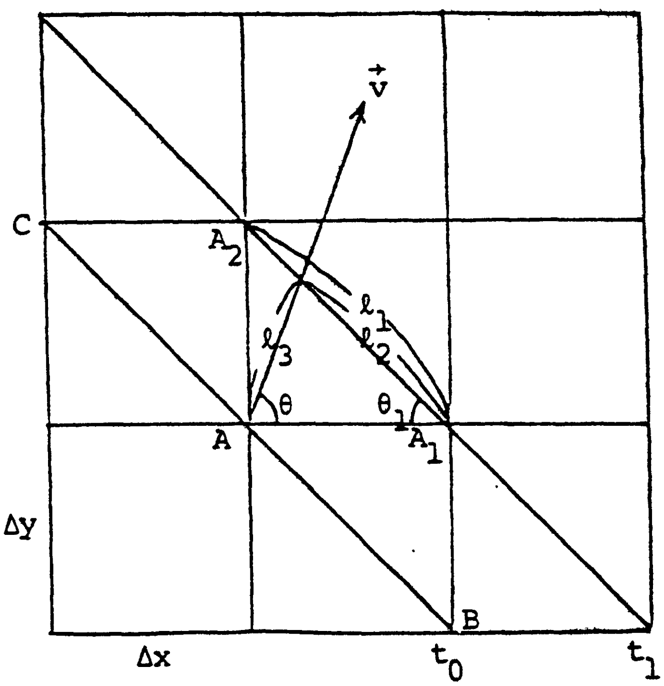

where $t_1 - t_0 = \Delta t = \ell_3/U$

$\tan\theta_1 = \Delta y/\Delta x$

$\tan\theta = v/u$

$$p = \frac{u/\Delta x}{\frac{u}{\Delta x} + \frac{v}{\Delta y}}$$

Fig. 4.3. Geometry for explanation of the cross-flow diffusion in a two dimensional Cartesian coordinate

element was on the line CAB at time t_0 and is translated in the velocity direction, $\vec{v}$.

The value Φ_A at the point A should reappear at the Point A'. In the donor cell scheme it is divided into two portions, $p\Phi_A$ and $(1-p)\Phi_A$ and appears at the points A_1 and A_2. The travel of the fluid element is analyzed in Fig. 4.4, which shows that the value Φ_A diffuses out along the fluid element. The diffusion occurs both to the right and left hand sides. The diffusion to the right hand side is considered first in the following.

$$\begin{pmatrix}\text{Gradient}\\ \text{of } \Phi\end{pmatrix} = \Phi_A/\ell_1$$

$$\begin{pmatrix}\text{Current}\\ \text{of } \Phi\end{pmatrix} = p\Phi_A \frac{\ell_2}{t_1 - t_0} = p\Phi_A \frac{\ell_2 U}{\ell_3}$$

Therefore,

$$\begin{pmatrix}\text{Diffusion}\\ \text{constant}\end{pmatrix} = \frac{(\text{Current})}{(\text{Gradient})} = pU\frac{\ell_2\ell_1}{\ell_3}$$

where

$$\ell_1 = \Delta x/\cos\theta_1$$

$$\ell_2 = \Delta x \sin\theta/\sin(\theta_1+\theta)$$

$$\ell_3 = \Delta x \sin\theta_1/\sin(\theta_1+\theta)$$

After substituting appropriate expression for each term, the following right hand side diffusion constant results.

$$D_{RHS} = U\Delta x \frac{\sin\theta \cos\theta}{\cos\theta_1 \sin(\theta+\theta_1)}$$

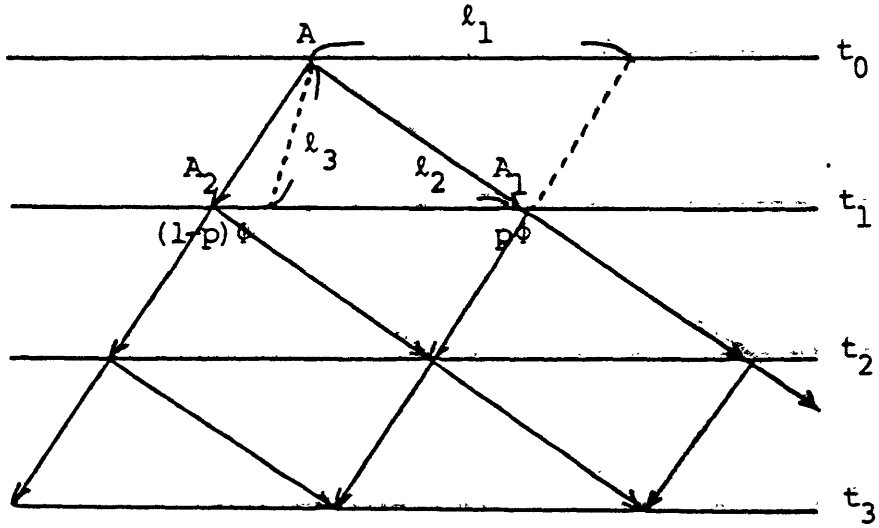

Fig. 4.4. Geometry for explanation of the cross-flow diffusion in a rotated two dimensional Cartesian coordinate

Repeating the same procedure for the left hand side we can find that the right and left hand side diffusion constants are equal to the following.

$$D_{RHS} = D_{LHS} = U\Delta x \frac{\sin\theta \cos\theta}{\cos\theta_1 \sin(\theta+\theta_1)} \qquad (4.38)$$

Equation 4.38 is the effective diffusion constant when the diffusion is confined to the one dimensional fluid element. There are two diffusion components in a two dimensional problem as follows.

$$\nabla^2 \Phi = \frac{\partial^2 \Phi}{\partial x^2} + \frac{\partial^2 \Phi}{\partial y^2}$$

The current on the one dimensional fluid element can be factored into the x and y components. The cross-flow diffusion constants are the ratios of the current and gradient of Φ in the x and y directions.

$$D_x = U\Delta x \frac{\sin\theta \cos\theta}{\sin(\theta+\theta_1)} \cos\theta_1$$

$$D_y = U\Delta x \frac{\sin\theta \cos\theta}{\sin(\theta+\theta_1)} \frac{\sin^2\theta_1}{\cos\theta_1} \qquad (4.39)$$

Equation 4.39 is identical to the following simple expressions.

$$D_x = u\Delta x(1-p)$$

$$D_y = v\Delta y\ p \qquad (4.40)$$

where

$$p = \frac{\frac{u}{\Delta x}}{\frac{u}{\Delta x} + \frac{v}{\Delta y}}$$

Equation 4.38 should be differentiated with respect to θ in order to find out the velocity direction with maximum cross-flow diffusion. It can be shown that,

$$\frac{D_{RHS}}{\partial\theta} = 0 \quad \text{when } \tan^3\theta = \tan\theta_1 \ . \tag{4.41}$$

Equation 4.41 shows that D_{RHS} (or D_{LHS}) is maximum at an angle of θ between $\pi/4$ and θ_1, that is to say, $\pi/4 \le \theta \le \theta_1$ or $\theta_1 \le \theta \le \pi/4$. De Vahl Davis and Mallinson [24] also derived the effective cross-flow diffusion constant and their result is given in Eq. 4.42.

$$D_{DM} = \frac{U\Delta x\Delta y \sin 2\theta}{4(\Delta y \sin^3\theta + \Delta x \cos^3\theta)} = U\Delta x \frac{\tan\theta_1 \sin 2\theta}{4(\tan\theta_1 \sin^3\theta + \cos^3\theta)} \tag{4.42}$$

Equation 4.42 underestimates the cross-flow diffusion as shown in Fig. 4.5. When both θ and θ_1 are equal to $\pi/4$, Eq. 4.40 and Eq. 4.42 give the same result.

Now the analysis will be extended to a three dimensional case in Fig. 4.6. In Fig. 4.6 the value at the point O is Φ and that value should reappear at the point X where the velocity vector meets the plane ABC. In the donor cell scheme the value Φ is divided into three portions $p_x\Phi$, $p_y\Phi$,

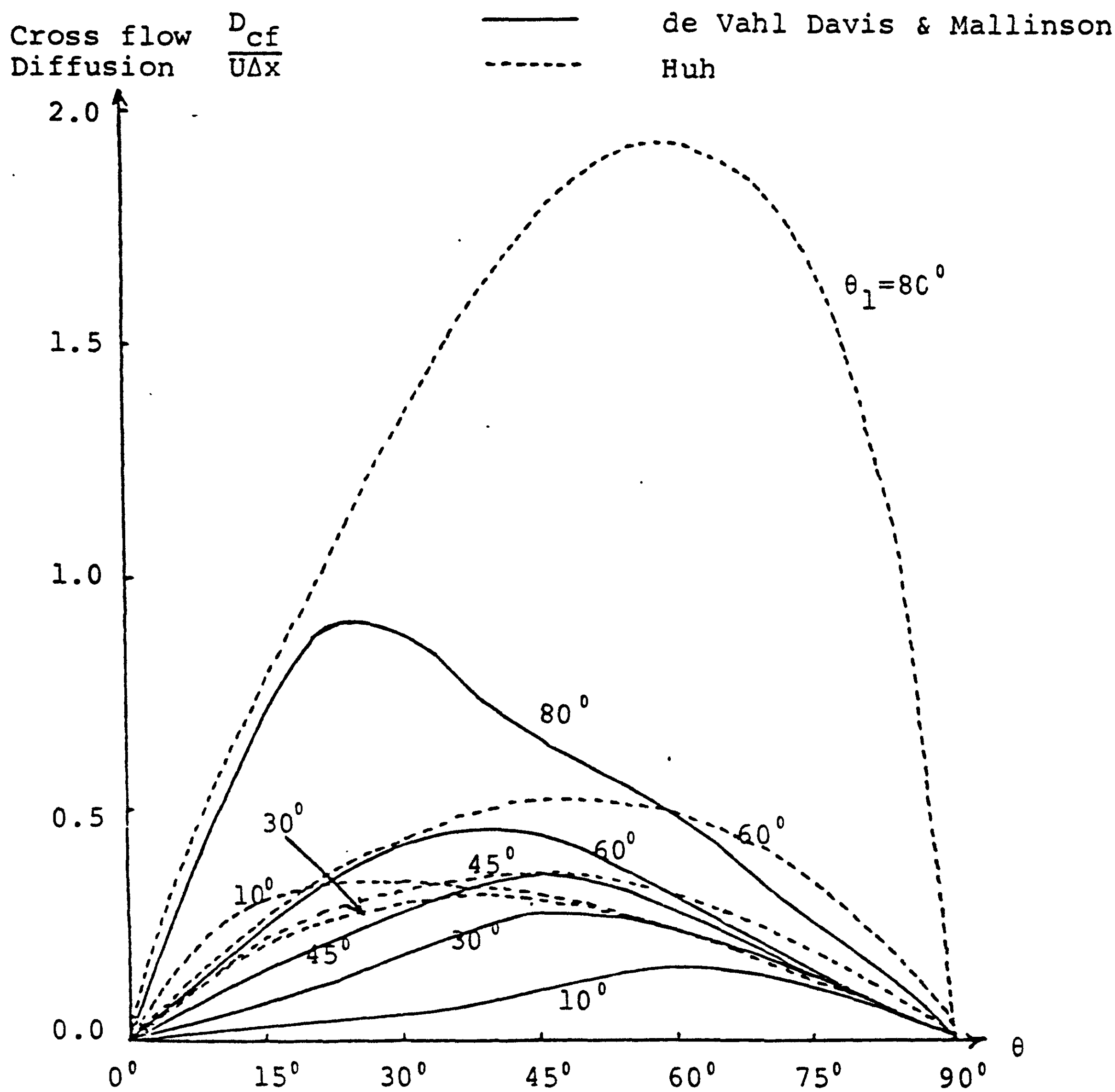

Fig. 4.5. Comparison of the prediction formulas for cross-flow diffusion constant by De Vahl Davis and Mallinson and Huh

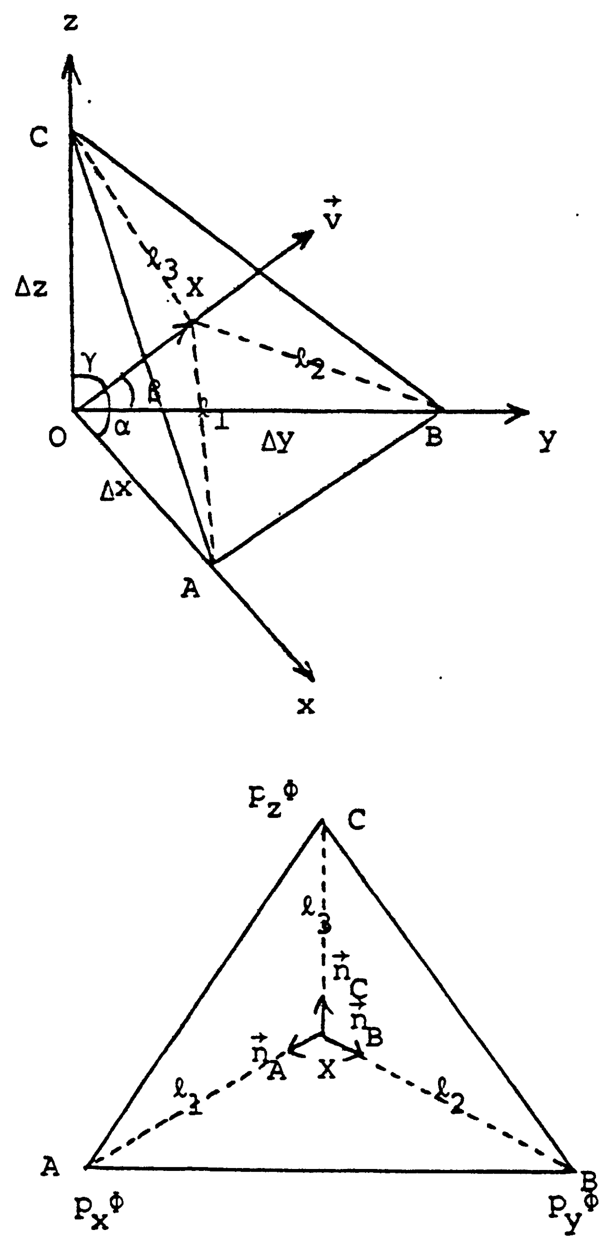

Fig. 4.6. Geometry for explanation of the cross-flow diffusion in a three dimensional Cartesian coordinate

$p_z\Phi$ occurring at the points A, B, and C instead of at the point X. This is the so-called cross-flow diffusion phenomenon. The currents due to the cross-flow diffusion are along the directions $\vec{XA}$, $\vec{XB}$, $\vec{XC}$, and $\vec{n}_A$, $\vec{n}_B$, $\vec{n}_C$ denote unit vectors along those directions. The coordinate of the point X is given as follows.

$$X(\ell_4\cos\alpha,\ \ell_4\cos\beta,\ \ell_4\cos\gamma)$$

Any point on the plane ABC should satisfy the following Eq. 4.43.

$$\frac{x}{\Delta x} + \frac{y}{\Delta y} + \frac{z}{\Delta z} = 1 \quad : \text{ plane ABC} \tag{4.43}$$

Since the point X is on the plane ABC, the following relation holds.

$$\ell_4\left(\frac{\cos\alpha}{\Delta x} + \frac{\cos\beta}{\Delta y} + \frac{\cos\gamma}{\Delta z}\right) = 1 \tag{4.44}$$

Therefore,

$$\ell_4 = \frac{1}{\dfrac{\cos\alpha}{\Delta x} + \dfrac{\cos\beta}{\Delta y} + \dfrac{\cos\gamma}{\Delta z}} \tag{4.45}$$

The lengths of AX, BX, CX which are denoted as ℓ_1, ℓ_2, ℓ_3 can be obtained as follows.

$$\ell_1 = AX = \sqrt{(\Delta x-\ell_4\cos\alpha)^2 + (\ell_4\cos\beta)^2 + (\ell_4\cos\gamma)^2}$$

$$= \sqrt{\Delta x^2 + \ell_4^2 - 2\Delta x\ell_4\cos\alpha}$$

$$\ell_2 = BX = \sqrt{(\ell_4\cos\alpha)^2 + (\Delta y-\ell_4\cos\beta)^2 + (\ell_4\cos\gamma)^2}$$

$$= \sqrt{\Delta y^2 + \ell_4^2 - 2\Delta y\ell_4\cos\beta}$$

$$\ell_3 = CX = \sqrt{(\ell_4\cos\alpha)^2 + (\ell_4\cos\beta)^2 + (\Delta z-\ell_4\cos\gamma)^2}$$

$$= \sqrt{\Delta z^2 + \ell_4^2 - 2\Delta z\ell_4\cos\gamma} \tag{4.46}$$

The unit vectors $\vec{n}_A$, $\vec{n}_B$, $\vec{n}_C$ can be obtained in terms of their components in x, y, z directions.

$$\vec{n}_A = \frac{\vec{XA}}{|\vec{XA}|} = \frac{\vec{OA} - \vec{OX}}{\ell_1} \tag{4.47}$$

etc.

Therefore,

$$\vec{n}_A = \frac{1}{\ell_1}[(\Delta x-\ell_4\cos\alpha), -\ell_4\cos\beta, -\ell_4\cos\gamma]$$

$$\vec{n}_B = \frac{1}{\ell_2}[-\ell_4\cos\alpha, (\Delta y-\ell_4\cos\beta), -\ell_4\cos\gamma]$$

$$\vec{n}_C = \frac{1}{\ell_3}[-\ell_4\cos\alpha, -\ell_4\cos\beta, (\Delta z-\ell_4\cos\gamma)] \tag{4.48}$$

The currents in the directions $\vec{n}_A$, $\vec{n}_B$, $\vec{n}_C$ can simply be given as the products of the transported quantities and velocities.

$$|(\text{Current})_{XA}| = p_x\Phi \frac{\ell_1}{\Delta t}$$

$$\left|(\text{Current})_{XB}\right| = p_y \Phi \frac{\ell_2}{\Delta t}$$

$$\left|(\text{Current})_{XC}\right| = p_z \Phi \frac{\ell_3}{\Delta t} \tag{4.49}$$

where

$$\Delta t = \ell_4/U$$

The gradients of Φ in the x, y, z directions are given as follows.

$$(\text{Grad})_x = \Phi/\Delta x$$

$$(\text{Grad})_y = \Phi/\Delta y$$

$$(\text{Grad})_z = \Phi/\Delta z \tag{4.50}$$

Now the x direction cross-flow diffusion constant may be given as the ratio of the current to the gradient of Φ in the x direction.

$$(\text{Current})_x = \frac{p_x \Phi}{\Delta t}(\Delta x - \ell_4 \cos\alpha) + \frac{p_y \Phi}{\Delta t}(-\ell_4 \cos\alpha) + \frac{p_z \Phi}{\Delta t}(-\ell_4 \cos\alpha)$$

$$(\text{Grad})_x = \Phi/\Delta x \tag{4.51}$$

Therefore,

$$D_x = \frac{p_x \Delta x}{\Delta t}(\Delta x - \ell_4 \cos\alpha) + \frac{p_y \Delta x}{\Delta t}(-\ell_4 \cos\alpha) + \frac{p_z \Delta x}{\Delta t}(-\ell_4 \cos\alpha)$$

$$D_x = \frac{p_x \Delta x^2}{\Delta t} - \frac{\Delta x}{\Delta t} \ell_4 \cos\alpha (p_x + p_y + p_z)$$

$$= \frac{p_x \Delta x^2}{\Delta t} - \frac{\Delta x}{\Delta t} \ell_4 \cos\alpha \qquad (4.52)$$

Inserting the expression for Δt given by $\Delta t = \ell_4/U$, we can simplify the result as follows.

$$D_x = u\Delta x [\frac{p_x \Delta x}{\ell_4 \cos\alpha} - 1]$$

$$= u\Delta x (1 - p_x) \qquad (4.53)$$

The cross-flow diffusion constants in the y and z directions can be obtained in the same way. The rotation of indices will also give the same result.

$$D_y = v\Delta y (1 - p_y)$$

$$D_z = w\Delta z (1 - p_z) \qquad (4.54)$$

4.3 Discussion of Skew Differencing and Corrective Schemes

The origins of the numerical diffusion and their effective diffusion constants have been given in the previous sections. This section is a review of the schemes that have been used to eliminate the numerical diffusion. The most important ones may be the skew differencing, tensor viscosity method, finite element method, etc. although none of them has been successful enough to be accepted widely.

Most of the schemes in Table 4.1 can be categorized into two types, skew differencing and corrective schemes. S. Chang's method [16] and Raithby's scheme [53] are of a skew differencing type while the tensor viscosity method [25] and Huh's corrective scheme that will be introduced in section 4.3.4 fall in the category of a corrective scheme. In the skew differencing type schemes finite differencing of the convection term is done not in terms of the x and y directions, but directly along the velocity direction. Since the upstream point in the velocity direction does not necessarily fall on the mesh point where the quantity under consideration is defined, the interpolation should be done between neighboring points to obtain the value at the upstream point. The donor cell treatment of the convection term results in a 5-point relationship in a two dimensional problem. In the skew differencing scheme the 5-point relationship becomes a 9-point relationship. Basically the inclusion of four additional corner points contributes to more accurate numerical modelling of the convection. However, the interpolation between neighboring points may still give some cross-flow diffusion. The cross-flow diffusion is not eliminated entirely in the skew differencing scheme, but just appreciably lower than that of the donor cell scheme.

The corrective scheme is to reduce the diffusion constants in order to compensate for the additional false

Classification	Contributor/method	Standard mesh?	Best mesh
Centered finite difference	Lillington	Yes	21 x 11
	Orlandi	–	40 x 40
Galerkin finite elements	Cliffe	–	65 x 33
	Donea et al.	–	41 x 21
	Grandotto	Yes	21 x 11
	Hickmott et al.	Yes	41 x 21
First-order upwind finite difference	Elbahar et al./PATANKAR	Pe = 10^6 only	41 x 21
	Lillington	Yes	21 x 11
	Orlandi	–	40 x 40
	Priddin	Yes	100 x 50
	Wada et al.	–	81 x 41
	Wilkes	–	100 x 50
Higher order upwind finite difference	Elbahar et al./QUICK	Yes	41 x 21
	Elbahar et al./LLUE	Pe = 10^6 only	41 x 21
	Hulme/QUICK	–	38 x 19
	Wilkes/LUE	–	80 x 40
Vector upwind difference	Lillington/SUD	Yes	21 x 11
	Lillington/VUD	Yes	21 x 11
	Lillington/VUDCC	Yes	21 x 11
Upwind finite element	Narusawa	Yes	21 x 11
Method of characteristics	Esposito	–	41 x 21
	Glass and Rodi	Yes	41 x 21
	Huffenus and Khalitzky	Yes	21 x 11
Finite analytic method	Chen	–	81 x 41
Tensor viscosity method	Ruel et al.	–	28 x 14
Self-adaptive method	Schonauer	–	See Table 2
Mesh transformation method	Sykes	–	21 x 11
Lax-Wendroff	Wada et al.	–	80 x 40[a]

Table 4.1. List of the schemes for numerical representation of advection presented at the Third Meeting of the International Association for Hydraulic Research, 1981 [65]

diffusion. The corrective scheme is valid only if the effective numerical diffusion constant can be predicted accurately. Since the cross-flow diffusion is dominant over the truncation error diffusion and the effective diffusion constants for the cross-flow diffusion can be predicted theoretically, the corrective scheme can give a numerical solution which is almost free from numerical diffusion. The tensor viscosity method is one example of the corrective scheme, although the validity of its correction formula is not clear. The correction formula used here is Eq. 4.53 and Eq. 4.54. The diffusion constants in x, y and z directions will be reduced by the amounts of D_x, D_y and D_z in Eq. 4.53 and Eq. 4.54.

4.3.1 Raithby's Scheme

Raithby's scheme [53] is an Eulerian type of approach, where the balance equation is set up for a given control volume by considering convection and diffusion at the control surface. It is therefore a conservative scheme. The finite difference equation for Raithby's scheme is derived on the assumption of a linear profile of Φ normal to the flow and a uniform profile in the flow direction.

$$\Phi = C_1 + C_2 n = C_1 + C_2 (y\frac{u}{U} - x\frac{v}{U}) \tag{4.55}$$

where n is the distance normal to the flow and $U = \sqrt{u^2+v^2}$.

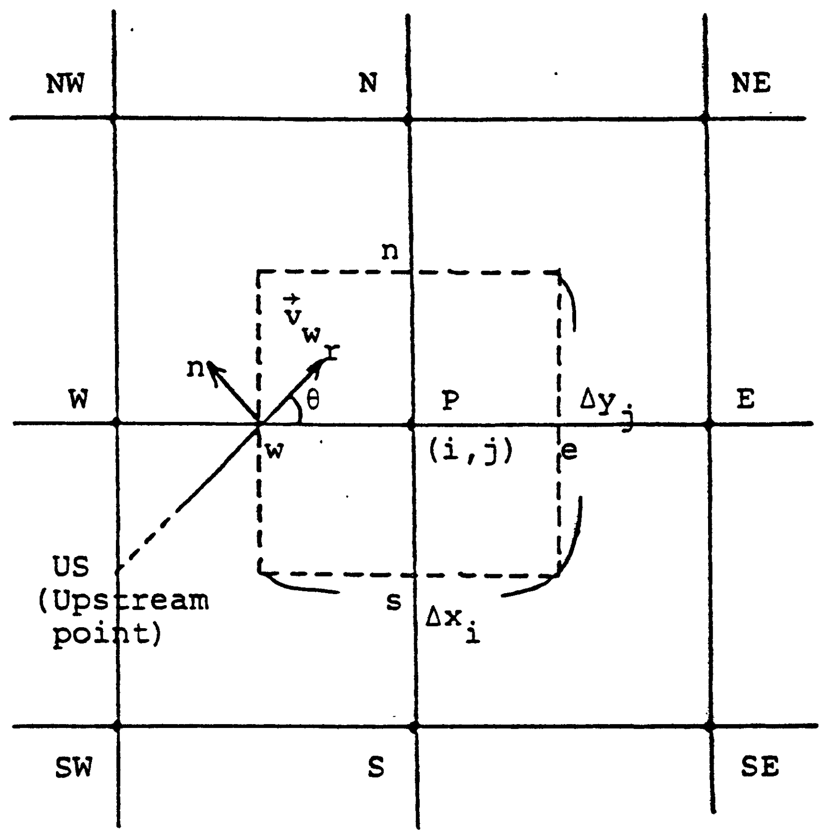

Fig. 4.7. A segment of the calculation domain showing grid lines, control volume and notations in Raithby's scheme

The convection quantity at the control surface is calculated from the upstream value in the flow direction and the upstream value is obtained by interpolating two neighboring points. This should be repeated for the four control surfaces of every mesh in a two dimensional problem, which may be too complicated and time consuming for a practical purpose. The inclusion of the four additional points also complicates the structure of the coefficient matrix in an implicit scheme.

4.3.2 Skew Differencing By Huh

Skew differencing scheme here treats the convection term in a Lagrangian way. The convection term is differenced in the velocity direction between mesh points, not in terms of the convection that occurs at mesh interfaces. Although this scheme is nonconservative, it is much simpler than Raithby's scheme and becomes conservative in a unidirectional flow.

$$u\frac{\partial \Phi}{\partial x} + v\frac{\partial \Phi}{\partial y} = U\frac{\partial \Phi}{\partial \xi} \tag{4.56}$$

where ξ is the coordinate in the velocity direction and $U = \sqrt{u^2+v^2}$.

$$\frac{\partial \Phi}{\partial \xi} = \frac{\Phi_{ij} - \Phi_{US}}{\ell} \tag{4.57}$$

where the upstream value Φ_{US} may be calculated by interpolating two neighboring points. Some of the results of this skew differencing scheme is given in section 5.3.2.

4.3.3 Tensor Viscosity Method

The tensor viscosity method treats the numerical diffusion constant as a tensor quantity. The expression for the tensor viscosity [25] is given in the following.

$$T = \tfrac{1}{2}\Delta t\ \vec{u}\vec{u}$$

$$= \tfrac{1}{2}\Delta t\begin{pmatrix} u^2 & uv \\ uv & v^2 \end{pmatrix} \qquad (4.58)$$

Eq. 4.58 for the numerical diffusion constant is apparently not consistent with the results in Eq. 4.53 and Eq. 4.54.

4.3.4 Corrective Scheme By Huh

The corrective scheme is to use the reduced diffusion constants, $D-D_x$, $D-D_y$, $D-D_z$ in x, y, z directions to compensate for the cross-flow diffusion effect. The validity of this scheme is based on the fact that the cross-flow diffusion can be predicted accurately. The expressions for the cross-flow diffusion constants D_x, D_y, D_z are derived in section 4.2.

$$D_x = u\Delta x(1-p_x)$$

$$D_y = v\Delta y(1-p_y)$$

$$D_z = w\Delta z(1-p_z) \tag{4.59}$$

where

$$p_x = \frac{\frac{u}{\Delta x}}{\frac{u}{\Delta x} + \frac{v}{\Delta y} + \frac{w}{\Delta z}} \quad \text{etc.}$$

Two implementation strategies have been tested so far, the mesh point implementation and mesh interface implementation. These two become identical when the flow field is uniform or a very fine mesh is used so that the flow change over neighboring meshes is negligible. In a coarse mesh or recirculating flow field the latter implementation strategy is definitely preferred.

4.3.4.1 Mesh Point Implementation

The mesh point implementation is to assign the cross-flow diffusion constants D_x, D_y, D_z at the center of a mesh where all quantities are defined except the flow field. The velocities at two boundary faces are averaged to get the representative velocity, which is used with the cell dimensions to get the cross-flow diffusion constants.

After the cross-flow diffusion constants are assigned to every mesh point, they should be averaged again between neighboring mesh points to calculate the cross-flow diffusion current at mesh interfaces.

4.3.4.2 Mesh Interface Implementation

The mesh interface implementation is to assign the cross-flow diffusion constants directly to the mesh interfaces where the cross-flow diffusion current should be calculated. The mesh interface implementation is always recommended although it has a more complex program logic than the mesh point implementation.

There are three possible cases that should be treated independently in a two dimensional case, as shown in Fig. 4.8. Note that the cross-flow diffusion constant for the interface with an inward velocity does not have to be considered in that mesh because it will be considered in the neighboring mesh. For the first two cases the cross-flow diffusion constants are zero because the velocity vector is aligned with the mesh configuration. For the second case the two outward velocities, U and V, can be directly used with cell dimensions in Eq. 4.59, and the resulting D_x and D_y will be assigned to each interface. The third case is expected to have a flow split as shown in the figure. The velocity U is split into two components, U1 and U2, so that they are proportional to V1 and V2. The two velocity sets (U1,V1) and (U2,V2) are used to give (D_{x1},D_{y1}) and (D_{x2},D_{y2}). The right interface will have the cross-flow diffusion constant $(D_{x1}+D_{x2})$ and the top and bottom interfaces, D_{y1} and D_{y2}. The same logic can easily be extended to a three dimensional case. Appendix C includes

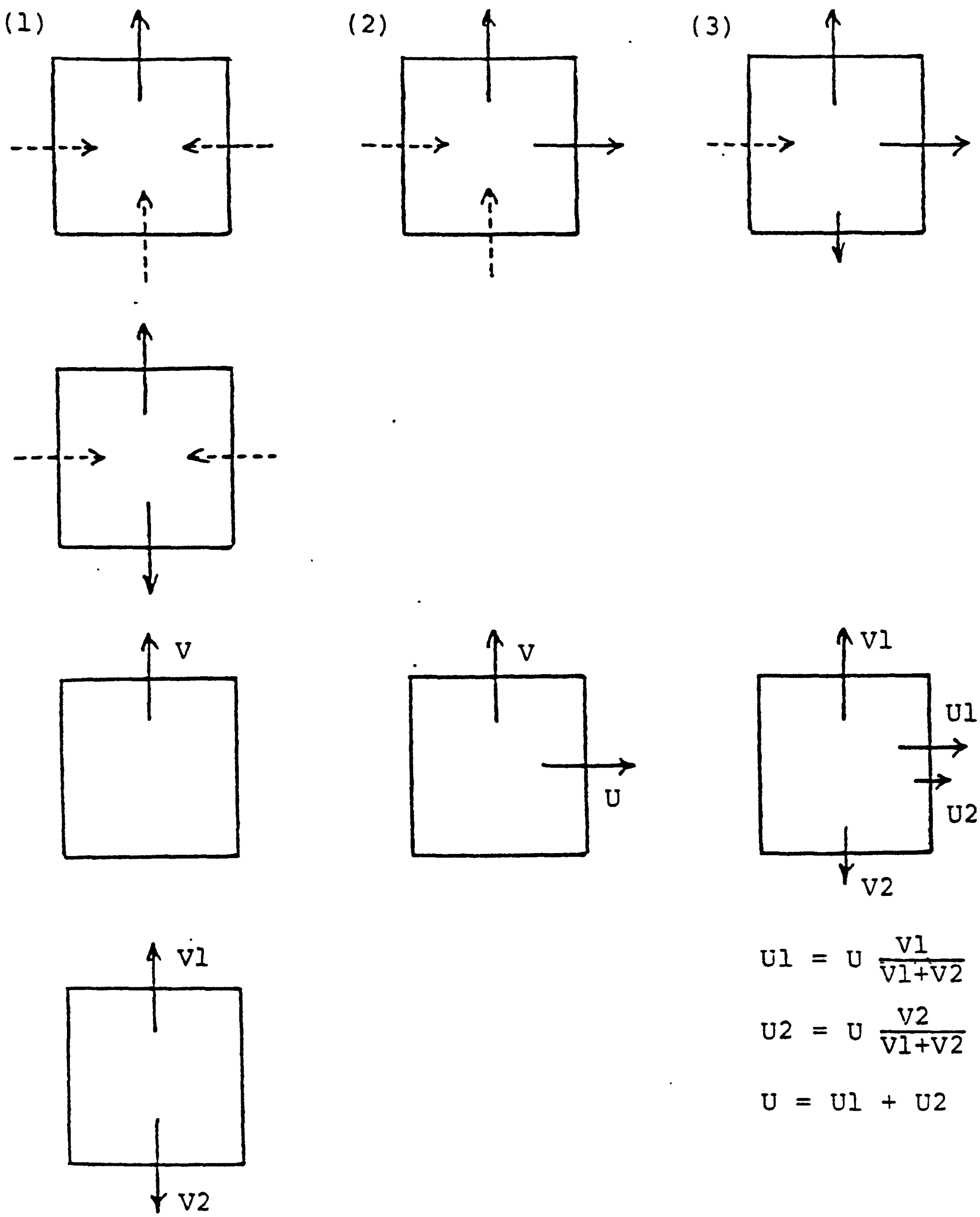

$$U1 = U \frac{V1}{V1+V2}$$

$$U2 = U \frac{V2}{V1+V2}$$

$$U = U1 + U2$$

Fig. 4.8. Three possible flow configurations for mesh interface implementation of the corrective scheme in a two dimensional problem

the fortran program for calculating cross-flow diffusion constants in an arbitrary flow field.

4.4 Comparison of Explicit, Implicit and ADI Schemes

There are three typical solution schemes, Explicit, Implicit and ADI (Alternate Direction Implicit), for the general conservation equation, Eq. 4.60, which is a parabolic partial differential equation. The pros and cons of the three schemes will be compared in the following four viewpoints.

1. conservation
2. physical constraint
3. accuracy
4. stability

$$\frac{\partial \Phi}{\partial t} + u\frac{\partial \Phi}{\partial x} + v\frac{\partial \Phi}{\partial y} + w\frac{\partial \Phi}{\partial z} = D\left(\frac{\partial^2 \Phi}{\partial x^2} + \frac{\partial^2 \Phi}{\partial y^2} + \frac{\partial^2 \Phi}{\partial z^2}\right) + S \tag{4.60}$$

Explicit (1-D):

$$\frac{\Phi_i^{n+1} - \Phi_i^n}{\Delta t} + \frac{u}{\Delta x}(\Phi_i^n - \Phi_{i-1}^n) = \frac{D}{\Delta x^2}(\Phi_{i+1}^n - 2\Phi_i^n + \Phi_{i-1}^n) + S \tag{4.61}$$

Implicit (1-D):

$$\frac{\Phi_i^{n+1} - \Phi_i^n}{\Delta t} + \frac{u}{\Delta x}(\Phi_i^{n+1} - \Phi_{i-1}^{n+1}) = \frac{D}{\Delta x^2}(\Phi_{i+1}^{n+1} - 2\Phi_i^{n+1} + \Phi_{i-1}^{n+1}) + S \tag{4.62}$$

ADI (2-D): (A)

$$\frac{\phi_{ij}^{n+\frac{1}{2}} - \phi_{ij}^{n}}{\frac{\Delta t}{2}} + u\frac{\phi_{ij}^{n+\frac{1}{2}} - \phi_{i-1j}^{n+\frac{1}{2}}}{\Delta x} + v\frac{\phi_{ij}^{n} - \phi_{ij-1}^{n}}{\Delta y}$$

$$= D\frac{\phi_{i+1j}^{n+\frac{1}{2}} - 2\phi_{ij}^{n+\frac{1}{2}} + \phi_{i-1j}^{n+\frac{1}{2}}}{\Delta x^2} + D\frac{\phi_{ij+1}^{n} - 2\phi_{ij}^{n} + \phi_{ij-1}^{n}}{\Delta y^2} + S$$

$$\frac{\phi_{ij}^{n+1} - \phi_{ij}^{n+\frac{1}{2}}}{\frac{\Delta t}{2}} + u\frac{\phi_{ij}^{n+\frac{1}{2}} - \phi_{i-1j}^{n+\frac{1}{2}}}{\Delta x} + v\frac{\phi_{ij}^{n+1} - \phi_{ij-1}^{n+1}}{\Delta y}$$

$$= D\frac{\phi_{i+1j}^{n+\frac{1}{2}} - 2\phi_{ij}^{n+\frac{1}{2}} + \phi_{i-1j}^{n+\frac{1}{2}}}{\Delta x^2} + D\frac{\phi_{ij+1}^{n+1} - 2\phi_{ij}^{n+1} + \phi_{ij-1}^{n+1}}{\Delta y^2} + S$$

ADI (2-D): (B)

$$\frac{\phi_{ij}^{*} - \phi_{ij}^{n}}{\Delta t} + u\frac{\phi_{ij}^{*} - \phi_{i-1j}^{*}}{\Delta x} = D\frac{\phi_{i+1j}^{*} - 2\phi_{ij}^{*} + \phi_{i-1j}^{*}}{\Delta x^2} + S$$

$$\frac{\phi_{ij}^{n+1} - \phi_{ij}^{*}}{\Delta t} + v\frac{\phi_{ij}^{n+1} - \phi_{ij-1}^{n+1}}{\Delta y} = \frac{\phi_{ij+1}^{n+1} - 2\phi_{ij}^{n+1} + \phi_{ij-1}^{n+1}}{\Delta y^2} + S \tag{4.63}$$

4.4.1 Conservation

The conservation principle is that the total amount of ϕ should be conserved ($S=0$), or affected only by the source term contribution ($S\neq0$), when the net inflow or outflow at the domain boundary is equal to zero. A scheme may be both stable and nonconservative and also both unstable and conservative because the conservative property is independent of the stability. When we are concerned with a steady state solution, the conservative property may not be crucial. For a long time transient, however, the conservative property is as important as the stability because the error from nonconservation may accumulate over many time steps. All the explicit, implicit and ADI schemes can be made conservative by using appropriate differencing forms for the convection term. In order to guarantee conservation, the same exchange term should be used for neighboring meshes. Although a conservative form is preferred to a nonconservative one, there are some nonconservative solution schemes like ICE (Implicit Continuous Eulerian), where the convection terms of momentum equations are linearized in a nonconservative way.

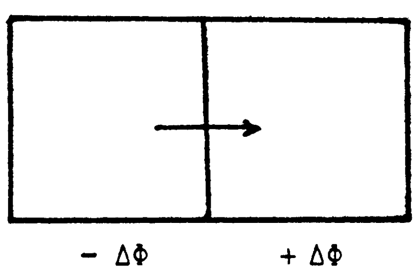

4.4.2 Physical Constraint

The physical constraint is closely related with the stability in a practical sense. Although they usually give similar constraints on the time step size and mesh spacing, they are from entirely different origins. The laws of physics impose some restrictions on the numerical scheme to get physically reasonable solutions. The Courant condition and Hirt's stability condition [36] that the finite domain of influence should at least include the continuum domain of influence are good examples of the physical constraint condition.

4.4.2.1 <u>Diffusion</u>

There is a maximum net flow that can occur between neighboring meshes by diffusion.

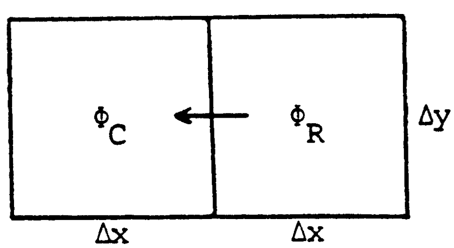

$$\Phi_R \geq \Phi_C$$

$$\left(\begin{array}{l}\text{Exchanged quantity of } \Phi \\ \text{by diffusion for time } \Delta t\end{array}\right) = D\frac{\Phi_R - \Phi_C}{\Delta x}\Delta y \ \Delta t$$

After the exchange of the diffusion current, new values of Φ are given as follows.

$$\Phi_C' \ \Delta x\Delta y = \Phi_C\Delta x\Delta y + D\frac{\Phi_R - \Phi_C}{\Delta x}\Delta y \ \Delta t$$

$$\Phi_R'\Delta x\Delta y = \Phi_R\Delta x\Delta y - D\frac{\Phi_R - \Phi_C}{\Delta x}\Delta y \ \Delta t$$

Since the relationship, $\Phi_R' \geq \Phi_C'$, should still hold, we have the following physical constraint.

$$\Delta x \Delta y(\Phi_R - \Phi_C) \geq 2D\frac{(\Phi_R - \Phi_C)}{\Delta x}\Delta y \Delta t$$

$$\frac{2D}{\Delta x^2}\Delta t \leq 1 \qquad (4.64)$$

Eq. 4.64 may be extended to a d-dimensional case as follows.

$$d\ \frac{2D}{\Delta x^2}\Delta t \leq 1 \qquad (4.65)$$

Equation 4.65 may be a too conservative criterion in a real problem. When the physical constraint is ignored and the time step size greater than that given by Eq. 4.64 or 4.65 is used, the solution will be unstable or stable with damping oscillations. Both of the oscillation and instability should be avoided in a transient problem. The ADI scheme given in Eq. 4.63 is unconditionally stable; however, there will be a damping oscillation in the solution when the time step size is greater than that given by Eq. 4.64 or 4.65. Therefore the physical constraint should be respected in addition to the stability condition to get a meaningful transient solution.

4.4.2.2 Convection

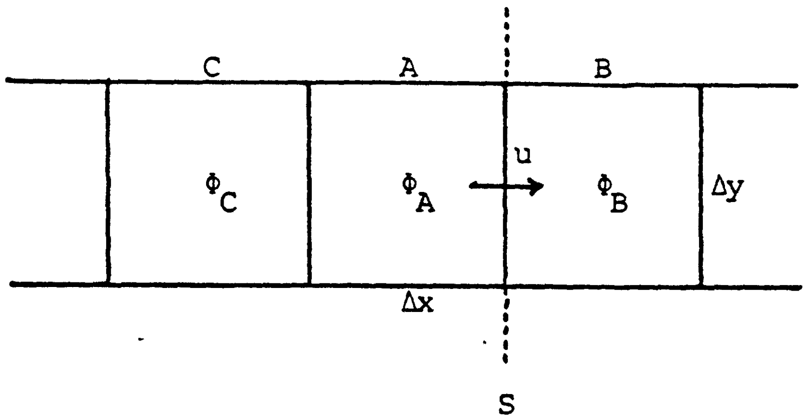

The explicit and donor cell treatment of the convection term gives the convection quantity at interface S as $u\phi_A\Delta t\Delta y$. It is based on the assumption that ϕ_A is the representative value of the control volume A. If Δt is greater than the Courant limit, a portion of the control volume C will cross the interface S. Then $u\phi_A\Delta t\Delta y$ is no more an appropriate expression for the convection quantity during Δt. Therefore,

$$\Delta t \leq \frac{\Delta x}{u} \tag{4.66}$$

When a time step size greater than the Courant limit is used, the damping oscillation or instability may occur as in the case of diffusion.

4.4.3 Accuracy

Realistic interpretation of a finite difference equation comes from an integral form of the conservation

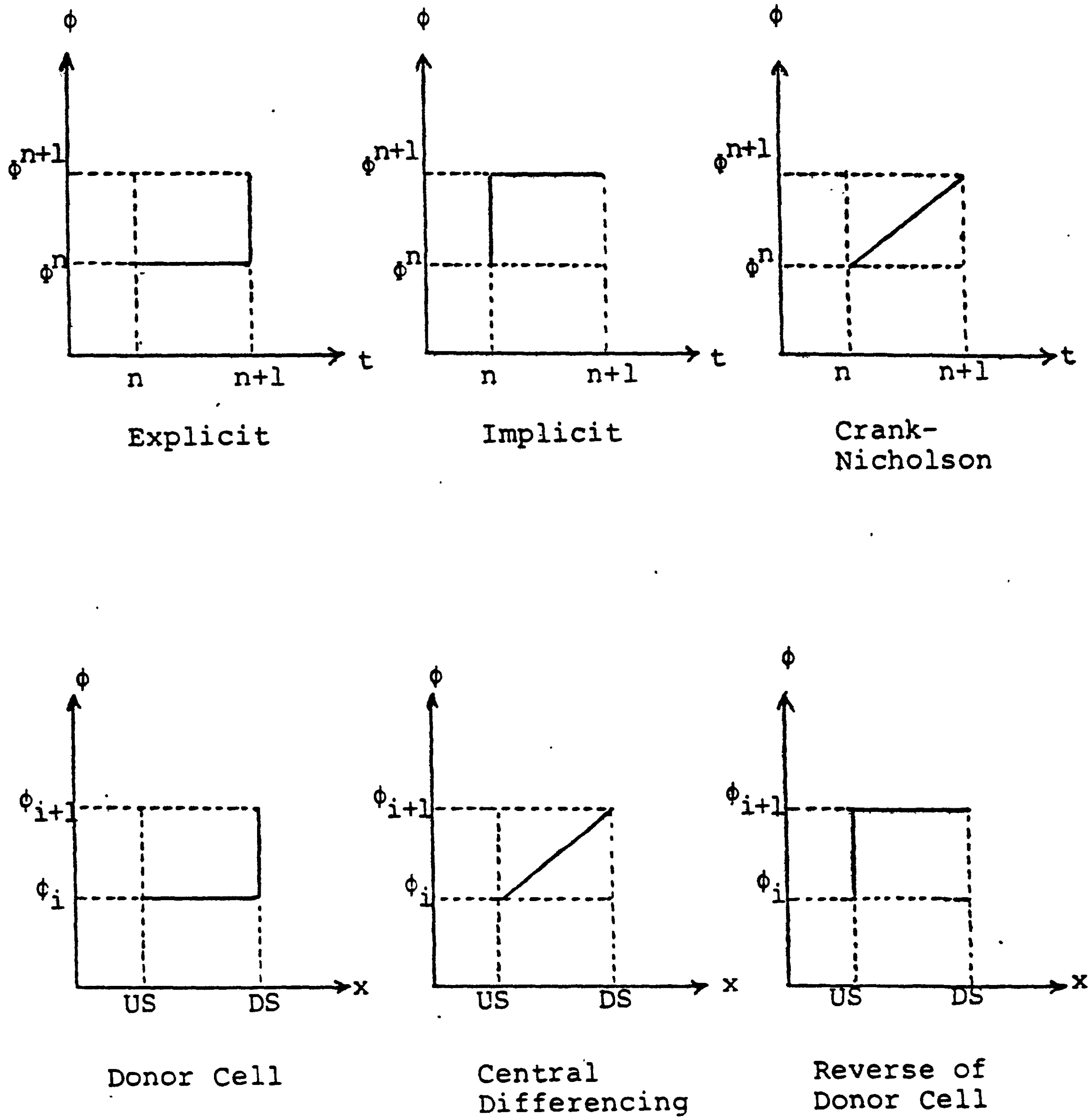

where US(Upstream)
DS(Downstream)

Fig. 4.9. Profile assumptions of ϕ in space and time for various differencing schemes

equation. The infinitesimal approximation of differential terms is not appropriate in most problems of our consideration. The accuracy expressed in terms of $0(\Delta t)$, $0(\Delta x^2)$ is also not appropriate for finitely large Δt and Δx. The accuracy depends on how well we can compute the convection and diffusion quantities at control surfaces over the time Δt. In other words, the accuracy depends on the profiles assumed for Φ in time and space because the exact profiles are not known a priori.

Since the exact profile depends on the Peclet and Strouhal numbers of the governing equation, appropriate schemes should be chosen according to those numbers or weighting should be done between neighboring time steps and mesh points to increase the accuracy of the solution. However, the accuracy is usually the least important among the given four considerations.

4.4.4 Stability

The stability is a mathematical problem, whether the error introduced at a certain step will increase or decrease as the calculation goes over to the following steps. It depends on the maximum eigenvalue of the iteration matrix. If its absolute magnitude is less than one, the error propagation is suppressed and the largest error contribution will be from the previous time step.

The stability can be checked by the theorems about matrix eigenvalues or Von Neumann analysis. The Von Neumann analysis is to expand the solution of a finite difference equation in Fourier series and check the decay of each mode separately. The stability is not a sufficient condition for an acceptable numerical scheme. In the following sections, stability criteria will be derived for the explicit, implicit and ADI schemes using the Von Neumann analysis.

4.4.4.1 Explicit Scheme

The Von Neumann stability analysis of a finite difference equation is simple in its idea, but its algebra may get complicated.

4.4.4.1.1 One Dimensional Central Differencing of Convection Term

The finite difference equation is given for a one dimensional general conservation equation with central differencing of the convection term.

$$\frac{\phi_i^{n+1} - \phi_i^n}{\Delta t} + u\frac{\phi_{i+1}^n - \phi_{i-1}^n}{2\Delta x} = D\frac{\phi_{i+1}^n - 2\phi_i^n + \phi_{i-1}^n}{\Delta x^2} \qquad (4.67)$$

The solution ϕ_i^n is expanded in Fourier series as follows.

$$\phi_i^n = \Sigma\zeta^n e^{Ii} \qquad (4.68)$$

where $I = \sqrt{-1}$.

The absolute value of ζ should be less than one for every mode to achieve stability. When Eq. 4.68 is substituted in Eq. 4.67, the following expression for ζ results.

$$\zeta = 1 - C_x \sin\theta_x I - 2d_x(1-\cos\theta_x) \tag{4.69}$$

where

$$C_x = \frac{u\Delta t}{\Delta x} ,$$

$$d_x = \frac{D\Delta t}{\Delta x^2} .$$

Therefore,

$$|\zeta|^2 = [1 - 2d_x(1-\cos\theta_x)]^2 + [C_x \sin\theta_x]^2 \leq 1 \tag{4.70}$$

Equation 4.70 may be rewritten as follows by defining $\cos\theta_x$ as t.

$$[1 - 2d_x(1-t)]^2 + C_x^2(1-t^2) \leq 1 \tag{4.71}$$

where

$$t = \cos\theta_x ,$$

$$-1 \leq t \leq 1 .$$

The function f(t) will be defined as follows.

$$f(t) = |\zeta|^2 - 1$$

$$= (4d_x^2 - C_x^2)t^2 + (-8d_x^2 + 4d_x)t + C_x^2 + 4d_x^2 - 4d_x \tag{4.72}$$

In order to get the stability of Eq. 4.67, the function

$f(t)$ should be less than or equal to zero for any t in $[-1,1]$.

$$f(t) \leq 0 \tag{4.73}$$

for any t in $[-1,1]$

Equation 4.73 can be solved by a graphical method using the characteristics of a quadratic equation. The parabola $f(t)$ always meets the t-axis because the discriminant is always greater than or equal to zero.

$$D(\text{Discriminant}) = (C_x^2 - 2d_x)^2 \geq 0 \tag{4.74}$$

One of the two meeting points with the t-axis is the point $t=1$ because $f(1)$ is equal to zero.

$$f(1) = 0 \tag{4.75}$$

The parabola $f(t)$ may have three distinct shapes according to the sign of the coefficient of the second order term.

(1) $4d_x^2 - C_x^2 > 0$: concave upward

(2) $4d_x^2 - C_x^2 = 0$: linear

(3) $4d_x^2 - C_x^2 < 0$: concave downward.

In case (1) $f(t)$ is a parabola concave upward and $f(-1)$ should be less than or equal to zero as shown in Fig. 4.10(1). Therefore,

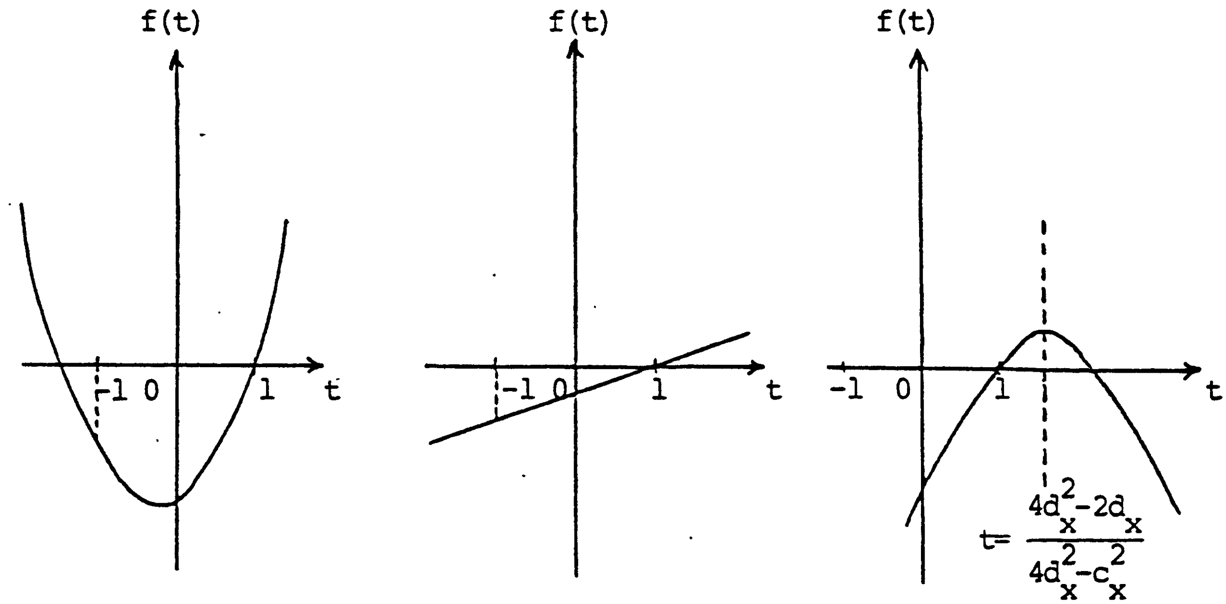

(1) $4d_x^2-c_x^2>0$ (2) $4d_x^2-c_x^2=0$ (3) $4d_x^2-c_x^2<0$

Fig. 4.10. Three distinct shapes of the parabola, f(t), according to the sign of the coefficient of second order term

$$f(-1) = 8d_x(2d_x-1) \leq 0$$

$$0 \leq d_x \leq \tfrac{1}{2} \qquad (4.76)$$

In case (2) f(t) is a straight line and f(-1) again should be less than or equal to zero. In case (3) the parabola f(t) is concave downward and the axis of symmetry should be on the right hand side of the point, t=1 as shown in Fig. 4.10(3).

$$\text{Axis of symmetry:} \quad t = \frac{4d_x^2 - 2d_x}{4d_x^2 - C_x^2} \geq 1$$

$$d_x \geq \tfrac{1}{2}C_x^2 \qquad (4.77)$$

Summing up the results in Eq. 4.76 and Eq. 4.77, we get the following stability conditions.

$$4d_x^2-C_x^2 \geq 0 \quad : \quad 0 \leq d_x \leq \tfrac{1}{2}$$

$$4d_x^2-C_x^2 < 0 \quad : \quad d_x \geq \tfrac{1}{2}C_x^2$$

The stable region in the coordinate system (C_x, d_x) is shown in Fig. 4.11.

4.4.4.1.2 <u>One Dimensional Donor Cell Differencing of Convection Term</u>

The following Eq. 4.78 is a finite difference equation with donor cell differencing of the convection term.

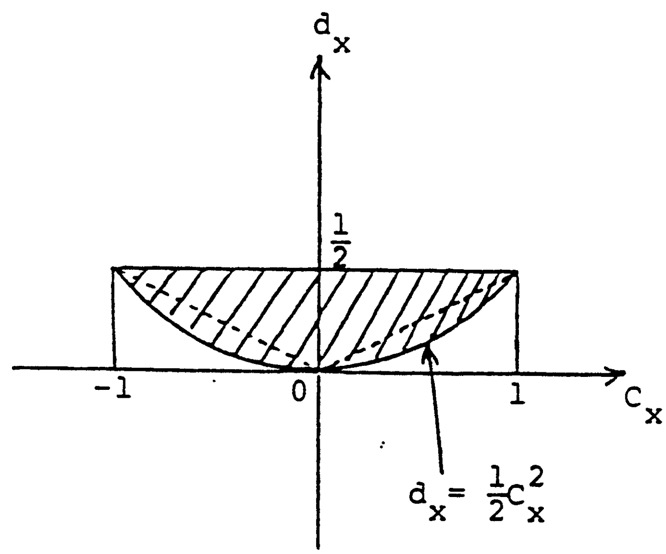

Fig. 4.11. Stability condition in the plane (c_x, d_x) for an explicit scheme with central differencing of convection term in a one dimensional problem

$$\frac{\phi_i^{n+1} - \phi_i^n}{\Delta t} + u\frac{\phi_i^n - \phi_{i-1}^n}{\Delta x} = D\frac{\phi_{i+1}^n - 2\phi_i^n + \phi_{i-1}^n}{\Delta x^2} \qquad (4.78)$$

where the velocity u is positive.

The Von Neumann analysis of Eq. 4.78 gives the following stability condition.

$$|\zeta|^2 = [1-(C_x+2d_x)(1-\cos\theta_x)]^2 + [C_x\sin\theta_x]^2 \leq 1 \qquad (4.79)$$

It can be shown that the value of $|\zeta|^2$ in Eq. 4.79 does not change when the velocity u is less than zero, if the Courant number, C_x, is defined such that it is always positive. The function f(t) is defined as follows to make it easier to solve Eq. 4.79.

$$f(t) = |\zeta|^2 - 1$$

$$= [(C_x+2d_x)^2-C_x^2]t^2 + [-2(C_x+2d_x)^2 + 2(C_x+2d_x)]t$$
$$+ [(C_x+2d_x)^2+C_x^2-2(C_x+2d_x)] \qquad (4.80)$$

The function f(t) in Eq. 4.80 should be less than or equal to zero for any t in [-1,1] for the stability of Eq. 4.78.

$$f(t) \leq 0 \quad \text{for any } t \text{ in } [-1,1] \qquad (4.81)$$

The parabola f(t) meets the t-axis at the point, t=1.

$$f(1) = 0 \qquad (4.82)$$

Equation 4.81 can be solved by the graphical method as in the previous section.

$$(C_x+2d_x)^2 - C_x^2 \geq 0 \quad : \quad 0 \leq C_x + 2d_x \leq 1 \tag{4.83}$$

$$(c_x+2d_x)^2 - C_x^2 < 0 \quad : \quad d_x \geq \tfrac{1}{2}(C_x^2 - C_x) \tag{4.84}$$

The results, Eq. 4.83 and Eq. 4.84, are shown graphically in Fig. 4.12.

4.4.4.1.3 Two and Three Dimensional Donor Cell Differencing of Convection Term

The two dimensional extension of Eq. 4.78 is given in the following.

$$\frac{\phi_{ij}^{n+1} - \phi_{ij}^{n}}{\Delta t} + u\frac{\phi_{ij}^{n} - \phi_{i-1j}^{n}}{\Delta x} + v\frac{\phi_{ij}^{n} - \phi_{ij-1}^{n}}{\Delta y}$$

$$= D\frac{\phi_{i+1j}^{n} - 2\phi_{ij}^{n} + \phi_{i-1j}^{n}}{\Delta x^2} + D\frac{\phi_{ij+1}^{n} - 2\phi_{ij}^{n} + \phi_{ij-1}^{n}}{\Delta y^2} \tag{4.85}$$

The Von Neumann analysis is applied to the finite difference equation, Eq. 4.85, yielding the following result.

$$\zeta - 1 = -C_x(1-e^{-I\theta_x}) - C_y(1-e^{-I\theta_y}) - 2d_x(1-\cos\theta_x)$$

$$- 2d_y(1-\cos\theta_y) \tag{4.86}$$

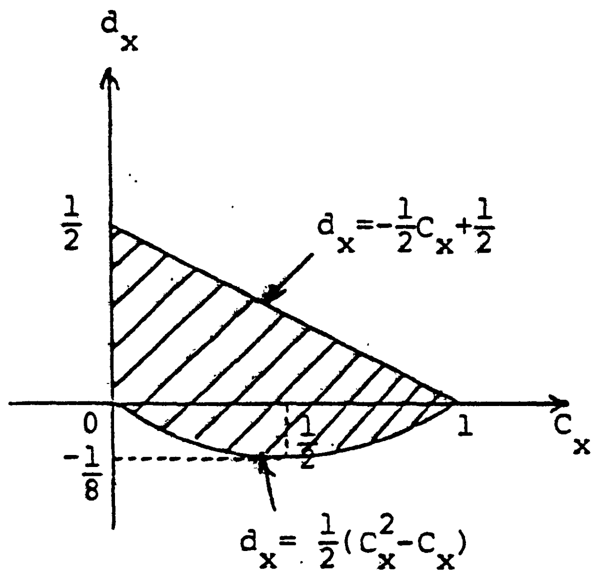

Fig. 4.12. Stability condition in the plane (C_x, d_x) for an explicit scheme with donor cell differencing of convection term in a one dimensional problem

where

$$C_x = \frac{u\Delta t}{\Delta x} \quad , \qquad C_y = \frac{v\Delta t}{\Delta y}$$

$$d_x = \frac{D\Delta t}{\Delta x^2} \quad , \qquad d_y = \frac{D\Delta t}{\Delta y^2}$$

The Courant numbers, C_x and C_y, are defined so that they are always positive, independent of the directions of the velocities u and v. Equation 4.86 can be simplified by defining α_1 and α_2 as given in the following Eq. 4.87.

$$\zeta = 1 + \alpha_1 + \alpha_2 \tag{4.87}$$

where

$$\alpha_1 = -C_x - 2d_x + (C_x+d_x)e^{-I\theta_x} + d_x e^{I\theta_x} \quad ,$$

$$\alpha_2 = -C_y - 2d_y + (C_y+d_y)e^{-I\theta_x} + d_y e^{I\theta_y} \quad .$$

The stability condition is that the absolute magnitude of ζ should be less than or equal to one for any values of θ_x and θ_y. From Fig. 4.13 and Fig. 4.14 it can be seen that α_1 and α_2 should satisfy the following conditions independently.

$$|\alpha_1+\tfrac{1}{2}| \leq \tfrac{1}{2} \tag{4.88}$$

$$|\alpha_2+\tfrac{1}{2}| \leq \tfrac{1}{2} \tag{4.89}$$

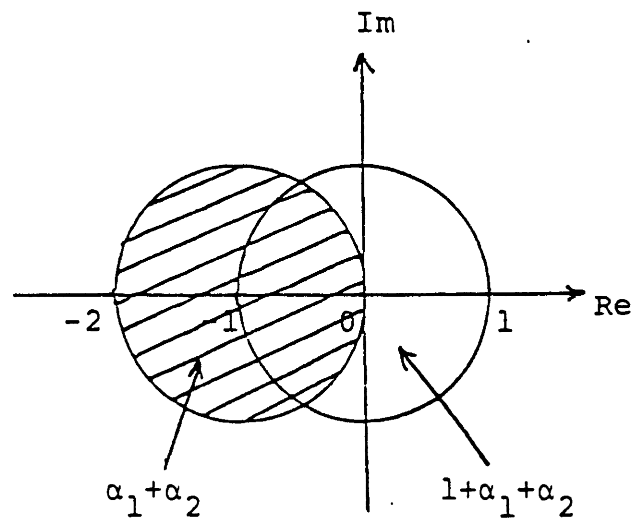

Fig. 4.13. The region in the complex plane where $(\alpha_1+\alpha_2)$ should exist for the stability of an explicit scheme with donor cell differencing of convection term in a general two dimensional problem

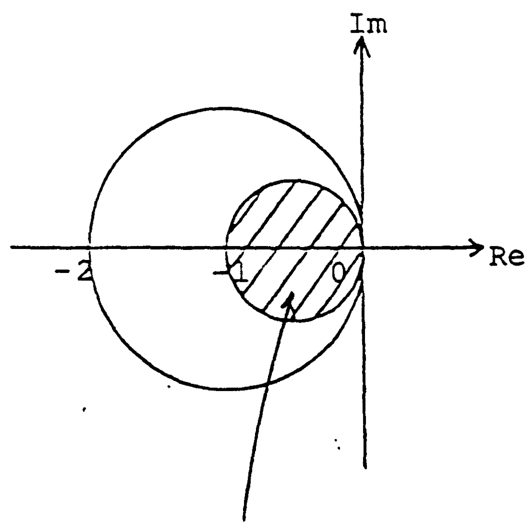

Both α_1 and α_2 should be in the shaded circle to ensure that $|\alpha_1+\alpha_2+1| < 1$.

Fig. 4.14. The region in the complex plane where the amplification factor, ζ, should exist for the stability of an explicit scheme with donor cell differencing of convection term in a general two dimensional problem

Both Eq. 4.88 and Eq. 4.89 can be solved by the graphical method as in the previous sections. The results are given in Fig. 4.15, where the points (C_x, d_x) and (C_y, d_y) should be in the shaded region for stability. A three dimensional case can also be solved through the same procedures and the results are given in Fig. 4.16. The stable region shrinks on a linear scale with dimensionality.

4.4.4.1.4 Stability Condition in Terms of Cell Reynolds Number

The stability conditions in the previous three sections are in terms of the dimensionless numbers, C_x and d_x, which depend on both the mesh spacing, Δx, and time step, Δt. When Δx and Δt are already given, the stability can be checked directly. However, our usual concern is the stable time step size for a given mesh spacing. Therefore, the stable range of C_x should be determined in terms of the cell Reynolds number C_x/d_x, which is independent of the time step size, Δt. The stability condition is again given by Eq. 4.88 and 4.89 and α_1 and α_2 may be rewritten as follows.

$$\alpha_1 = C_x[-1 - \frac{2}{R_x} + (1+\frac{1}{R_x})e^{-I\theta_x} + \frac{1}{R_x} e^{I\theta_x}] \tag{4.90}$$

$$\alpha_2 = C_y[-1 - \frac{2}{R_x} + (1+\frac{1}{R_y})e^{-I\theta_y} + \frac{1}{R_y} e^{I\theta_y}] \tag{4.91}$$

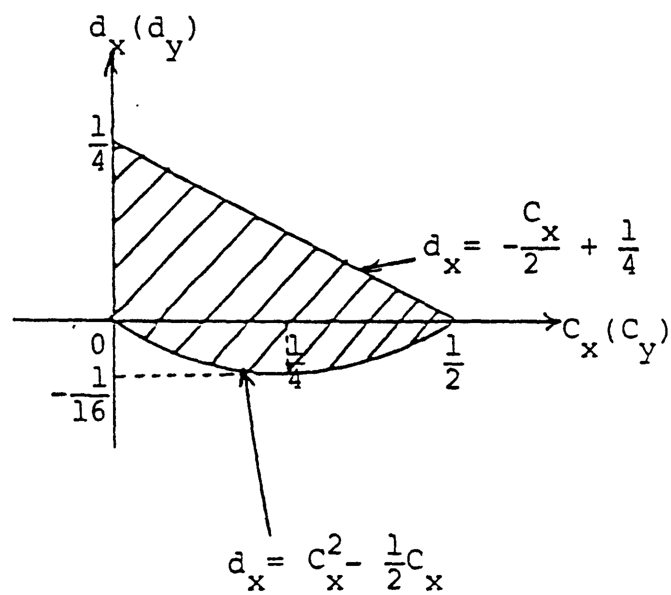

Fig. 4.15. Stability condition in the planes (C_x, d_x) and (C_y, d_y) for an explicit scheme with donor cell differencing of convection term in a general two dimensional problem.

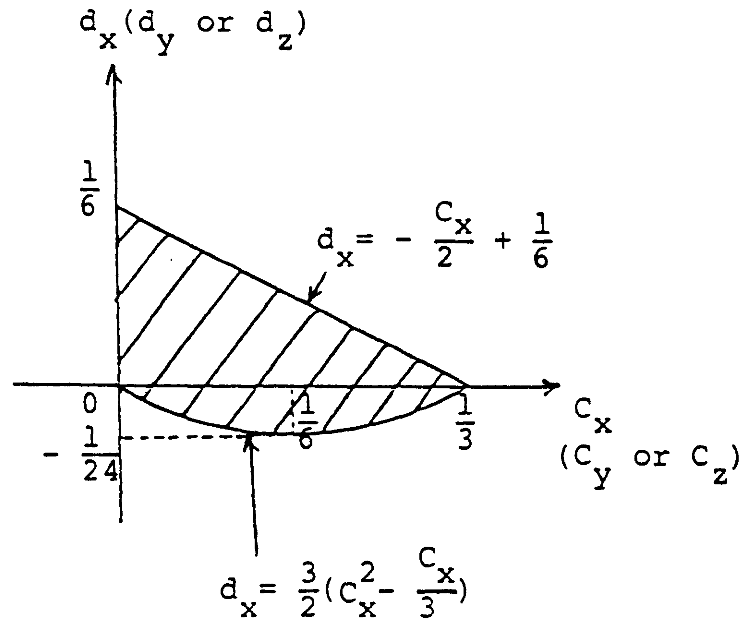

Fig. 4.16. Stability condition in the planes (C_x,d_x) etc. for an explicit scheme with donor cell differencing of convection term in a general three dimensional problem

The following condition for C_x and R_x can be derived from Eq. 4.88 and Eq. 4.90.

$$[\tfrac{1}{2} - C_x(1+\frac{2}{R_x})(1-\cos\theta_x)]^2 + [C_x \sin\theta_x]^2 \leq \tfrac{1}{4} \tag{4.92}$$

Equation 4.92 can be simplified as follows.

$$\begin{aligned} f(t) &= C_x(1+K)^2(1-t)^2 - C_x K(1-t) + C_x^2(1-t^2) \\ &= (C_x^2K^2 - C_x^2)t^2 + (2C_x^2K^2 + C_xK)t + C_x^2K^2 - C_xK \\ &\quad + C_x^2 \leq 0 \end{aligned} \tag{4.93}$$

where $K = 1 + \frac{2}{R_x}$, and

$t = \cos\theta_x$.

The stability condition is now that f(t) should be less than or equal to zero for any t in [-1,1] .

$$f(1) = 0 \tag{4.94}$$

$$D(\text{Discriminant}) = C_x^2(K-2C_x)^2 \geq 0 \tag{4.95}$$

The function f(t) satisfies Eq. 4.94 and Eq. 4.95, and has distinct shapes for the following three cases.

(1) $C_x^2(K^2-1) > 0$: concave upward

(2) $C_x^2(K^2-1) = 0$: linear

(3) $C_x^2(K^2-1) < 0$: concave downward

For case (1) and (2), f(-1) should be less than or equal to zero. For case (3) the axis of symmetry of the parabola should be on the right hand side of the point, t=1. The solution procedure is similar to those in the previous sections and the results are given in the following as,

$$R_x > 0 \quad : \quad 0 \leq C_x \leq \frac{1}{2(1+\frac{2}{R_x})} \quad , \quad \text{and} \tag{4.96}$$

$$R_x < -1 \quad : \quad 0 \leq C_x \leq \tfrac{1}{2}(1+\frac{2}{R_x}) \quad . \tag{4.97}$$

The results in Eq. 4.96 and Eq. 4.97 are shown in Fig. 4.17. The same result will be obtained for the y-direction, therefore the subscript x may be replaced with the subscript y in Fig. 4.17. The stability condition in Fig. 4.17 is applicable to all general 2-D problems, although it can be relaxed if there is a constraint on the velocity direction and mesh spacings such that the following relation is satisfied.

$$f = \frac{\frac{v}{\Delta y}}{\frac{u}{\Delta x}} \leq 1 \tag{4.98}$$

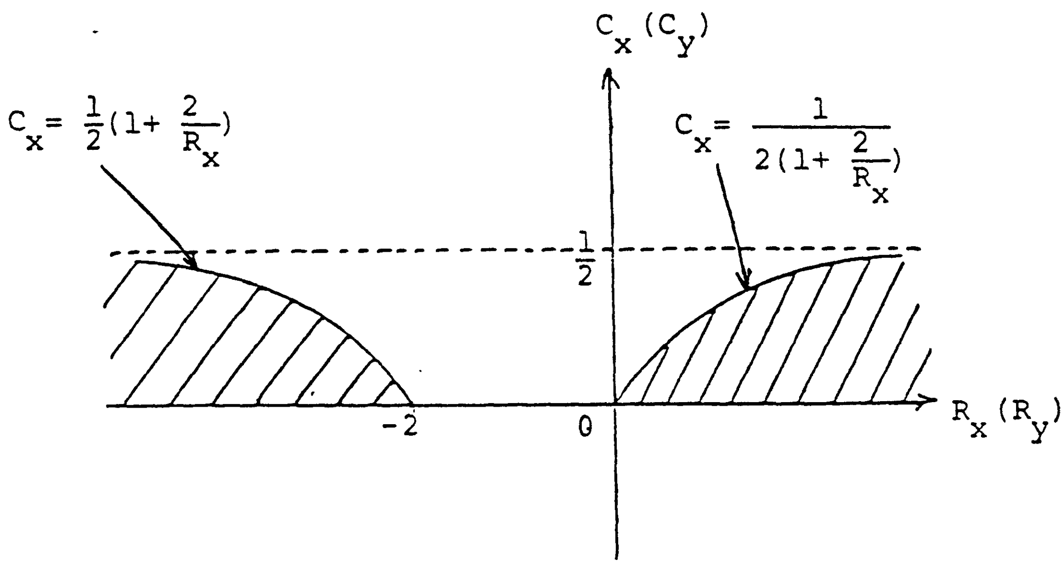

Fig. 4.17. Stability condition in the plane (R_x, C_x) and (R_y, C_y) for an explicit scheme with donor cell differencing of convection term in a general two dimensional problem

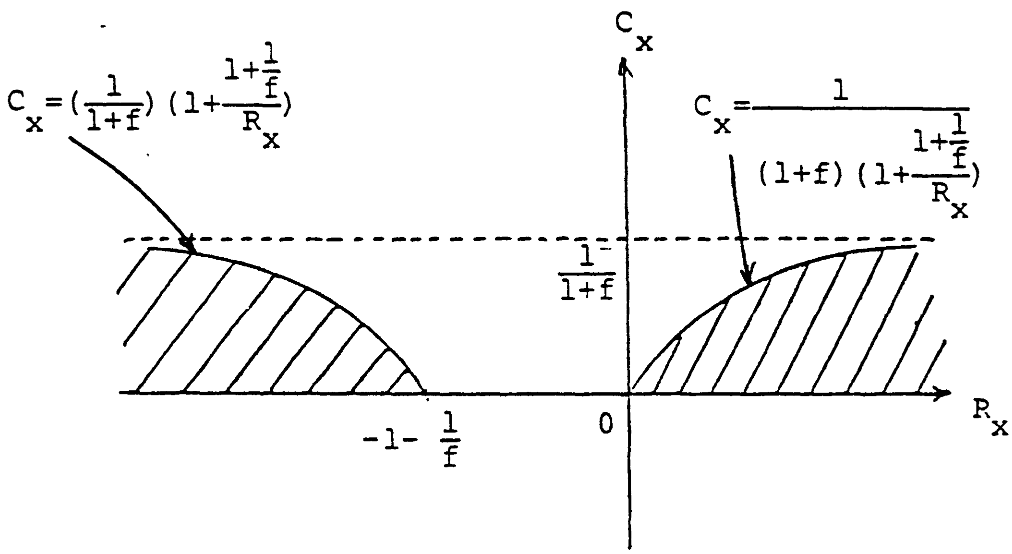

$$\text{where} \quad f = \frac{\frac{v}{\Delta y}}{\frac{u}{\Delta x}}$$

Fig. 4.18. Stability condition in the plane (R_x, C_x) for an explicit scheme with donor cell differencing of convection term in a two dimensional problem with $f = \frac{v/\Delta y}{u/\Delta x}$

Then the number ½ on the C_x-axis in Fig. 4.17 should be replaced with $\frac{1}{1+f}$ in Fig. 4.18. Table 4.2 shows the comparison between the analytical result in Fig. 4.17 and numerical experiments.

4.4.4.2 Implicit Scheme

The following Eq. 4.99 is a fully implicit finite difference equation for a general one dimensional problem and the Von Neumann analysis will be applied in the same way as in the explicit scheme.

$$\frac{\Phi_i^{n+1} - \Phi_i^n}{\Delta t} + u\frac{\Phi_i^{n+1} - \Phi_{i-1}^{n+1}}{\Delta x} = D\frac{\Phi_{i+1}^{n+1} - 2\Phi_i^{n+1} + \Phi_{i-1}^{n+1}}{\Delta x^2} \tag{4.99}$$

The stability condition is shown in Fig. 4.19 and Fig. 4.20, and it can be seen that the implicit scheme is unconditionally stable if the diffusion constant is greater than $-\frac{1}{2}u\Delta x$.

$$d_x \geq -\tfrac{1}{2}C_x \tag{4.100}$$

For a general two dimensional problem, the stability condition is found to be the following.

$$d_x \geq -\tfrac{1}{2}C_x \tag{4.101}$$

$$d_y \geq -\tfrac{1}{2}C_y \tag{4.102}$$

R_x	Maximum Stable C_x Von Neumann Analysis	Maximum Stable C_x Numerical Experiments
0.833	0.147	0.180
8.333	0.403	0.540
83.333	0.488	0.660
833.3	0.499	0.660
-8.333	0.380	0.780
-4.167	0.260	0.720
-2.629	0.120	0.120
-2.083	0.019	0.060

Table 4.2. Comparison of the stability conditions in terms of the cell Reynolds number by Von Neumann analysis and numerical experiments in a two dimensional explicit scheme with donor cell differencing of convection term

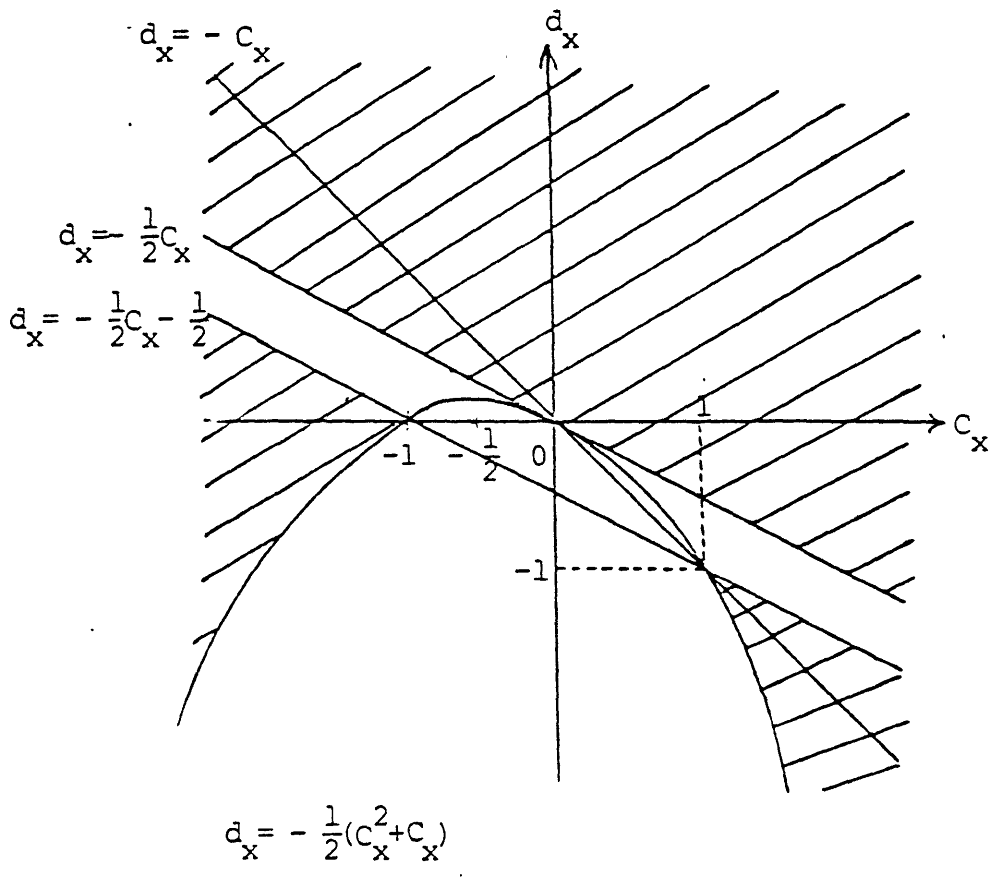

Fig. 4.19. Stability condition in the plane (C_x, d_x) for an implicit scheme with donor cell differencing of convection term in a one dimensional problem

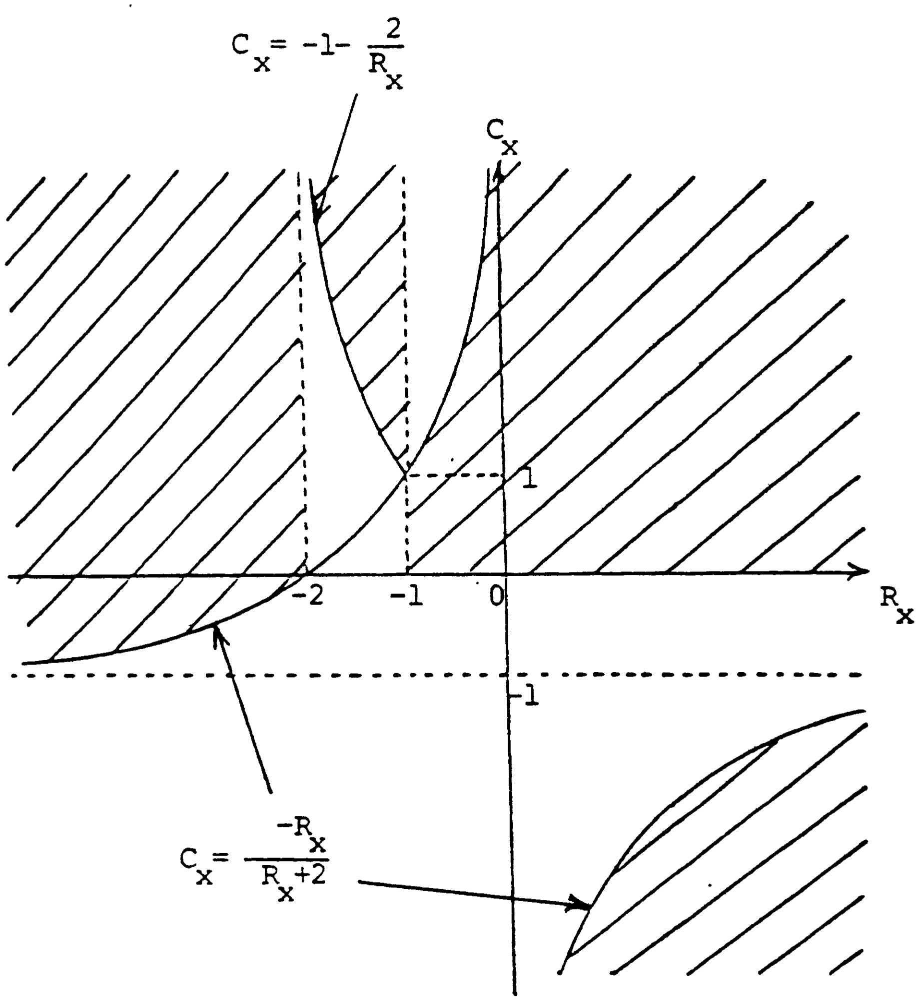

Fig. 4.20. Stability condition in the plane (R_x, C_x) for an implicit scheme with donor cell differencing of convection term in a one dimensional problem

4.4.4.3 ADI Scheme

There are two possible formulations of the Alternate Direction Implicit (ADI) scheme given in Eq. 4.63. One of the formulations has both the x and y direction components in each step, treating them implicitly one by one at each fractional step and the other formulation has only the x or y direction component treated implicitly in each step.

The Von Neumann analysis of the first formulation in Eq. 4.63 gives the following stability condition.

$$|\zeta|^2 = \frac{\{[(1-\cos\theta_x)(\frac{C_x}{2}+d_x)]^2 + [\frac{C_x}{2}\sin\theta_x]^2\}\{[(1-\cos\theta_y)(\frac{C_y}{2}+d_y)]^2\}}{\{[1+(1-\cos\theta_x)(\frac{C_x}{2}+d_x)]^2+[\frac{C_x}{2}\sin\theta_x]^2\}\{[1+(1-\cos\theta_y)(\frac{C_y}{2}+d_y)]^2 + [\frac{C_y}{2}\sin\theta_y]^2\}} \tag{4.103}$$

$$|\zeta| \leq 1$$

In order for $|\zeta|$ to be less than or equal to one, the following condition should be satisfied.

$$d_x \geq -\frac{C_x}{2} - \tfrac{1}{4} \tag{4.104}$$

The same condition should hold for the y-direction.

$$d_y \geq -\frac{C_y}{2} - \tfrac{1}{4} \qquad (4.105)$$

The stability condition of the second formulation in Eq. 4.63 can also be given by the Von Neumann analysis as follows.

$$d_x \geq -\frac{C_x}{2} \qquad (4.106)$$

$$d_y \geq -\frac{C_y}{2} \qquad (4.107)$$

Therefore the second formulation of the ADI scheme in Eq. 4.63 has the same stability condition as the fully implicit scheme.

CHAPTER 5

RESULTS

Some calculations are performed to validate the physical models and numerical schemes in the previous chapters. The physical models are tested in a natural convection problem and the numerical schemes are tested in a simple geometry to compare numerical solutions with exact solutions. Finally, the ADI scheme is explored to use a time step size larger than the Courant limit to save the overall computational time.

5.1 Natural Convection Results

The containment is modelled as a two dimensional rectangular compartment with an obstacle as a heat sink. Natural convection occurs due to the heat transfer between the obstacle and containment air. Updating of the reference state, energy convection and heat transfer models are considered and the resulting flow fields are given in Fig. 5.1 and Fig. 5.2.

5.1.1 Updating of the Reference State

The state of air is determined by any two independent properties. For example, density is determined by temperature and pressure. Since the natural convection of air occurs as a result of the buoyancy force due to density

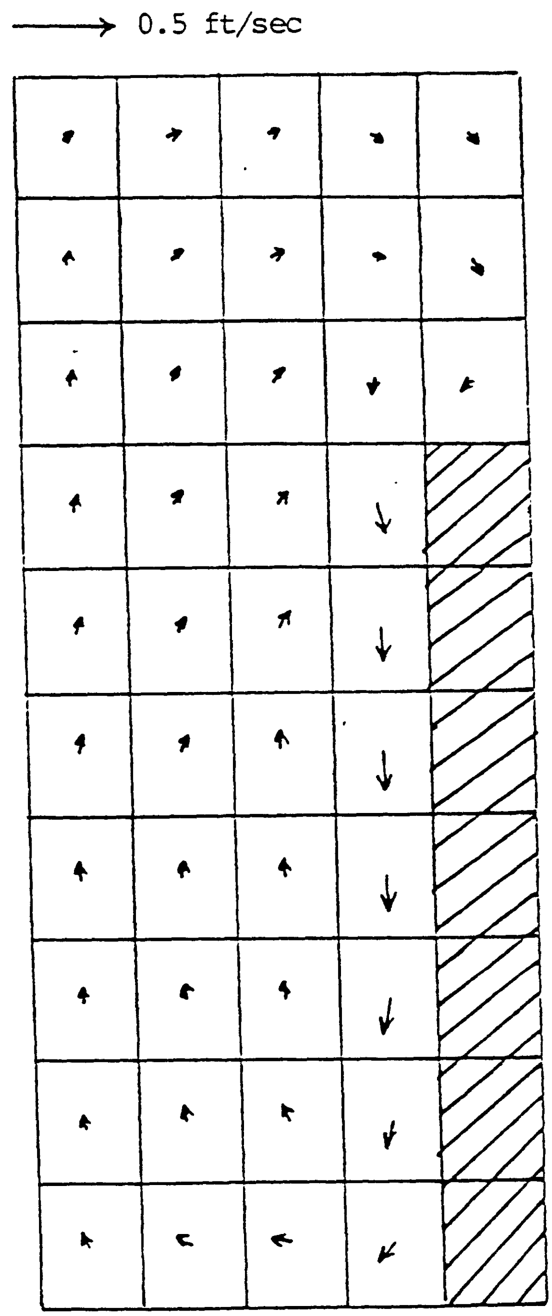

$h = 1.8537\text{x}10^{-4}\text{Btu/ft}^{2\,0}\text{F sec}$

$(c_p)_{ob} = 1.0$ Btu/lbm ^{0}F

$(M)_{ob} = 208.29$ lbm

$A = 2$ ft^2

$\tau_i = 677.4$ sec

$\Delta T = 10^0$F

$T_{air} = 68^0$F

$T_{ob} = 58^0$F

Fig. 5.1. Natural convection flow field due to heat transfer between the obstacle and air in the containment at t = 10.8 sec

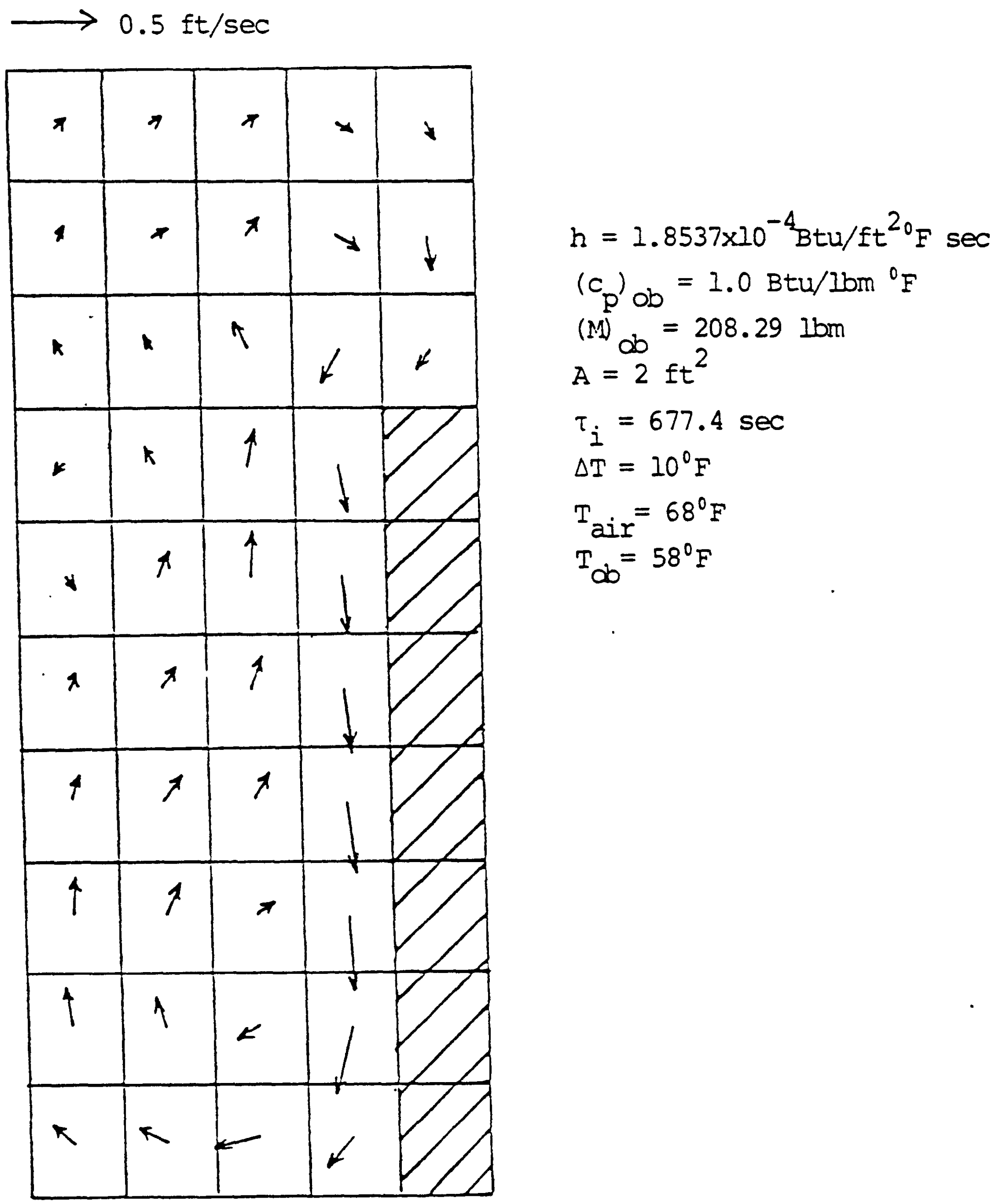

Fig. 5.2. Natural convection flow field due to heat transfer between the obstacle and air in the containment at t = 62.5 sec

gradients, temperature and pressure are equally important parameters in determining the flow field. The density change of liquid, however, depends primarily on the temperature, not on the pressure because of a high modulus of elasticity.

The equation of state of an ideal gas is given in the following.

$$\rho_{new} = \frac{P_{new}}{RT_{new}} \tag{5.1}$$

$$P_{new} = P_{old} \frac{T_{old} + \dfrac{Q_{total}}{c_v M_{f,total}}}{T_{old}}$$

$$T_{new} = T_{old} + \frac{Q_{cell}}{c_v M_{f,cell}}$$

where

ρ_{old}, ρ_{new}: Density of the fluid at old and new time steps.

P_{old}, P_{new}: Pressure of the fluid at old and new time steps.

T_{old}, T_{new}: Temperature of the fluid at old and new time steps.

c_v : Specific heat of the fluid at constant volume.

$M_{f,cell}$, $M_{f,total}$: Mass of the fluid in one cell and in the total domain.

Q_{cell}, Q_{total} : Heat input to the fluid in one cell and in the total domain.

The VARR calculations [21] have shown that the magnitude of velocity can be affected by a factor two by updating the reference pressure at every time step.

5.1.2 Energy Convection

Another difference between liquid and gas is the ratio of the specific heats, $k = c_p/c_v$. The value of k is 1.0 for liquid and 1.4 for air. Monatomic, diatomic and polyatomic gases have different values of k. Therefore, the convection energy transfer should be in terms of enthalpy instead of internal energy. The energy convection will be underestimated by a factor of 1.4 when internal energy is used for enthalpy in air flow.

5.1.3 Heat Transfer Modelling

The heat transfer to the obstacle is modelled as a natural convection from a vertical surface. The Nussett and Grashof numbers here are based on the axial length of one computational mesh, but they may also be based on the vertical height of the obstacle. An experimental correlation is given in Eq. 5.2 in terms of the dimensionless numbers.

$$Nu = C(Gr \cdot Pr)^n \qquad (5.2)$$

$$Gr = \frac{g\beta(\Delta T)L^3\rho^2}{\mu^2} \qquad (5.3)$$

$Pr = 0.708$ (air)

$Gr \cdot Pr$	C	n
$10^5 - 10^9$	0.555	0.25
$> 10^9$	0.021	0.4

The following data are used to calculate the heat transfer coefficient at the obstacle wall.

$L = 2$ ft

$\Delta T = 50°F$

$\rho = 0.0763$ lbm/ft^3

$g = 32.2$ ft/sec^2

$\mu = 1.2179 \times 10^{-5}$ lbm/ft$\cdot$sec

$\beta = 1.923 \times 10^{-3}$

Therefore,

$Gr = 9.7134 \times 10^8$

$Nu = 89.876$

The heat transfer coefficient is given as,

$h = 1.8537 \times 10^{-4}$ Btu/ft$^2\cdot$°F$\cdot$sec .

This may be a typical value for the natural convection heat transfer in the containment without any phase change.

The VARR input [21] requires the time constant of the heat transfer instead of the heat transfer coefficient.

$$CQ = c_{p,ob} \frac{1}{\tau}(T_f - T_{ob}) \tag{5.4}$$

where -CQ is the source term in the energy equation of fluid. The time constant, τ, can be obtained from heat balance between the obstacle and fluid as follows.

$$\tau = \frac{(Mc_p)_{ob}\rho_f}{hA\rho_{ob}} \tag{5.5}$$

where

- M : Mass of one computational mesh.
- A : Heat transfer area between the obstacle and fluid over one computational mesh.
- ρ_f : Fluid density.
- ρ_{ob}: Obstacle density.
- c_p : Specific heat at constant pressure.
- h : Heat transfer coefficient between the fluid and obstacle.

Therefore,

τ = 677.4 sec.

5.1.4 Turbulence Modelling

Laminar flow is assumed in obtaining the results in Fig. 5.1 and Fig. 5.2. If the flow is turbulent, the heat transfer to the obstacle will be enhanced and the diffusion transport of momentum and energy will also be enhanced in the containment air.

5.2 Numerical Diffusion

The truncation and cross-flow diffusion errors are compared in a simple geometry where an analytical solution can be obtained. The skew differencing and corrective schemes are tested for various problems. Huh's formula is compared with De Vahl Davis and Mallinson's in predicting the magnitude of cross-flow diffusion. The corrective scheme is tested in recirculating flow problems for mesh point and mesh interface implementations.

5.2.1 Truncation Error and Cross-flow Diffusion

The truncation error diffusion is compared with the cross-flow diffusion in a two dimensional, steady-state problem in Fig. 5.3. The flow in Fig. 5.3(A) is parallel with the mesh orientation so that no cross-flow diffusion occurs. The results in Fig. 5.4 and Fig. 5.5 show that the numerical solutions is close to the analytical solution and the truncation error can be neglected. The flow in Fig. 5.3(B) is skewed at 45° to the mesh orientation and both truncation error and cross-flow diffusions are included in the solution error. Figure 5.6 and Fig. 5.7 show that excessive numerical diffusion has occurred due to the

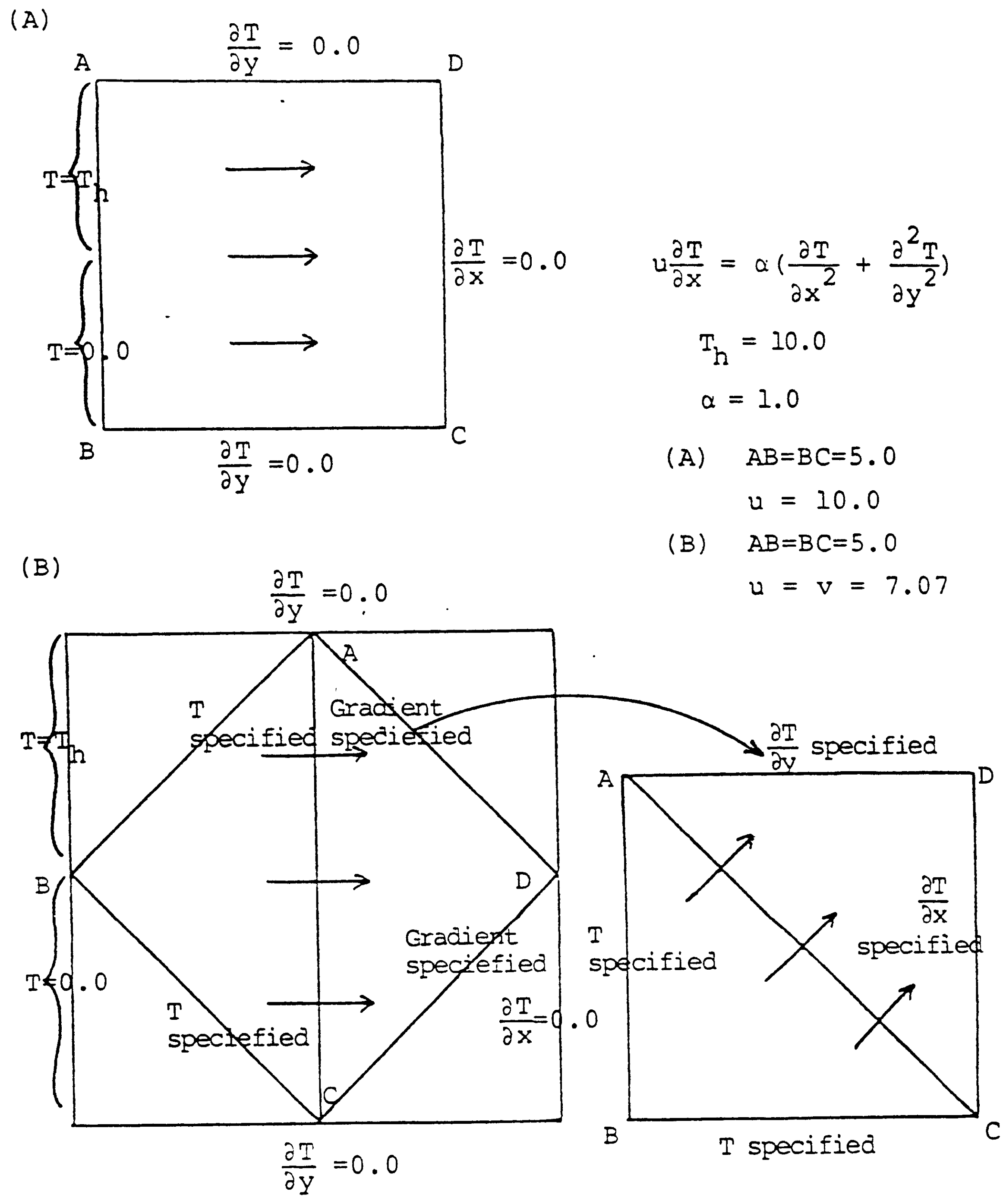

Fig. 5.3. Problem geometry for the two cases, (A) parallel flow and (B) cross flow, for evaluation of numerical diffusion

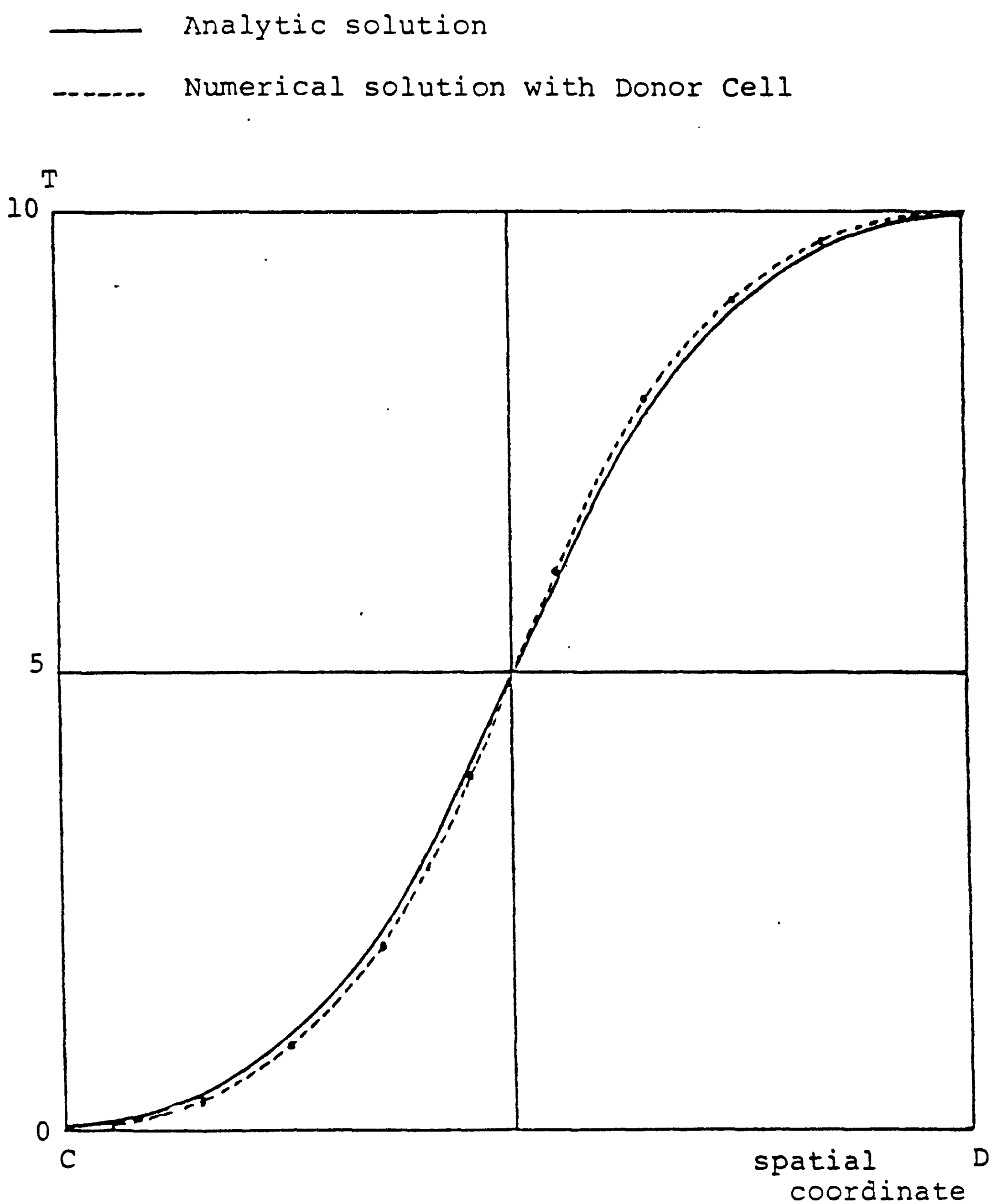

Fig. 5.4. Comparison of the analytic solution and numerical solution with donor cell differencing of convection term in 10x10 meshes along the line CD in Fig. 5.3(A)

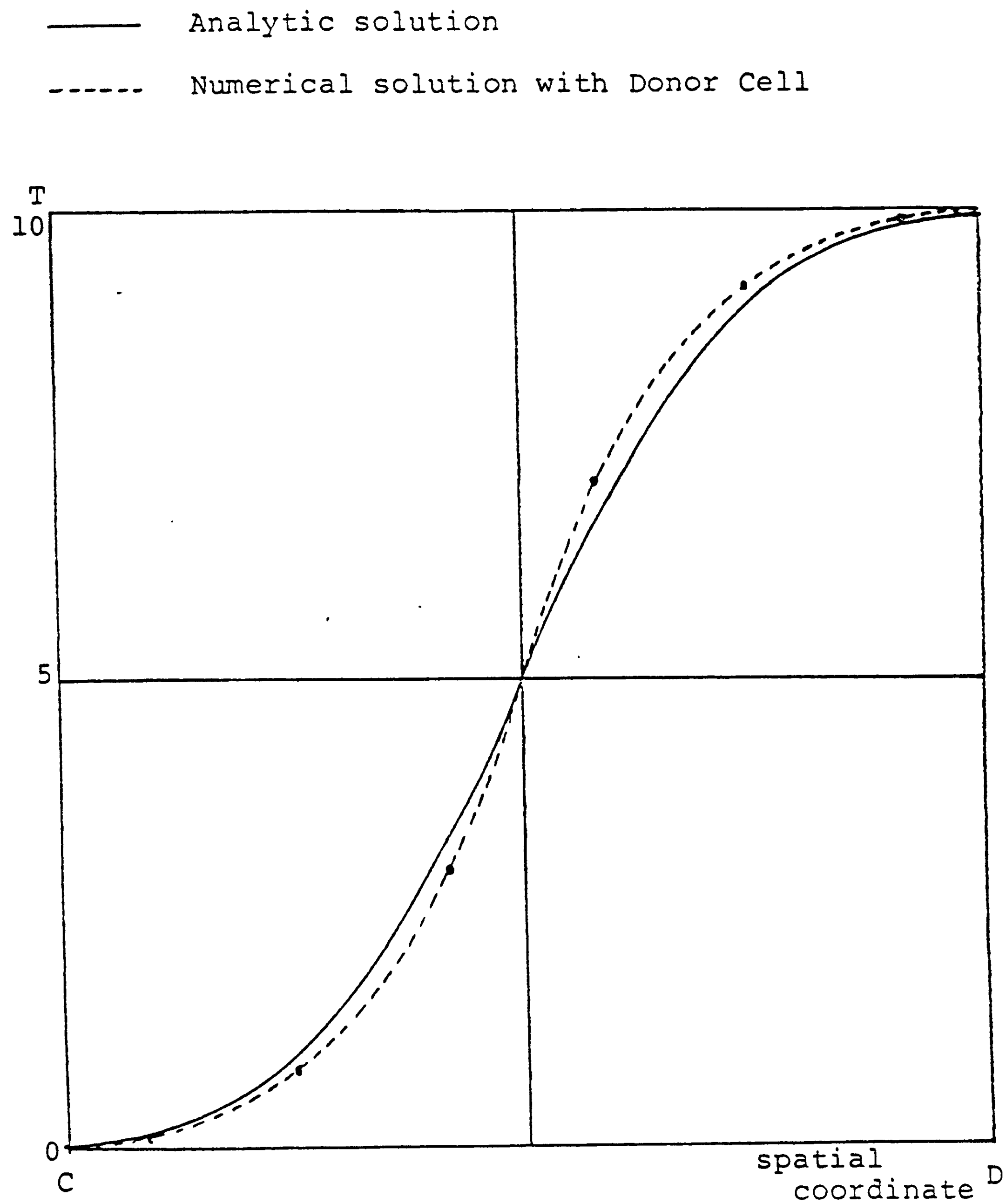

Fig. 5.5. Comparison of the analytic solution and numerical solution with donor cell differencing of convection term in 6x6 meshes along the line CD in Fig. 5.3(A)

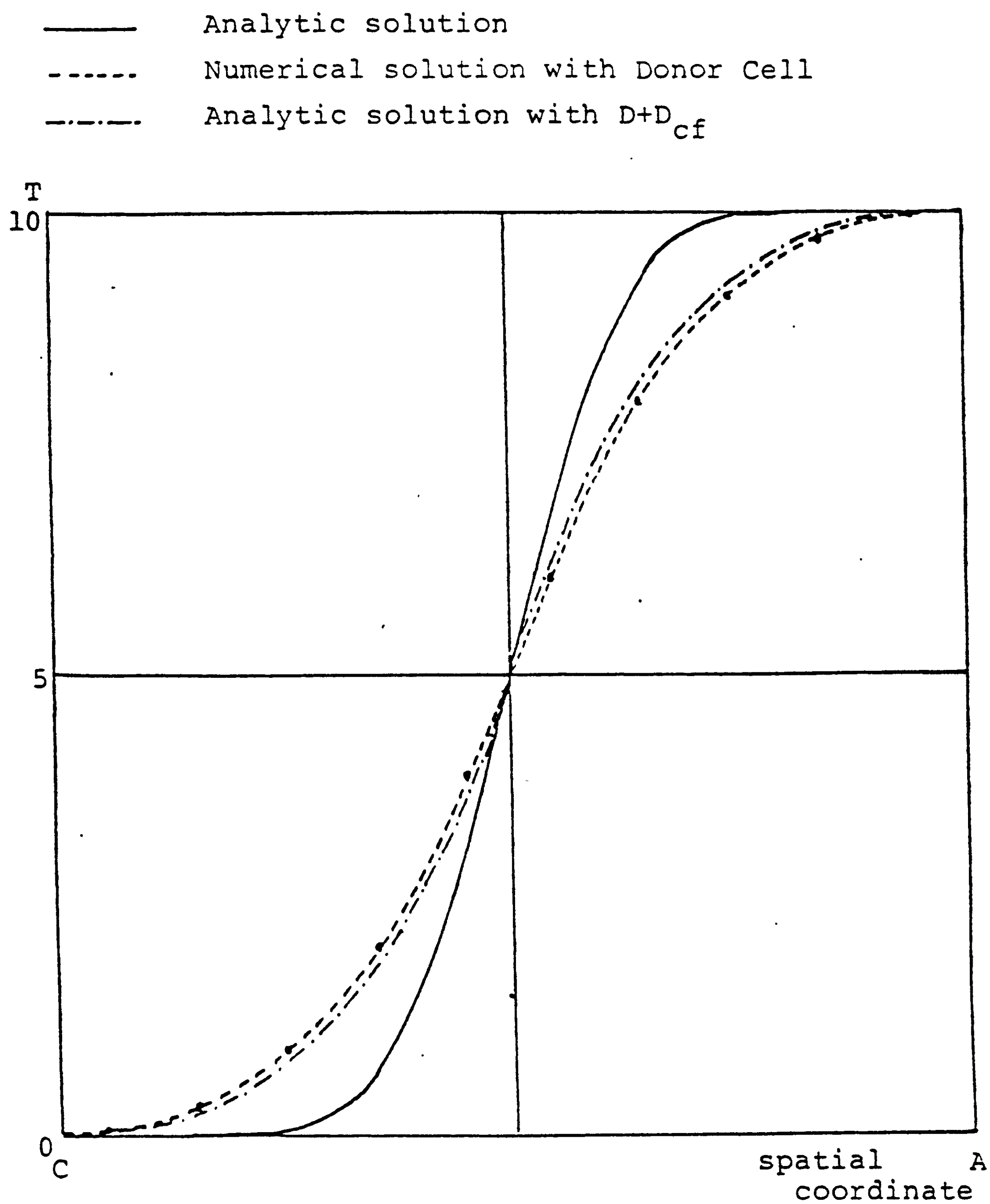

Fig. 5.6. Comparison of the analytic solution, analytic solution with increased diffusion constant and numerical solution with donor cell differencing of convection term in 10x10 meshes along the line CA in Fig. 5.3(B)

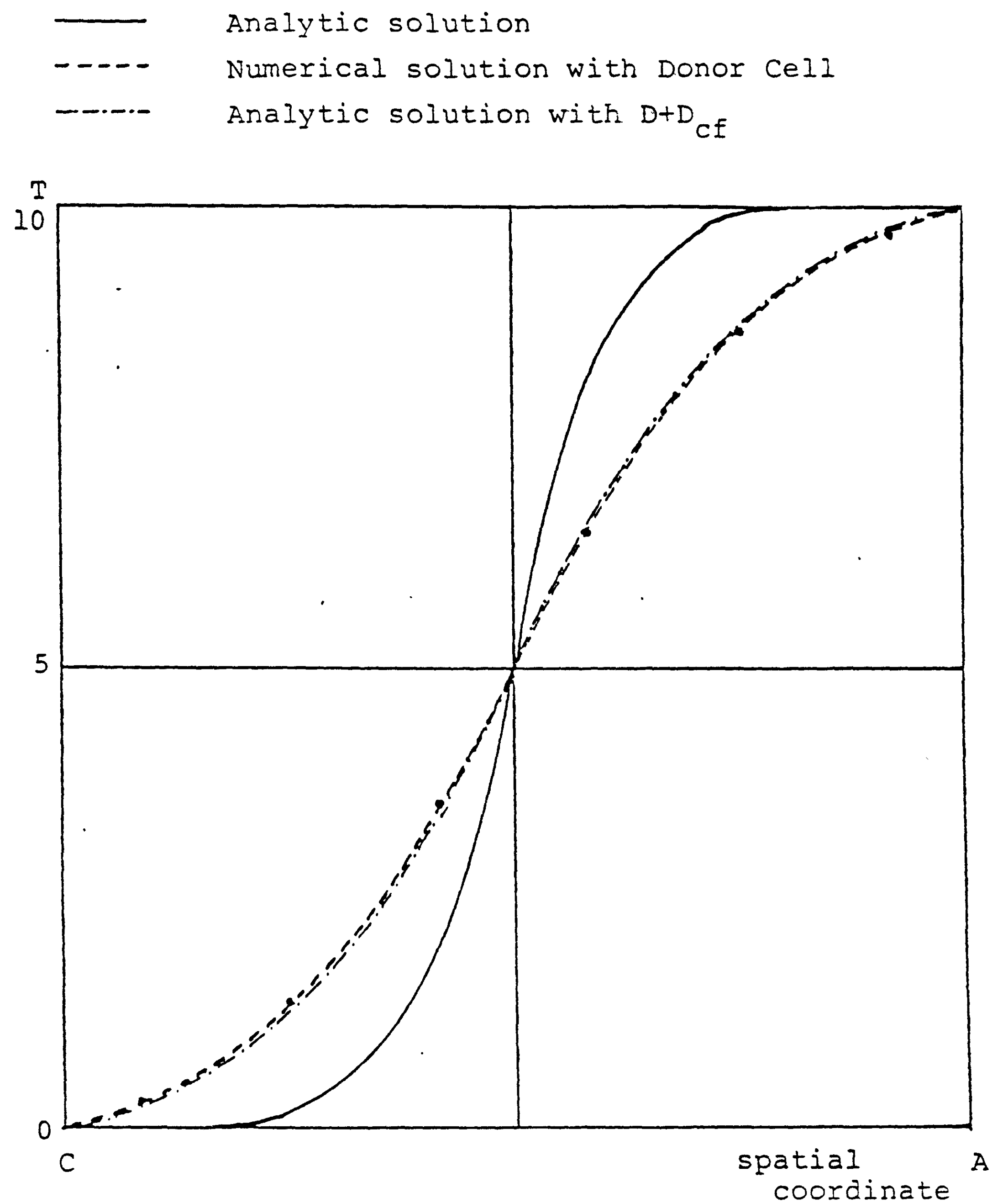

Fig. 5.7. Comparison c: the analytic solution, analytic solution with increased diffusion constant and numerical solution with donor cell differencing of convection term in 6x6 meshes along the line CA in Fig. 5.3(B)

cross-flow diffusion. Figure 5.4 and Fig. 5.6 are for 10 x 10 meshes and Fig. 5.5 and Fig. 5.7 are for 6 x 6 meshes. It is seen that a finer mesh gives a better solution. Since the cross-flow diffusion constant is proportional to the mesh spacing, more diffusion has occurred in Fig. 5.7 than in Fig. 5.6.

5.2.2 Validation of Huh's Correction Formula

The cross-flow diffusion can be predicted by Huh's formula, Eq. 4.53 and Eq. 4.54. Since the corrective scheme is based on the validity of those correction formulas, it is necessary to test them for various cases.

Figure 5.6 and Fig. 5.7 show that the numerical solution can be reproduced by the analytical solution with increased diffusion constants by the amount given by Huh's formula. De Vahl Davis and Mallinson's and Huh's formulas give the same cross-flow diffusion constants for the case, $\theta = \theta_1 = 45°$. The problem geometry in Fig. 5.8 has the arbitrary angles of θ and θ_1 such that $\theta = 60°$ and $\theta_1 = 76.81°$. Figure 5.9 is the result by Huh's formula and Fig. 5.10 by De Vahl Davis and Mallinson's for the problem in Fig. 5.8. It can be seen that the former result is much better than the latter.

5.2.3 Skew Differencing Scheme

Two skew differencing schemes, Raithby's and Huh's, are tested in Fig. 5.11 and Fig. 5.12 for a simple pure

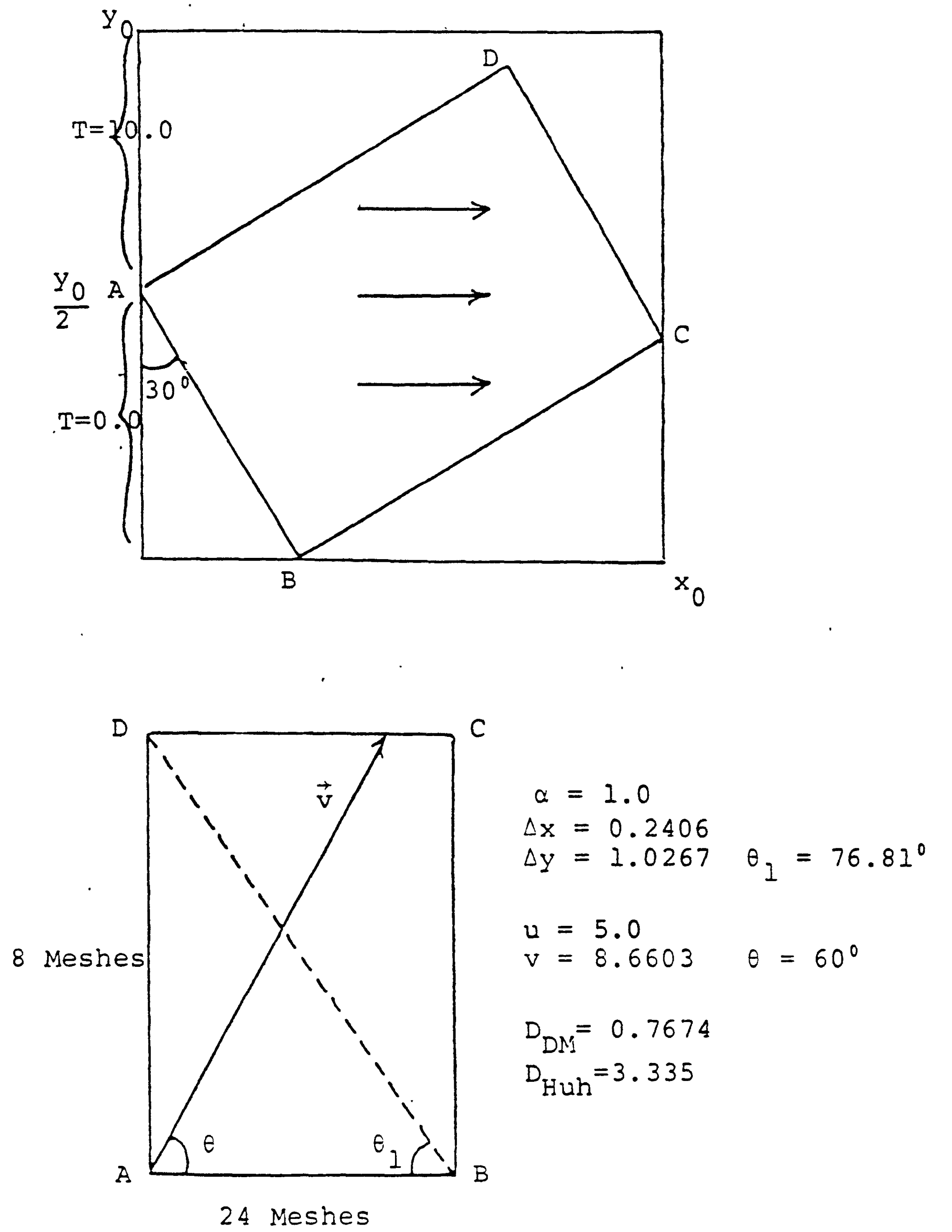

Fig. 5.8. Problem geometry with arbitrary angles of θ and θ_1 to compare De Vahl Davis and Mallinson's and Huh's formulas for prediction of cross-flow diffusion constant

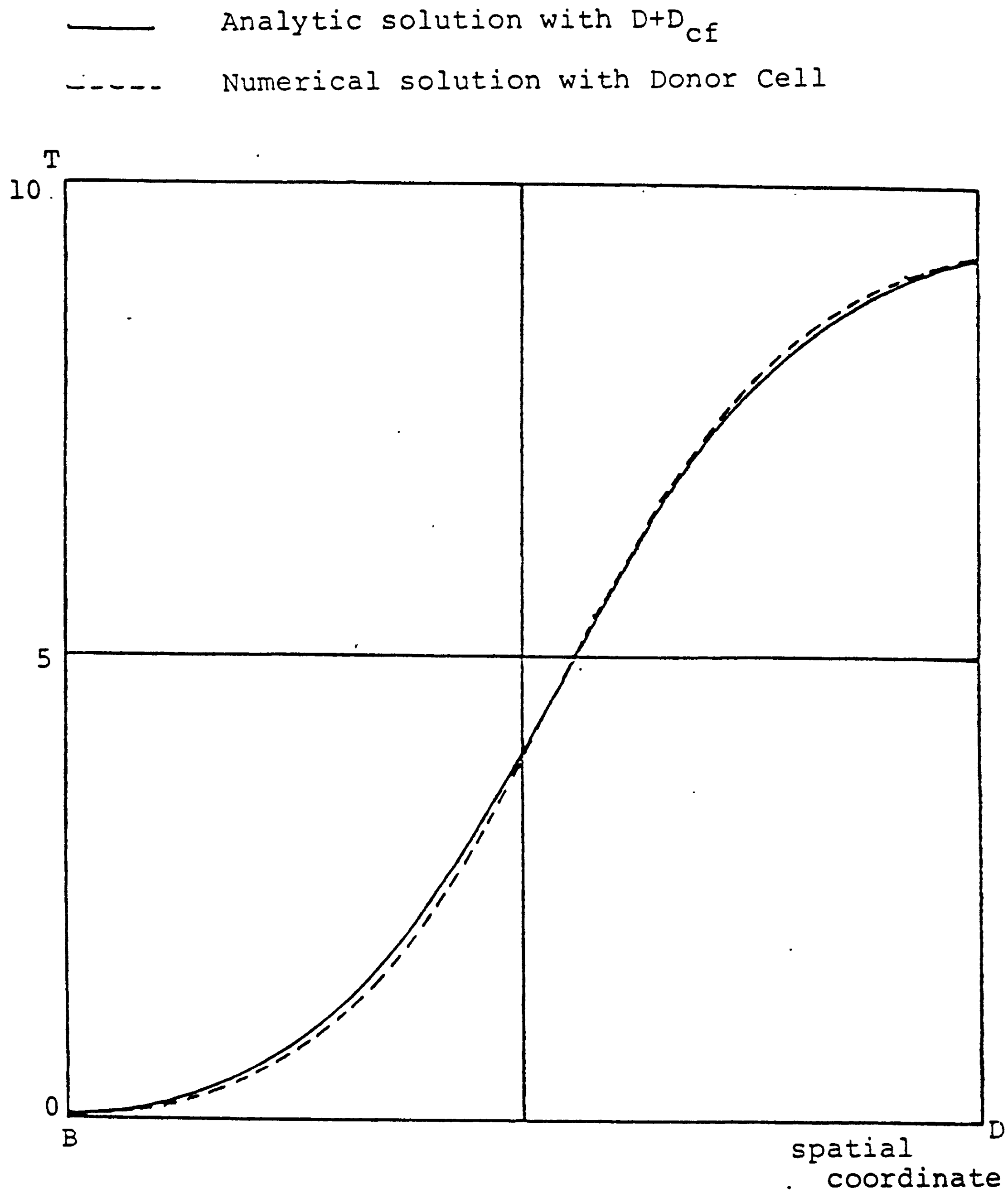

Fig. 5.9. Comparision of the numerical solution with donor cell differencing of convection term and analytic solution with increased diffusion constant, $(D+D_{cf})$, by Huh's formula along the line BD in Fig. 5.8

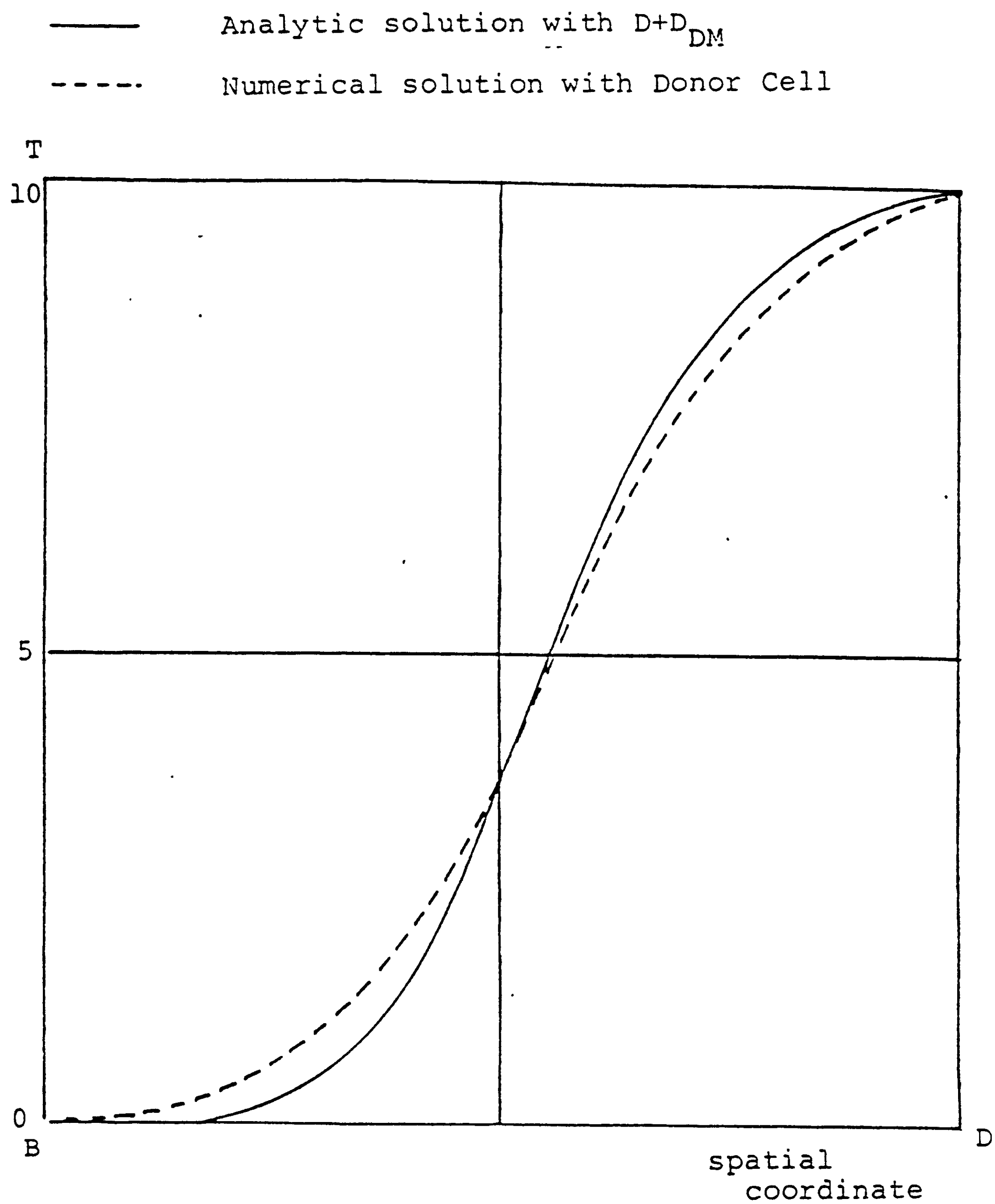

Fig. 5.10. Comparision of the numerical solution donor cell differencing of convection term and analytic solution with increased diffusion constant, (D+D_{DM}), by De Vahl Davis and Mallinson's formula along the line BD in Fig. 5.8

Donor cell

100	93.75	81.25	65.63	50
100	87.5	68.75	50	34.38
100	75	50	31.25	18.75
100	50	25	12.5	6.25
100	0	0	0	0

Skew differencing
by Raithby

100	100	100	100	50
100	100	100	50	0
100	100	50	0	0
100	50	0	0	0
50	0	0	0	0

Skew differencing
by Huh
(True solution)

100	100	100	100	50
100	100	100	50	0
100	100	50	0	0
100	50	0	0	0
50	0	0	0	0

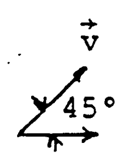

Fig. 5.11. Comparison of the true solution and solutions by donor cell scheme, skew differencing scheme by Raithby and skew differencing scheme by Huh in a pure convection problem with θ = 45°

Donor cell

100	80.25	53.91	31.96	17.33
100	70.37	40.74	20.99	10.01
100	55.56	25.93	11.11	4.52
100	33.33	11.11	3.70	1.23
50	0	0	0	0

Skew differencing by Raithby

100	96.91	71.43	7.47	-23.15
100	90.74	38.89	-22.83	6.50
100	72.22	-9.25	-1.86	2.26
100	16.67	-5.56	1.85	-0.62
50	0	0	0	0

Skew differencing by Huh

100	90.63	59.38	21.88	3.13
100	81.25	37.50	6.25	0
100	62.5	12.5	0	0
100	25	0	0	0
50	0	0	0	0

True solution

100	100	50	0	0
100	100	25	0	0
100	50	0	0	0
100	25	0	0	0
50	0	0	0	0

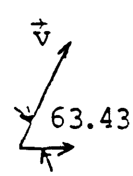

Fig. 5.12. Comparison of the true solution and solutions by donor cell scheme, skew differencing scheme by Raithby and skew differencing scheme by Huh in a pure convection problem with θ = 63.43°

convection problem. The details of those schemes are given in sections 4.3.1 and 4.3.2. Figure 5.11 has a flow at a 45° angle with respect to the mesh orientation and shows that the donor cell scheme introduces appreciable cross-flow diffusion while Raithby's and Huh's skew differencing schemes give the true solution. Fig. 5.12 has a flow at a 63.43° angle and neither Raithby's nor Huh's scheme can reproduce the true solution. It is indicated that Raithby's scheme may give unphysical results in problems with steep gradients of the quantity under consideration. Some cross-flow diffusion has occurred in Huh's scheme, but less than in the donor cell scheme.

Figure 5.13 and Fig. 5.14 show that the analytical solution can be reproduced by Huh's skew differencing scheme for the case, $\theta = \theta_1 = 45°$. Raithby's scheme is an Eulerian method while Huh's scheme is Lagrangian. Therefore, the former is conservative while the latter is not. However, both of them are conservative in a uni-directional flow.

5.2.4 Corrective Scheme

The prediction formulas of the cross-flow diffusion constants are validated by showing that the numerical solution can be reproduced by the analytical solution with the appropriately increased diffusion constant. The purpose of the corrective scheme is, however, to obtain the true solution by subtracting the additional cross-flow diffusion

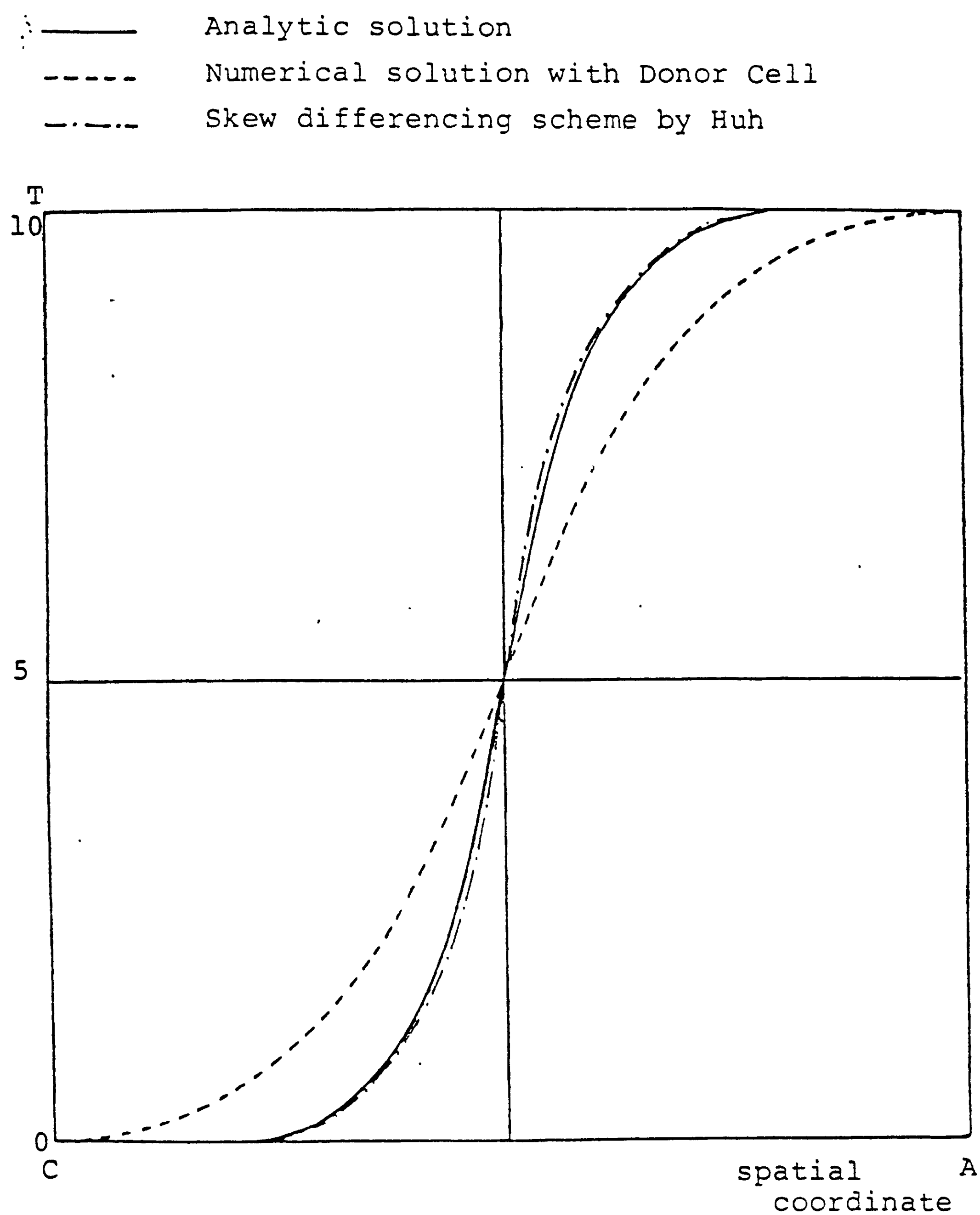

Fig. 5.13. Comparison of the analytic solution and numerical solutions by donor cell scheme and skew differencing scheme by Huh for 10x10 meshes along the line CA in Fig. 5.3(B)

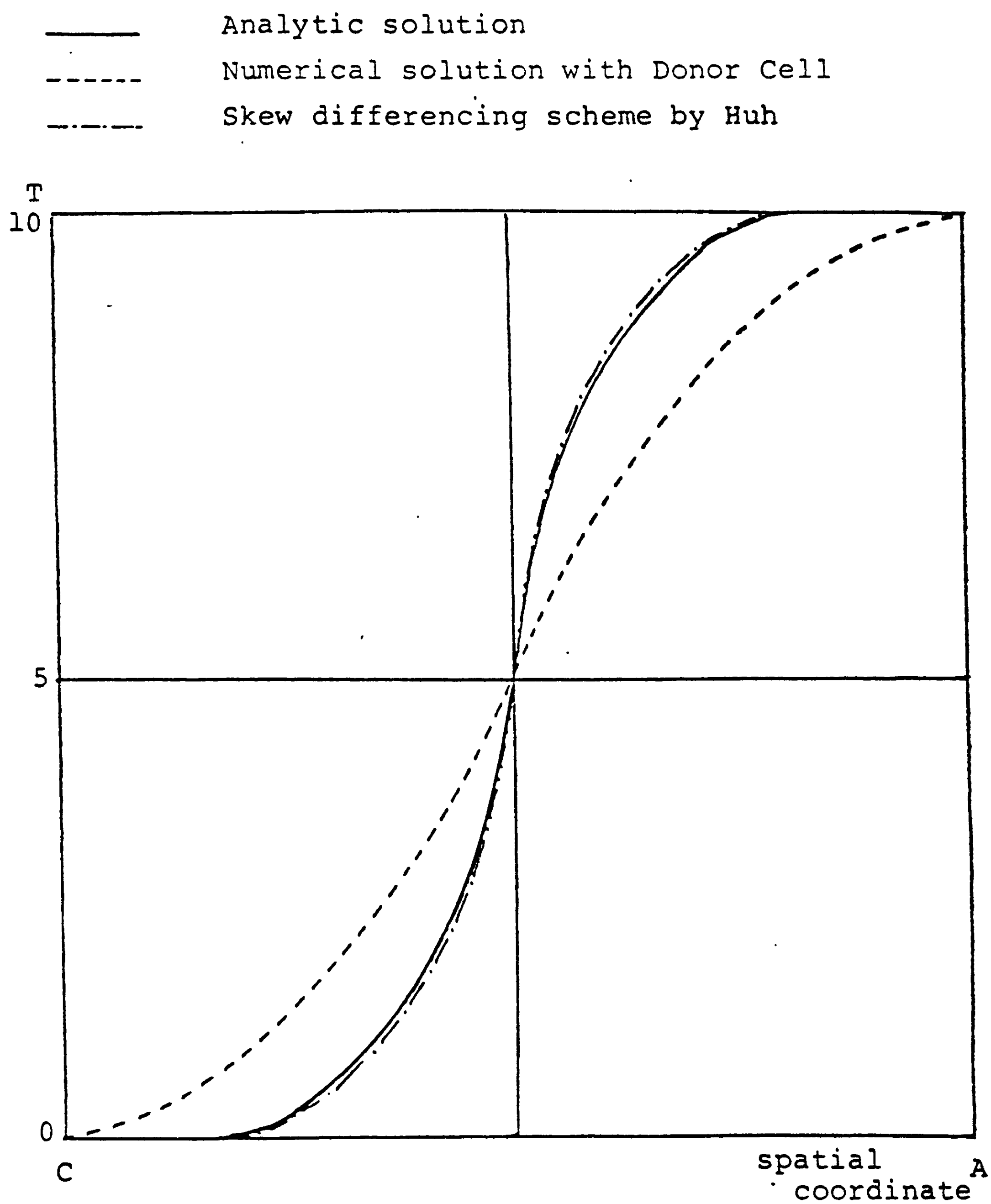

Fig. 5.14. Comparison of the analytic solution and numerical solutions by donor cell scheme and skew differencing scheme by Huh for 6x6 meshes along the line CA in Fig. 5.3(B)

constant from the total diffusion constant of the finite difference equation.

In Fig. 5.15 numerical solutions are given for a simple pure convection problem with various diffusion corrections. The flow is at a 45° angle with respect to the mesh orientation. The full correction of the cross-flow diffusion gives the true solution without any numerical diffusion error. Fig. 5.16 has a flow with $\theta = 63.43°$. The corrective scheme gives a physically reasonable solution, although not identical to the true solution.

The corrective scheme is also tested in the problem geometry of Fig. 5.3(B). Figure. 5.17 and Fig. 5.18 show that the cross-flow diffusion can be eliminated by the corrective scheme and that a finer mesh spacing always gives a better solution.

Two implementation strategies of the corrective scheme, mesh point and mesh interface, are introduced in Chapter 4. Both of them are tested in a recirculating flow problem with pure convection. Figure 5.19 is a hypothetical 3 x 3 recirculating flow field where the inlet boundary values are specified on the left and bottom surfaces. Fig. 5.20 shows the diffusion corrections of the mesh point and mesh interface implementations at each interface. Figure 5.21 gives the true solution, donor cell solution and the solutions by mesh point and mesh interface implementations. The mesh point implementation gives an unphysical solution

D=0.0

10	8.75	6.88	5
10	7.5	5	3.13
10	5	2.5	1.25
	0	0	0

D=-0.1

4.01	7.12	5.0
7.71	5.0	2.88
5.0	2.29	0.99

D=-0.3

9.59	7.92	5.0
8.29	5.0	2.08
5.0	1.71	0.41

D=-0.5 (True Solution)

10	10	5
10	5	0
5	0	0

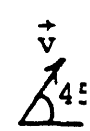

$u=v=1$

$\Delta x=\Delta y=1$

$D_x=D_y=0.5$

Fig. 5.15. Donor cell solutions with various diffusion corrections for a pure convection problem with $\theta = 45°$

D=0.0

10	7.04	4.07	2.10
10	5.56	2.59	1.11
10	3.33	1.11	0.37
	0	0	0

$D=-\frac{2}{3}$

9.96	3.93	0.73
6.91	0.82	-0.07
3.07	0.41	0.11

True Solution

10	2.5	0
5	0	0
2.5	0	0

$u=1,\ v=2$

$x= y=1$

$D_x=D_y=-\frac{2}{3}$

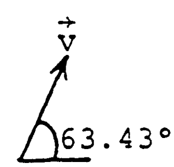

Fig. 5.16. True solution and donor cell solutions with and without diffusion correction for a pure convection problem with θ = 63.43°

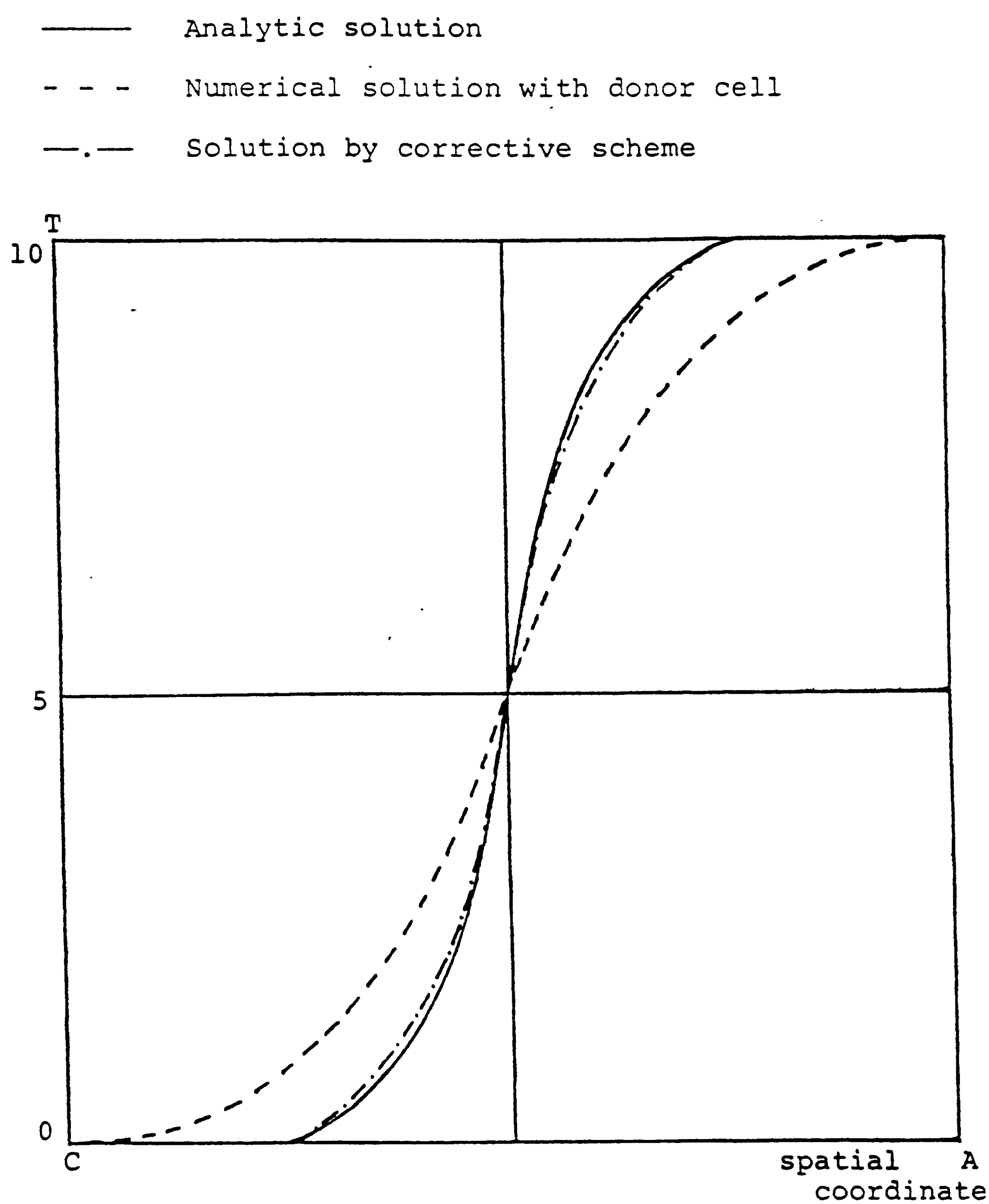

Fig. 5.17. Comparison of the analytic solution, numerical solution by donor cell scheme and numerical solution by corrective scheme for 10x10 meshes along the line CA in Fig. 5.3(B)

———— Analytic solution

- - - - Numerical solution with donor

—·—·— Solution by corrective scheme

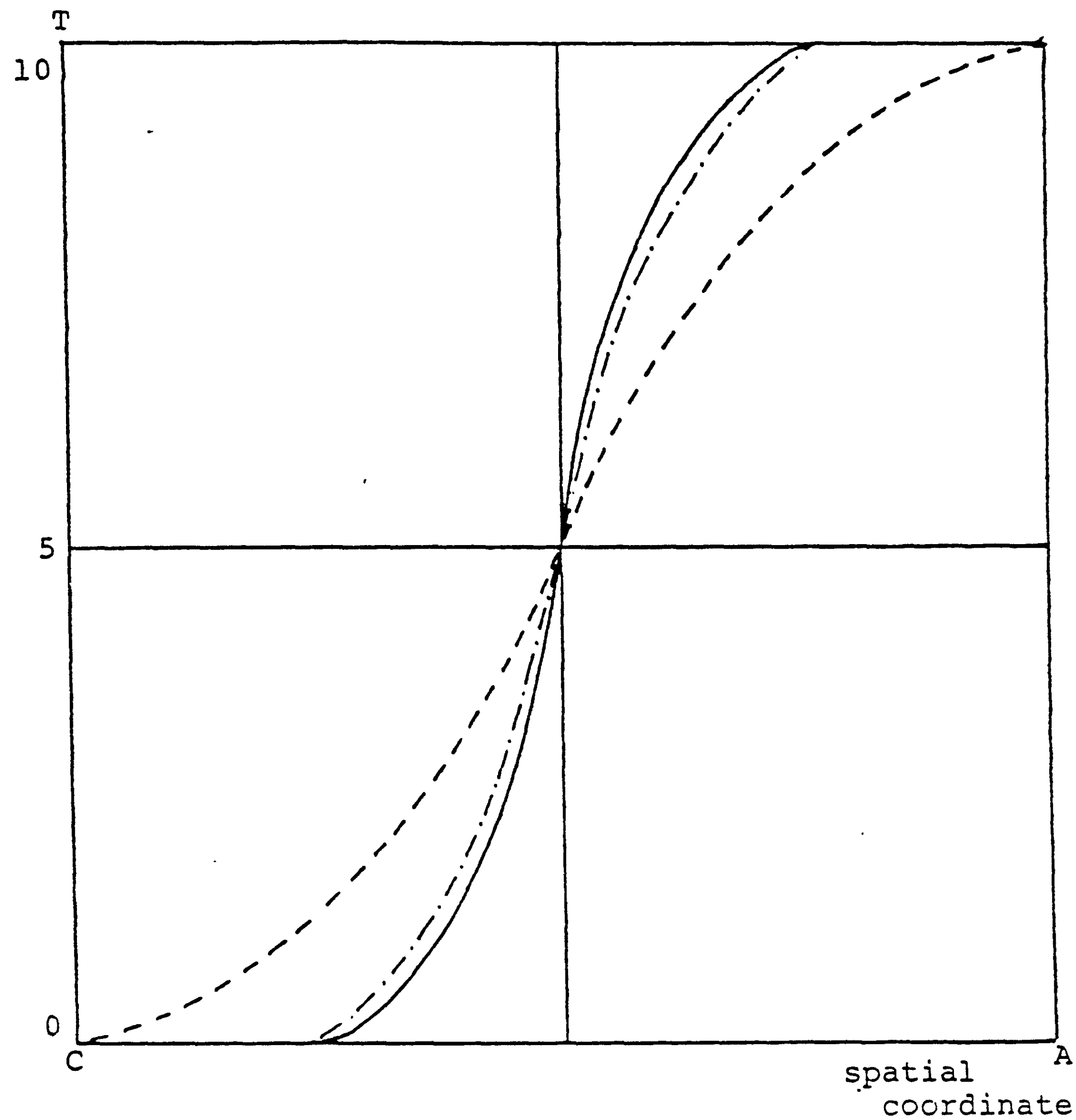

Fig. 5.18. Comparison of the analytic solution, numerical solution by donor cell scheme and numerical solution by corrective scheme for 6x6 meshes along the line CA in Fig. 5.3(B)

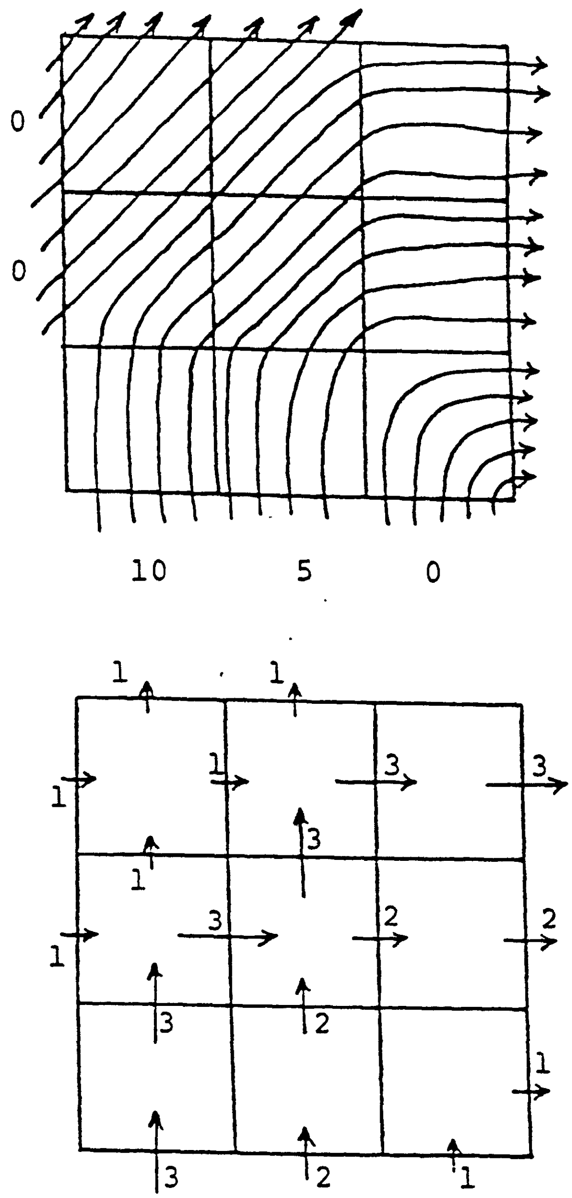

$\Delta x = \Delta y = 1$

Fig. 5.19. Simple recirculating flow field for test of the implementation strategies of the corrective scheme

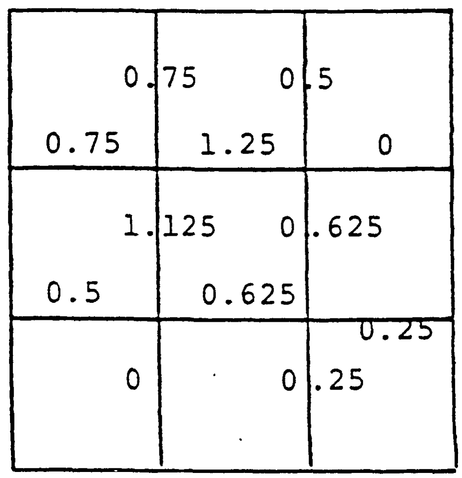

mesh point implementation

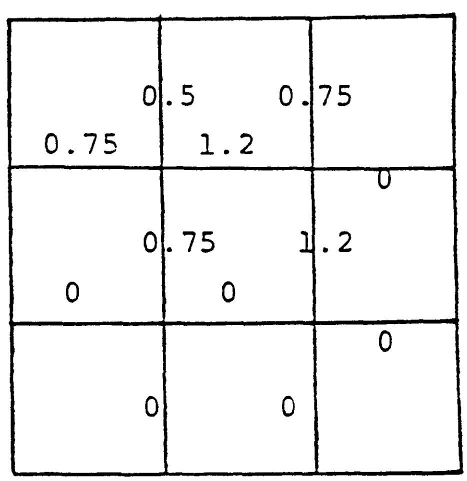

mesh interface implementation

Fig. 5.20. Diffusion constant corrections at each interface for the mesh point and mesh interface implementations of the corrective for the recirculating flow field given in Fig. 5.19

True solution

0	7.5	10
7.5	8	5
10	5	0

Donor cell

3.75	5.81	5.81
7.5	6.5	6.5
10	5	0

mesh point implementation

-5.18	7.21	7.21
11.26	8.86	12.94
9.75	6.08	-9.51

mesh interface implementation

-0.83	6.16	6.16
9.82	8.10	8.10
10	5	0

Fig. 5.21. Comparison of the true solution, donor cell solution and solutions by the mesh point and mesh interface implementations of the corrective scheme for the recirculating flow field given in Fig. 5.19

while the mesh interface implementation gives a physically reasonable solution. The true solution cannot be reproduced because some of the information about the flow field has already been lost in Fig. 5.19.

Another test calculation is done for a two dimensional, rectangular containment with an arbitrary recirculating flow field. There was initially air in the containment and steam is introduced in the source mesh at the rate of 0.2 kg/sec. After a while a flow field is set up in the containment by the input mass and momentum of steam. This flow field is used here to test the mesh point and mesh interface implementations of the corrective scheme. Since the steam concentration distribution and flow field are given at the start of the calculation, the steam concentration for the new time step can be calculated in an explicit way. Figure 5.22 shows the flow field in the containment and more detailed information about the flow field is given in Fig. 5.23. The steam concentration distribution at the beginning is given in Fig. 5.24 in which the source mesh has the highest steam concentration. Figure 5.25 and Fig. 5.26 show the diffusion constant corrections of the mesh point and mesh interface implementations and Fig. 5.27 and Fig. 5.28 show the steam concentration distributions after one time step, 0.3 sec with the corrections in Fig. 5.25 and Fig. 5.26, respectively. The result in Fig. 5.28 is not a reasonable solution while the mesh interface implementation result in Fig. 5.27 is physically reasonable and even better

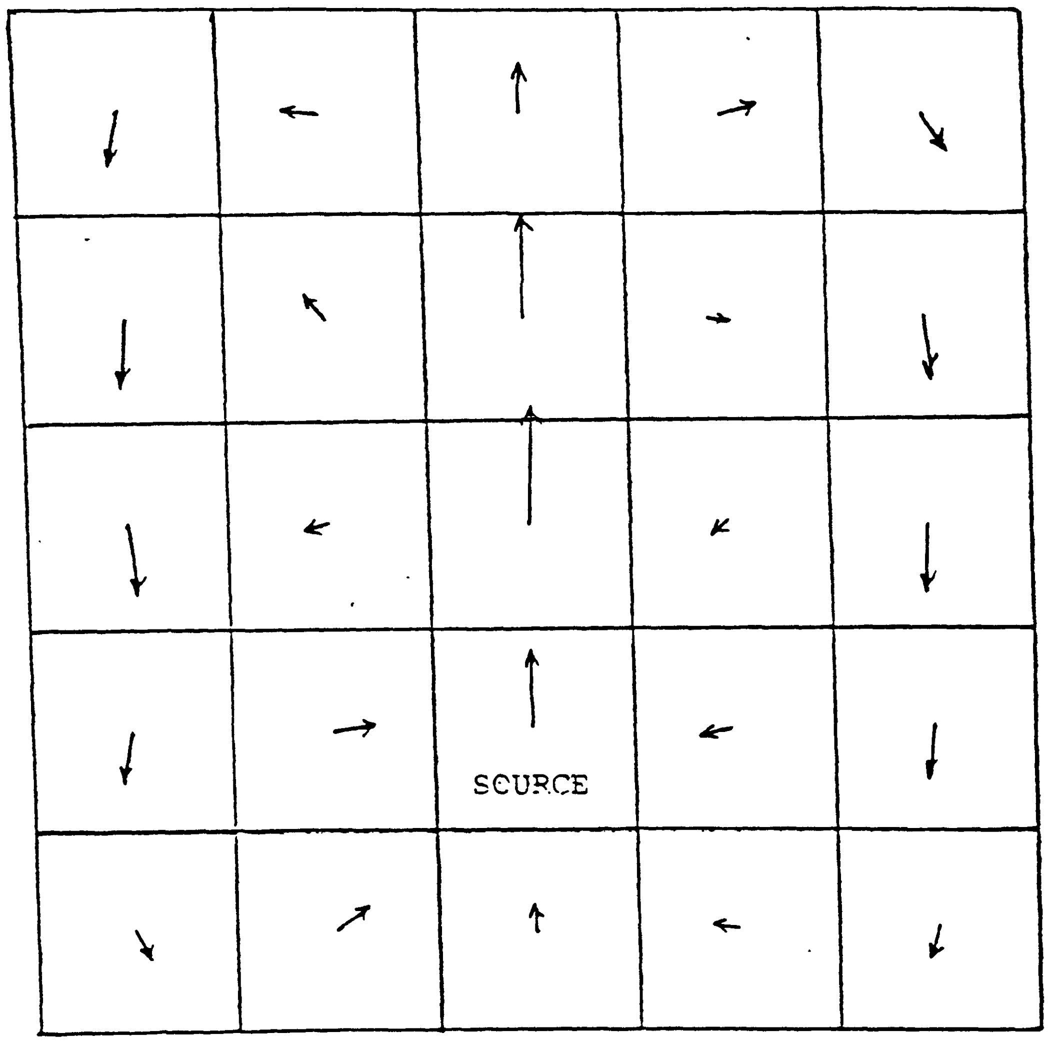

$\Delta x = 0.5m$

$\Delta y = 1.0m$

Fig. 5.22. Recirculating flow field for calculation of the steam concentration distribution in the two dimensional containment to test the mesh point and mesh interface implementations of the convective scheme

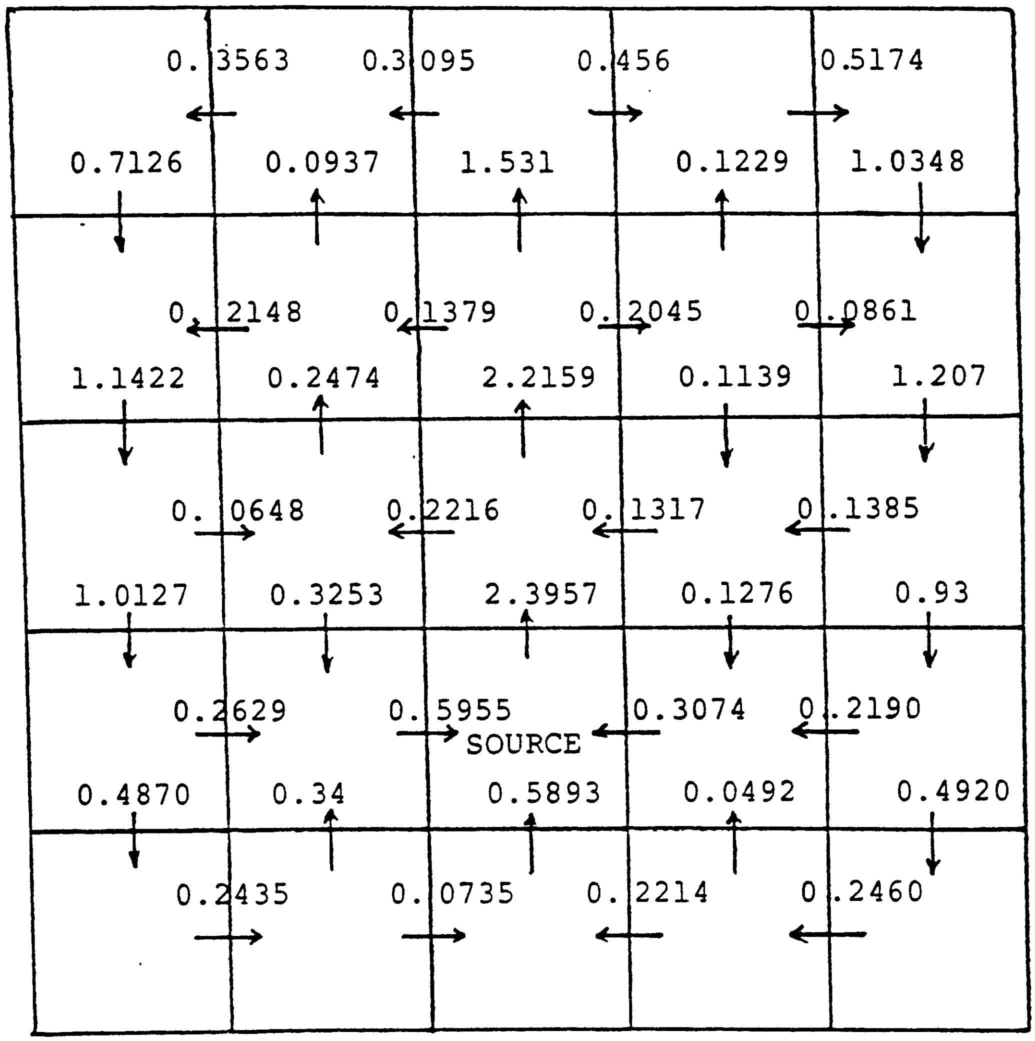

velocity [m/sec]

$\Delta x = 0.5$ m $\Delta y = 1$ m

Fig. 5.23. Detailed flow field for calculation of the steam concentration distribution in the two dimensional containment to test the mesh point and mesh interface implementations of the corrective scheme

0.0819	0.1420	0.1750	0.1592	0.1085
0.0620	0.1178	0.1712	0.1266	0.0676
0.0358	0.1244	0.1710	0.0305	0.0346
0.0179	0.0298	0.1859 SOURCE	0.0095	0.0136
0.0049	0.0011	0.0002	0.0007	0.0031

$\Delta x = 0.5$m
$\Delta y = 1$m
steam concentration in [kg/m^3]

Source: 0.2 kg/sec of steam

Fig. 5.24. Initial steam concentration distribution in the two dimensional containment to test the mesh point and mesh interface implementations of the corrective scheme

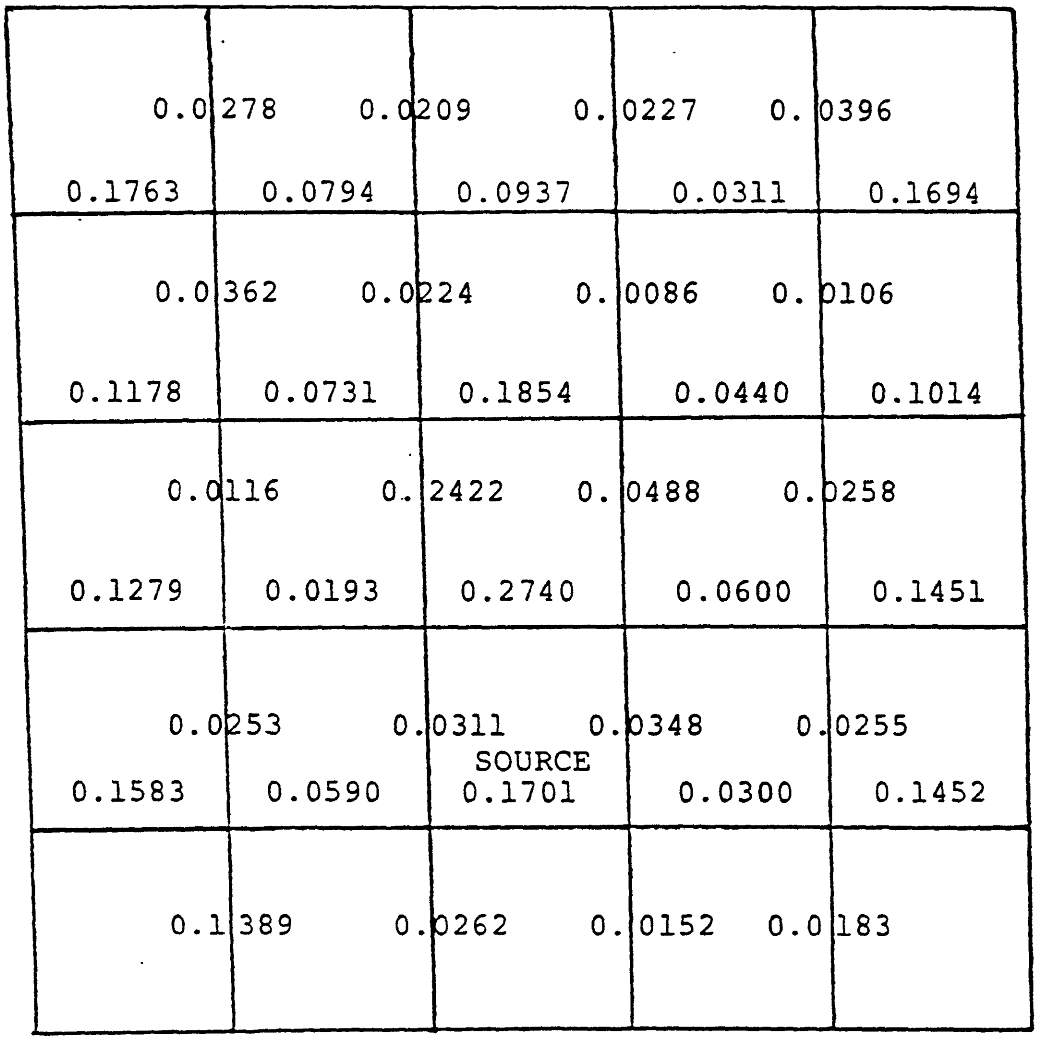

$\Delta x = 0.5m$

$\Delta y = 1m$

Diffusion constant in [m^2/sec]

Fig. 5.25. Diffusion constant corrections of the mesh point implementation of the corrective scheme for calculation of the steam concentration distribution in the two dimensional containment

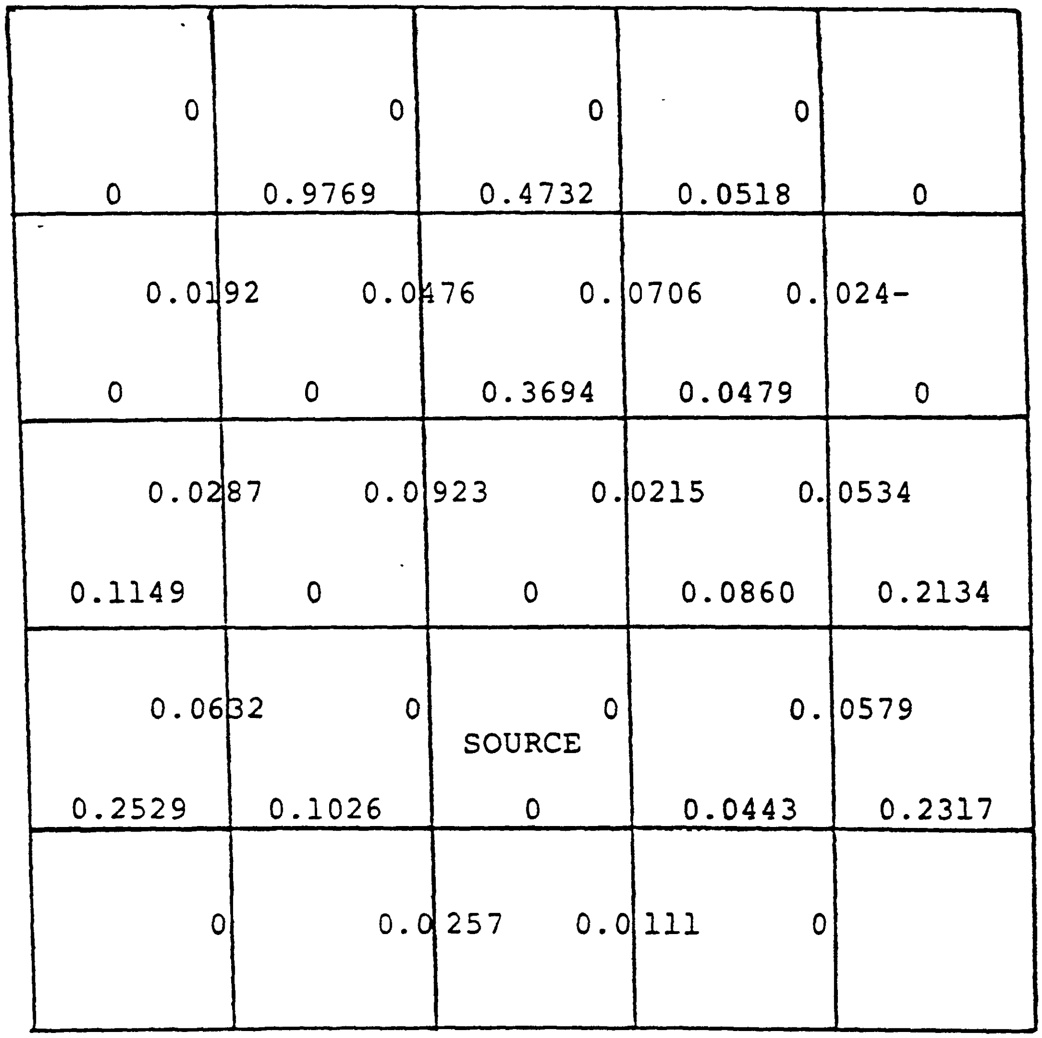

Δx = 0.5m

Δy = 1m

Diffusion constant in [m^2/sec]

Fig. 5.26. Diffusion constant corrections of the mesh interface implementation of the corrective scheme for calculation of the steam concentration distribution in the two dimensional containment

0.0947	0.1475	0.1733	0.1623	0.1243
0.0735	0.1135	0.1711	0.1321	0.0833
0.0448	0.1363	0.1706	0.0342	0.0465
0.0233	0.0342	0.1847 SOURCE	0.0107	0.0195
0.0068	0.0016	0.0003	0.0011	0.0046

$\Delta x = 0.5m$

$\Delta y = 1m$

steam concentration in [kg/m^3]

Source: o.2 kg/sec of steam

Fig. 5.27. Steam concentration distribution after one time step, 0.3 sec, with donor cell differencing of convection term without any diffusion correction

0.0937	0.1493	0.1747	0.1646	0.1240
0.0709	0.1797	0.1729	0.1334	0.0815
0.0433	0.1247	0.1911	0.0250	0.0465
0.0229	0.0287	0.2086 SOURCE	0.0029	0.0355
0.0068	0.0005	-0.0092	0.0010	0.0042

$\Delta x = 0.5m$

$\Delta y = 1m$

steam concentration in [kg/m^3]

Source: 0.2 kg/sec of steam

Fig. 5.28. Steam concentration distribution after one time step, 0.3 sec, with mesh point implementation of the corrective scheme

0.0947	0.1487	0.1738	0.1628	0.1243
0.0722	0.1112	0.1756	0.1310	0.0815
0.0424	0.1342	0.1794	0.0295	0.0481
0.0228	0.0360	0.1847 SOURCE	0.0100	0.0192
0.0058	0.0007	0.0003	0.0010	0.0039

$\Delta x = 0.5m$

$\Delta y = 1m$

steam concentration in [kg/m^3]

Source: 0.2 kg/sec of steam

Fig. 5.29. Steam concentration distribution after one time step, 0.3 sec, with mesh interface implementation of the corrective scheme

than the donor cell solution. In the meshes at the top of the source mesh, the steam concentration should decrease as the flow goes up to the ceiling because most of the steam introduced in the source mesh goes upward and gets distributed by convection and diffusion.

5.3 ADI Solution

The ADI scheme is tested to use a time step size larger than the Courant limit. Although the Von Neumann analysis shows that the ADI scheme is unconditionally stable, it has the maximum time step size that can give a physically reasonable solution. It is found that a wise use of the ADI scheme can reduce the overall computation time in comparison with the explicit and implicit schemes.

The results of the ADI and explicit schemes are compared in the problem geometry of Fig. 5.30. In Fig. 5.30 there is an inflow from the bottom surface at the velocity of $v=1.0$ and the inlet boundary value of Φ is, $\Phi=10.0$. There is a source of Φ on the right boundary over two computational meshes and the profile of Φ along the dotted line is affected by that source. Figure 5.31 shows the profiles of Φ along the dotted line for the time step size of 0.5 sec, when the Courant limit is 1 sec. The ADI and explicit schemes give almost identical results during all the transient. Figure 5.32 shows the profiles of Φ at the same location for the time step size of 1 sec, which is exactly the

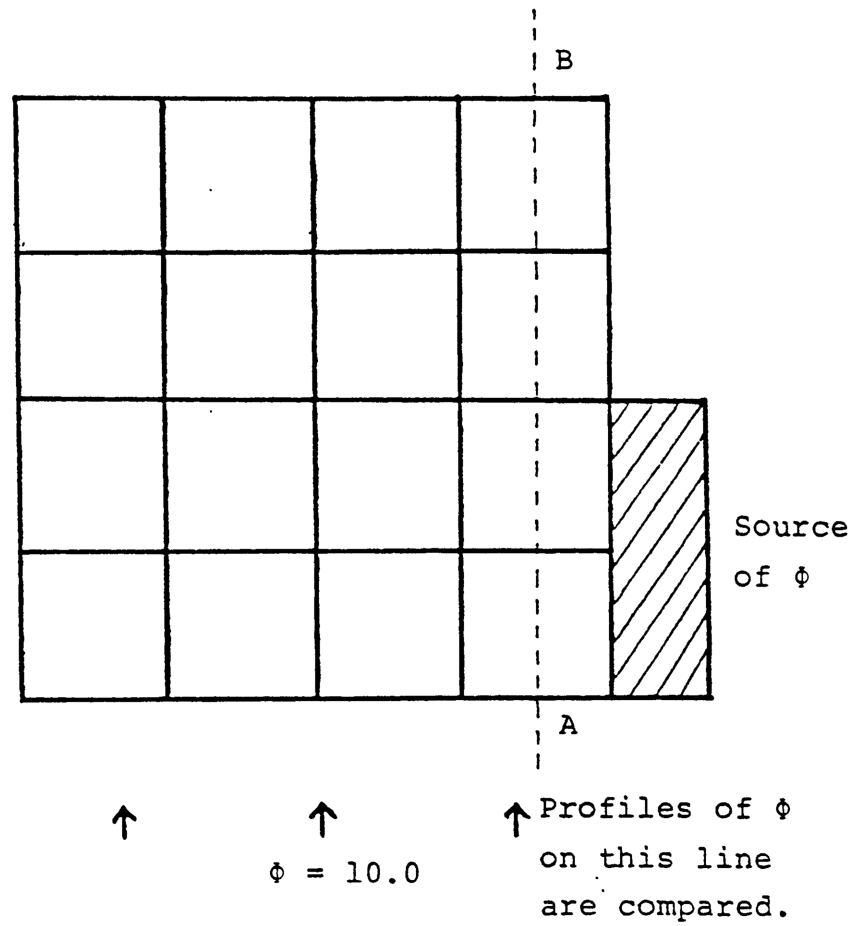

$v = 1.0$

$\alpha = 1.0$

$\Delta x = \Delta y = 1.0$

Fig. 5.30. Problem geometry for comparison of the explicit and ADI solution schemes

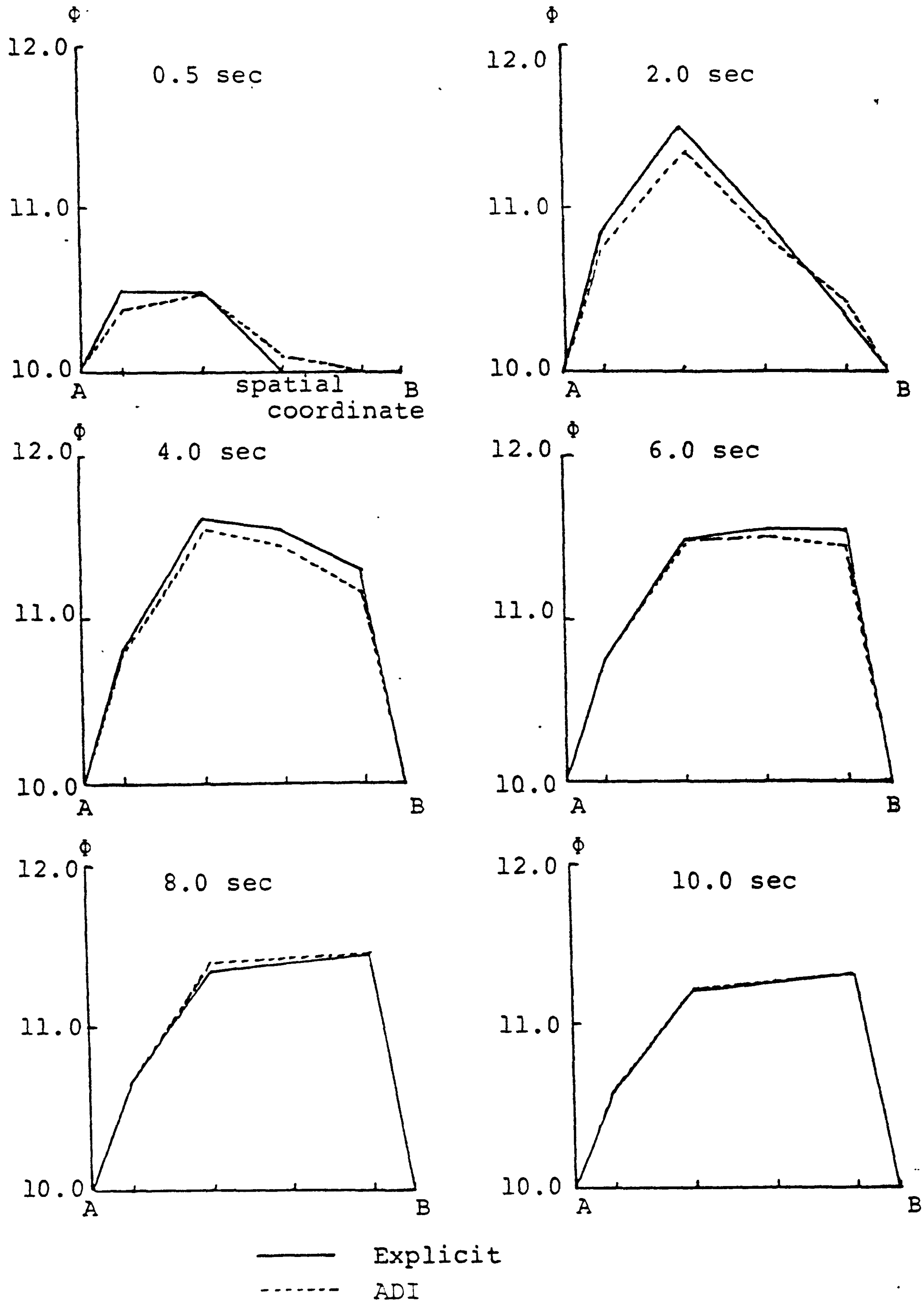

Fig. 5.31. Comparison of the explicit and ADI solutions for the profile of Φ along the line AB in Fig. 5.30 for Δt=0.5 sec and the Courant limit of 1.0 sec

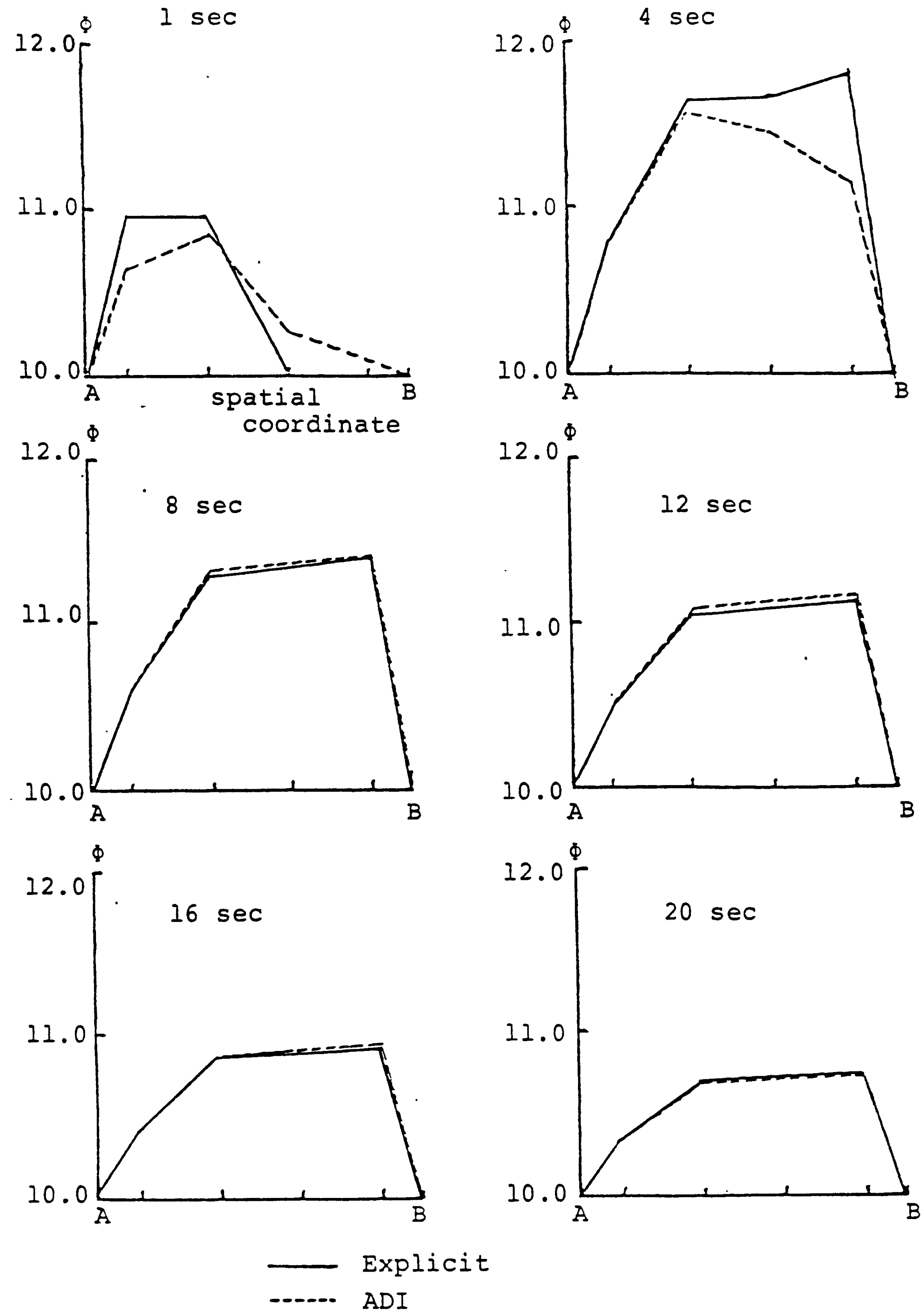

Fig. 5.32. Comparison of the explicit and ADI solutions for the profile of Φ along the line AB in Fig. 5.30 for Δt=1.0 sec and the Courant limit of 1.0 sec

the Courant limit. Initially, there is some deviation between the two results, but it damps out rapidly and the ADI scheme gives almost identical results with the explicit scheme. No cross-flow diffusion corrections are involved in the results of Fig. 5.31, Fig. 5.32 and Fig. 5.33. Fig. 5.33 shows that the ADI scheme can use a time step size up to five times the Courant limit. The deviation for the time step size of 5 sec is expected to damp out as the calculation goes over to the next time steps because of the unconditional stability.

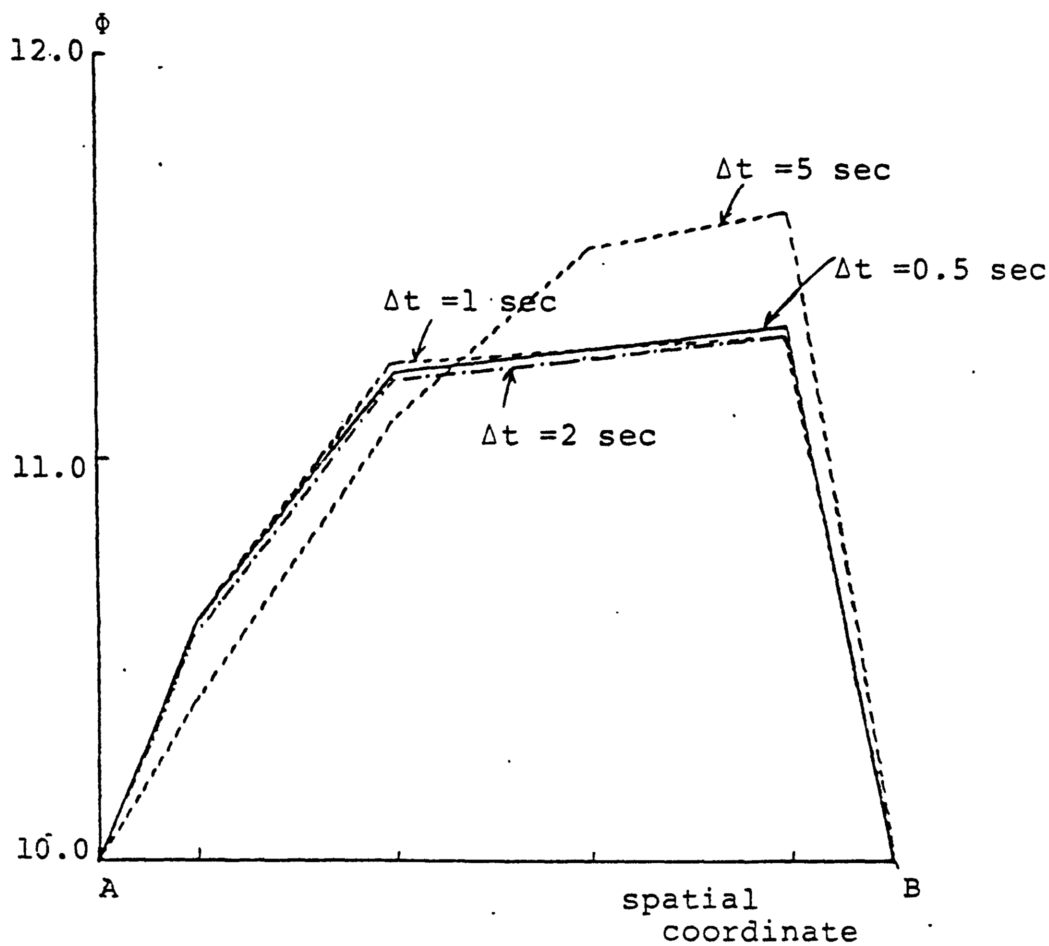

Fig. 5.33. Comparison of the ADI solutions for the profile of Φ at t=10.0 sec along the line AB in Fig. 5.30 with different time step sizes

CHAPTER 6

CONCLUSION

6.1 Physical Models

(1) The solution scheme presented in Chapter 2 has been adequate for modelling the slow mixing stage in the containment after a loss-of-coolant accident. The continuity/momentum equations are decoupled from the scalar transport equations and solved by the SMAC scheme to obtain the flow field. The mass diffusion, energy, and turbulence equations are solved separately using that flow field. The thermal equilibrium is assumed and the phase change occurs to maintain 100% relative humidity, or superheated steam as may be appropriate.

(2) The models of laminar and turbulent diffusions in Chapter 3 may be adequate for predicting the hydrogen transport in the containment. The total diffusion constant is the sum of the laminar and turbulent diffusion constants.

6.2 Numerical Schemes

(1) There are two numerical diffusion sources, truncation error and cross-flow diffusion, in the finite difference donor cell treatment of convection. Cross-flow diffusion occurs due to the donor cell treatment of the convection term in a multi-dimensional problem. The

effective diffusion constants of the truncation error and cross-flow diffusion are of the same order of magnitude, $\sim u\Delta x$. The truncation error diffusion occurs in the flow direction while the cross-flow diffusion occurs in the diagonal direction of neighboring mesh points. The gradient of the scalar quantity under consideration is usually small in the flow direction in comparison with that in the direction normal to the flow. Therefore, most of the numerical diffusion error in a multi-dimensional, convection dominant, recirculating flow problem is due to the cross-flow diffusion.

(2) Two types of approaches, skew differencing and corrective schemes, have been tried in order to eliminate the numerical diffusion. The skew differencing scheme gives good results for some problems, but not always. It gives unphysical results for most recirculating flow and coarse mesh problems. The inclusion of corner points complicates the matrix structure and a fully implicit scheme should be used for maintenance of stability. The corrective scheme is based on the fact that the additional cross-flow diffusion can be predicted theoretically for every mesh at every time step. It is conservative and an explicit scheme can be used without affecting the simple solution structure. Therefore, the corrective scheme is generally preferred to the skew differencing scheme.

(3) Two implementation strategies, mesh point and mesh interface, are tried for the corrective scheme. They are identical in a unidirectional flow. The mesh interface implementation is always preferred to the mesh point implementation in a recirculating flow problem. The results of various sample problems show that the mesh interface implementation of the corrective scheme always gives a physically reasonable solution with negligible numerical diffusion error.

(4) The Von Neumann stability analysis is applied to various finite difference forms of a general conservation equation. The graphical method is used to obtain the stability condition in terms of the Courant, diffusion and cell Reynolds numbers, i.e., C_x, d_x and R_x, using the characteristics of a quadratic equation. The results of numerical experiments are found to be consistent with the Von Neumann analysis.

(5) The maximum time step size is limited by the Courant condition in an explicit scheme. The Alternate Direction Implicit (ADI) scheme can be used to increase the time step size and decrease the overall computational effort. Although the Von Neumann analysis shows that the ADI scheme is unconditionally stable, it has its own limitations due to the following factors.

First, the physical constraint in section 4.4.2 imposes a maximum time step size that can give a physically reasonable solution.

Second, the ADI scheme is a fractional step method. The asymmetry of the given problem may give different results according to the sweeping sequence. For example, a steady-state solution may never be reached due to the fact that one time step is composed of a few fractional steps.

CHAPTER 7

RECOMMENDATIONS FOR FUTURE WORK

7.1 Physical Models

Since both the laminar and turbulent flow regimes are possible in a complicated geometry and flow field, it is necessary to predict the flow regime in order to use appropriate physical models. A criterion for the flow regime should be developed in such a form that it may be implemented into a computer code. The important parameters may be the velocity, geometry (e.g., distance from the wall), velocity gradient, previous time step information, time step size, etc.

The flow regime criterion may be replaced with a model that covers all the turbulent, transitional and laminar flow regimes. The model should show proper limiting behaviors as the Reynolds number goes to infinity (turbulent) and zero (laminar). The modified $k-\varepsilon$ model in a low Reynolds number flow may be a guide in this approach.

7.2 Numerical Schemes

There have been two approaches, skew-differencing and corrective schemes, to eliminate the cross-flow diffusion. They may still be improved further to get an accurate solution in a transient, multi-dimensional recirculating flow problem.

Corrective scheme

The corrective scheme has been successful by the mesh interface implementation strategy in the scope of this work. More tests and validation calculations are required in recirculating flow problems.

Skew differencing scheme

1. The conservative form of the skew differencing scheme is complicated and time consuming in comparison with the corrective scheme. It may be possible to develop a reasonably simple form that may or may not include the corner points. The solution in Appendix A may be a useful guide in this work.

2. The stability of the skew-differencing scheme is open to question in the explicit, ADI and implicit schemes although only the implicit scheme has been used up to now.

REFERENCES

[1] Amsden, A.A. and Harlow, F.H., "Transport of Turbulence in Numerical Fluid Dynamics," Journal of Comp. Phys. 3, 94-110 (1968).

[2] Amsden, A.A. and Harlow, F.H., "The SMAC method: A numerical technique for calculating incompressible flows," LA-4370 (May 1970).

[3] Amsden, A.A. and Harlow, F.H., "A Simplified MAC Technique for Incompressible Fluid Flow Calculations," Journal of Comp. Phys. 6, 332-325 (1970).

[4] Baliga, B.R. and Patankar, S.V., "A New Finite Element Formulation for Convection-Diffusion Problems," Numerical Heat Transfer 3, 393-409 (1980).

[5] Bird, R.B., Stewart, W.E. and Lightfoot, E.N., Transport Phenomena, John Wiley & Sons (1960).

[6] Bloom, G.R. et al., "Hydrogen Distribution in a Containment With a High-Velocity Hydrogen-Steam Source," HEDL-SA-2682 (October 1982).

[7] Boyle, D.R., "Transient Effects in Turbulence Modelling," MIT Ph.D. thesis (1979).

[8] Bradshaw, P., Cebeci, T. and Whitelaw, J.H., Engineering Calculation Methods for Turbulent Flow, Academic Press (1981).

[9] Briggs, D.G., "A Finite Difference Scheme for the Incompressible Advection-Diffusion Equation," Comp. Methods in Applied Mech. and Eng. 6, 233-241 (1975).

[10] Briley, W.R. and McDonald, H., "Solution of the Multi-dimensional Compressible Navier-Stokes Equations by a Generalized Implicit Method," Journal of Comp. Phys. 24, 372-397 (1977).

[11] Briley, W.R. and McDonald, H., "On the Structure and Use of Linearized Block Implicit Schemes," Journal of Comp. Phys. 34, 54-73 (1980).

[12] Broadus, C.R. et al., "BEACON/MOD 3: A Computer Program for Thermal-hydraulic Analysis of Nuclear Reactor Containments - User's Manual," NUREG/CR-1148 (EGG-208), (April 1980).

[13] Carbajo, J.J., "Study of Non-homogeneous Conditions in Reactor Containments Due to Separation Effects," Nuclear Eng. and Design 69, 95-107 (1982).

[14] Cebeci, T., Hirsh, R.S., Keller, H.B., Williams, P.G., "Studies of Numerical Methods for the Plane Navier-Stokes Equations," Comp. Methods in Applied Mech. and Eng. 27, 13-44 (1981).

[15] Chang, S.H., "Buoyancy Effects in Mathematical and Numerical Turbulence Modelling," MIT M.S. thesis (1980).

[16] Chang, S.H., "Comparative Analysis of Numerical Methods for the Solution of Navier-STokes Equations," MIT Ph.D. thesis (1981).

[17] Chen, Y.B., "Coolant Mixing in the LMFBR Outlet Plenum," MIT Ph.D. thesis (1977).

[18] Cheng, S.I., "Accuracy of Difference Formulation of Navier-Stokes Equations," The Phys. of Fluids Supplement 2 (1969).

[19] Clark, M., Jr. and Hansen, K.F., "Numerical Methods of Reactor Analysis, Academic Press (1964).

[20] Cloutman, L.D., Hirt, C.W. and Romero, N.C., "SOLA-ICE: A Numerical Solution Algorithm for Transient Compressible Fluid Flows," LA-6236 (July 1976).

[21] Cook, J.L. and Nakayama, P.I., "VARR-2 - A Computer Program for Calculating Time-dependent Turbulent Fluid Flows with Slight Density Variation," CRBRP-ARD-0106, Vol. 1 (Nov. 1976).

[22] Covelli, B., Varadi, G., Nielsen, L. and Lewis, M., "Simulation of Containment Cooling with Outside Spray After a Core Meltdown," Nuclear Eng. and Design 69, 127-137 (1982).

[23] Crowley, W.P., "Second-Order Numerical Advection," Journal of Comp. Phys. 1, 471-484 (1967).

[24] De Vahl Davis, G. and Mallison, G.D., "An Evaluation of Upwind and Central Difference Approximations by a Study of Recirculating Flow," Computers and Fluids, Vol. 4, 29-43 (1976).

[25] Dukowicz, J.K. and Ramshaw, J.D., "Tensor Viscosity Method for Convection in Numerical Fluid Dynamics," Journal of Comp. Phys. 32, 71-79 (1979).

[26] Fromm, J.E., "Practical Investigation of Convective Difference Approximations of Reduced Dispersion," The Phys. of Fluids Supplement 2 (1969).

[27] Gebhart, B., "Buoyancy Induced Fluid Motions Characteristic of Applications in Technology - The 1978 Freeman Scholar Lecture," Journal of Fluids Eng., Vol. 101, 5-28 (March 1979).

[28] Gupta, M.M. and Marohar, R.P., "On the Use of Central Difference Scheme for Navier-Stokes Equations," Int. J. for Num. Methods in Eng., Vol. 15, 557-573 (1980).

[29] Hamza, R. and Golay, M.W., "Behavior of Buoyant Moist Plumes in Turbulent Atmospheres," MIT-EL 81-020 (June 1981).

[30] Han, T., Humphrey, J.A.C. and Launder, B.E., "A Comparison of Hybrid and Quadratic Upstream Differencing in High Reynolds Number Elliptic Flows," Comp. Methods in Applied Mech. and Eng., 29, 81-95 (1981).

[31] Harlow, F.H. and Amsden, A.A., "Numerical Calculation of Almost Incompressible Flow," Journal of Comp. Phys., 3, 80-93 (1968).

[32] Harlow, F.H. and Amsden, A.A., "A Numerical Fluid Dynamics Calculation Method for All Flow Speeds," Journal of Comp. Phys., 8, 197-213 (1971).

[33] Harlow, F.H. and Amsden, A.A., "Numerical Calculation of Multiphase Fluid Flow," Journal of Comp. Phys., 17, 19-52 (1975).

[34] Hinze, J.O., Turbulence, McGraw-Hill Book Company, 2nd ed. (1975).

[35] Hirschfelder, J.O., Curtiss, C.F. and Bird, R.B., Molecular Theory of Gases and Liquids, Wiley, New York (1954).

[36] Hirt, C.W., "Heuristic Stability Theory for Finite Difference Equations," Journal of Comp. Phys., 2, 339-355 (1968).

[37] Hirt, C.W., "Computer Studies of Time-dependent Turbulent Flows," The Phys. of Fluids Supplement 2 (1969).

[38] Hoffman, G.H., "Improved Form of the Low Reynolds Number k-ε Turbulence Model," The Phys. of Fluids, Vol. 18, 309-312 (March 1975).

[39] Houston, M.H., Jr. and De Braemaecker, J. Cl., "ADI Solution of Free Convection in a Variable Viscosity Fluid," Journal of Comp. Phys., 16, 221-239 (1974).

[40] Jones, W.P. and Launder, B.E., "The Prediction of Laminarization with a Two-equation Model of Turbulence," Int. J. Heat Mass Transfer, Vol. 15, 301-314 (1972).

[41] Jones, W.P. and Launder, B.E., "The Calculation of Low Reynolds Number Phenomena with a Two-equation Model of Turbulence," Int. J. Heat Mass Transfer, Vol. 16, 1119-1130 (1973).

[42] Keenan, J.H. and Keyes, F.G., Steam Tables, John Wiley & Sons (1978).

[43] Lam, C.K.G. and Bremhorst, K., "A Modified Form of the k-ε Model for Predicting Wall Turbulence," Trans. of the ASME, Vol. 103, 456-460 (Sept. 1981).

[44] Langer, G. et al., "Experimental Investigation of Hydrogen Distribution in a Containment of a Light Water Reactor Following a Coolant Loss Accident," BF-63.363-3, Battelle Institute e.V. Frankfurt, translated (October 1980).

[45] Launder, B.E. and Spalding, D.B., "The Numerical Comparison of Turbulent Flows," Comp. Methods in Applied Mech. and Eng., 3, 269-289 (1974).

[46] Launder, B.E., Reece, G.J. and Rodi, W., "Progress in the Development of a Reynolds Stress Turbulence Closure," J. Fluid Mech., Vol. 68, part 3, 537-566 (1975).

[47] Leschziner, M.A., "Practical Evaluation of Three Finite Difference Schemes for the Computation of Steady-State Recirculating Flows," Comp. Methods in Applied Mech. and Eng., 23, 293-312 (1980).

[48] Manno, V.P. and Golay, M.W., "Analytical Modelling of Hydrogen Transport in Reactor Containments," Report submitted to 2nd International Topical Meeting on Nuclear Reactor Thermalhydraulics (March 1982).

[49] Manno, V.P., "Analytical Modelling of Hydrogen Transport In Reactor Containments," MIT Sc.D. thesis (1983).

[50] Nakamura, S., Computational Methods in Engineering and Science, John Wiley & Sons, Inc. (1977).

[51] Patankar, S.V. and Spalding, D.B., "A Calculational Procedure for Heat, Mass and Momentum Transfer in Three Dimensional Parabolic Flows," Int. J. Heat Mass Transfer, 15, 1787-1806 (1972).

[52] Patankar, S.V., Numerical Heat Transfer and Fluid Flow, Hemisphere Publishing Corporation (1980).

[53] Raithby, G.D. and Torrance, K.E., "Upstream-weighted Differencing Schemes and Their Application to Elliptic Problems Involving Fluid Flow," Computers and Fluids, Vol. 2, 191-206 (1974).

[54] Raithby, G.D., "A Critical Evaluation of Upstream Differencing Applied to Problems Involving Fluid Flow," Comp. Methods in Applied Mech. and Eng., 9, 75-103 (1976).

[55] Raithby, G.D., "Skew-Upstream Differencing Schemes for Problems Involving Fluid Flow," Comp. Methods in Applied Mech. and Eng., 9, 153-164 (1976).

[56] Reid, R.C. and Sherwood, T.K., The Properties of Gases and Liquids, McGraw-Hill, New York (1958).

[57] Roache, P.J., "On Artificial Viscosity," Journal of Comp. Phys., 10, 169-184 (1972).

[58] Roache, P.J., Computational Fluid Dynamics, Hermosa Publishers, Albuquerque, New Mexico (1976).

[59] Roberts, K.B. and Weiss, N.O., "Convective Difference Schemes," Mathematics of Computation, 20 (1966).

[60] Rodi, W., "A Note on the Empirical Constant in the Kolmogorov-Prandtl Eddy-Viscosity Expression," Trans. of the ASME, 386-389 (Sept. 1975).

[61] Rodi, W., Turbulent Buoyant Jets and Plumes, Pergamon Press (1982).

[62] Runchal, A.K., "Convergence and Accuracy of Three Finite Difference Schemes for a Two Dimensional Conduction and Convection Problem," Int. J. for Num. Methods in Eng., 4, 541-550 (1972).

[63] Schonauer, W., "Numerical Experiments with a Difference Model for the Navier-Stokes Equations (Turbulence Model)," The Phys. of Fluids Supplement 2 (1969).

[64] Shin, Y.W. and Valentin, R.A., "Numerical Analysis of Fluid Hammer Waves by the Method of Characteristics," Journal of Comp. Phys., 20, 220-237 (1976).

[65] Smith, R.M. and Hutton, A.G., "The Numerical Treatment of Advection: A Performance Comparison of Current Methods," Numerical Heat Transfer, 3, 411-428 (1980).

[66] Spalding, D.B., "A Novel Finite Difference Formulation for Differential Expressions Involving Both First and Second Derivatives," Int. J. For Num. Methods in Eng., 4, 551-559 (1972).

[67] Stubley, G.D., Raithby, G.D. and Strong, A.B., "Proposal for a New Discrete Method Based on an Assessment of Discretization Errors," Numerical Heat Transfer, 3, 411-428 (1980).

[68] Stubley, G.D., Raithby, G.D., Strong, A.B. and Woolner, K.A., "Simulation of Convection and Diffusion Processes by Standard Finite Difference Schemes and by Influence Schemes," Comp. Methods in Applied Mech. and Eng., 35, 153-168 (1982).

[69] Stuhmiller, J.H., "Development and Validation of a Two-Variable Turbulence Model," SAI-74-509-LJ, (Jan. 1974).

[70] Tennekes, H. and Lumley, J.L., A First Course in Turbulence, MIT Press (1970).

[71] Torrance, K.E., "Comparison of Finite Difference Computations of Natural Convection," Journal of Research of the National Bureau of Science - B. Mathematical Sciences, Vol. 72B, No. 4 (Oct.-Dec. 1968).

[72] Trent, D.S., Budden, M.J. and Eyler, L.L., "TEMPEST: A Three-dimensional Time-dependent Computer Program for Hydrothermal Analysis," FATE-80-114 (Jan. 1981).

[73] Wilke, C.R., "Diffusional Properties of Multicomponent Gases," Chemical Engineering Progress, Vol. 46, No. 2, 95-102 (1950).

APPENDIX A

ANALYTICAL SOLUTION FOR THE PROBLEM IN FIGURE 5.3(B)

A steady state two dimensional energy conservation equation without any source is given in the following Eq. A.1.

$$\rho c_p u \frac{\partial T}{\partial x} = k\left(\frac{\partial^2 T}{\partial x^2} + \frac{\partial^2 T}{\partial y^2}\right) \tag{A.1}$$

In Eq. A.1 convection occurs in the x direction and diffusion occurs in both x and y directions. The boundary conditions are specified in Fig. 5.3(B) and the constants can be grouped into one constant, c, as follows.

$$\alpha = \frac{k}{\rho c_p}$$

$$c = \frac{u}{2\alpha}$$

Therefore, Eq. A.1 is reduced to the following form.

$$2c\frac{\partial T}{\partial x} = \frac{\partial^2 T}{\partial x^2} + \frac{\partial^2 T}{\partial y^2} \tag{A.2}$$

Equation A.2 is simplified further by substitution of Φ for T as follows.

$$\frac{\partial^2 \Phi}{\partial x^2} + \frac{\partial^2 \Phi}{\partial y^2} = c^2 \Phi \tag{A.3}$$

where

$$\Phi = e^{-cx}T \tag{A.4}$$

The boundary conditions should also be expressed in terms of Φ as given in Fig. A.1.

Equation A.3 can be solved by the method of separation of variables. The variable Φ is separated into two variables, X and Y, which are functions of x and y only respectively.

$$\Phi(x,y) = X(x)Y(y) \tag{A.5}$$

Then Eq. A.3 is reduced to the following form.

$$\frac{1}{X}\frac{d^2X}{dx^2} + \frac{1}{Y}\frac{d^2Y}{dy^2} = c^2 \tag{A.6}$$

The two terms on the left hand side of Eq. A.6 should be equal to some constants because they are functions of x and y only respectively and the sum of them is equal to a constant, c^2.

$$\frac{1}{X}\frac{d^2X}{dx^2} = \alpha^2 \tag{A.7}$$

$$\frac{1}{Y}\frac{d^2Y}{dy^2} = c^2 - \alpha^2 = -\beta^2 \tag{A.8}$$

where $\alpha > c > 0$

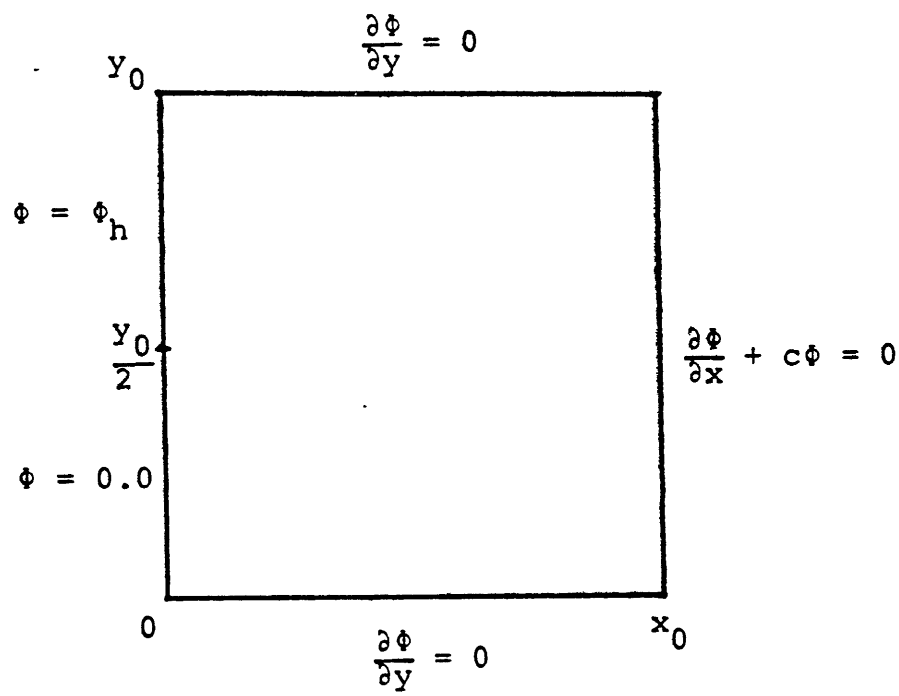

Fig. A.1. Boundary conditions in terms of Φ for the problem in Fig. 5.3(B) where Φ is given by,
$\Phi = e^{-cx}\ T$

The solutions to Eq. A.7 and Eq. A.8 can be easily obtained as follows.

$$X = C_1 e^{\alpha x} + C_2 e^{-\alpha x} \tag{A.9}$$

$$Y = C_3 \sin\beta y + C_4 \cos\beta y \tag{A.10}$$

The boundary conditions in Fig. A.1 may be given in terms of the variables X and Y as follows. The boundary condition at x=0 will be considered later.

$$\left(\frac{dY}{dy}\right)_{y=0} = 0 \tag{A.11}$$

$$\left(\frac{dY}{dy}\right)_{y=y_0} = 0 \tag{A.12}$$

$$\left(\frac{dX}{dx} - cX\right)_{x=x_0} = 0 \tag{A.13}$$

In order to satisfy the boundary conditions given in Eq. A.11, Eq. A.12 and Eq. 13, the constants in Eq. A.9 and Eq. A.10 should satisfy the following relations.

$$C_3 = 0 \tag{A.14}$$

$$\beta_n y_0 = n\pi \tag{A.15}$$

$$\frac{C_2}{C_1} = \left(\frac{\alpha_n + c}{\alpha_n - c}\right) e^{2\alpha_n x_0} \qquad (\alpha_n \neq c) \tag{A.16}$$

where

$$\alpha_n^{\,2} = c^2 + \left(\frac{n\pi}{y_0}\right)^2$$

$$= c^2 + \beta_n^{\,2} \, .$$

Therefore, the final solution can be expressed as follows.

$$\Phi = A_0 e^{-\alpha_n x} + \sum_{n=1}^{\infty} A_n \left[e^{\alpha_n x} + \left(\frac{\alpha_n + c}{\alpha_n - c}\right) e^{2\alpha_n x_0} \, e^{-\alpha_n x} \right] \cos\beta_n y$$

(A.17)

$$T(x,y) = e^{cx}\Phi(x,y) \qquad (A.18)$$

where

$$\beta_n = \frac{n\pi}{y_0}$$

$$\alpha_n = \sqrt{c^2 + \beta_n^2}$$

Since the boundary condition at x=0 should also be satisfied, the constants A_i are determined as follows.

$$A_0 = \frac{T_h}{2.0}$$

$$A_n = \frac{-2T_h}{n\pi} \, \frac{1}{1 + \left(\frac{\alpha_n + c}{\alpha_n - c}\right) e^{2\alpha_n x_0}} \, \sin\frac{n\pi}{2} \qquad (n=1,2,3\ .\ .\ .)$$

(A.19)

APPENDIX B

ADI SCHEME FOR MOMENTUM EQUATION

The ADI scheme can replace the explicit scheme in the momentum equation in order to eliminate the Courant condition for the time step size. When the tilde phase of the SMAC scheme and other scalar transport equations are solved by the ADI scheme, the computational effort for one time step is greater than that of the explicit scheme. Therefore, the time step size in the ADI should be at least two or three times the Courant limit in order to have a gain in the overall computational efforts required for a problem. The time step size limitation in the ADI scheme comes from the semi-implicit treatment of the non-linear convection term. Since there are two steps involved in solving the momentum equation in each direction, there are six sweeps in a three dimensional problem and four sweeps in a two dimensional problem. The sequence of the sweeps is arbitrary and depends on the problem under consideration. The most important sweep should be given the first priority and most updated information.

The ADI scheme is applied to a two dimenaional momentum equation in the following Eq. B.1-Eq. B.4. They are formulated for a natural convection problem where the gravity acts in the z-direction. Equations B.1 and B.3 are the z and x direction sweeps of the x direction momentum equation. Equations B.2 and B.4 are the x and z direction sweeps of the z-direction momentum equation. The z direction sweep of the z direction momentum equation is treated as the last one in order to be given the most updated information.

$$\frac{u^{*}_{i+\frac{1}{2}j} - u^{n}_{i+\frac{1}{2}j}}{\Delta t} + \frac{w^{n}_{i+\frac{1}{2}j+\frac{1}{2}}u^{*}_{i+\frac{1}{2}j} - w_{i+\frac{1}{2}j-\frac{1}{2}}u^{*}_{i+\frac{1}{2}j-1}}{\Delta z}$$

$$= \nu\frac{u^{*}_{i+\frac{1}{2}j+1} - 2u^{*}_{i+\frac{1}{2}j} + u^{*}_{i+\frac{1}{2}j-1}}{\Delta z^{2}} - \frac{1}{2}\frac{\partial P}{\partial r} - \frac{1}{2}RX_{i+\frac{1}{2}j}u^{n}_{i+\frac{1}{2}j}u^{*}_{i+\frac{1}{2}j} \tag{B.1}$$

$$\frac{w^{*}_{ij+\frac{1}{2}} - w^{n}_{ij+\frac{1}{2}}}{\Delta t} + \frac{u^{*}_{i+\frac{1}{2}j+\frac{1}{2}}w^{*}_{ij+\frac{1}{2}} - u^{*}_{i-\frac{1}{2}j+\frac{1}{2}}w^{*}_{i-1j+\frac{1}{2}}}{\Delta r}$$

$$= \nu\frac{w^{*}_{i+1j+\frac{1}{2}} - 2w^{*}_{ij+\frac{1}{2}} + w^{*}_{i-1j+\frac{1}{2}}}{\Delta r^{2}} - \frac{1}{2}\frac{\partial P}{\partial z} - \frac{1}{2}RZ_{ij+\frac{1}{2}}w^{n}_{ij+\frac{1}{2}}w^{*}_{ij+\frac{1}{2}} \tag{B.2}$$

$$\frac{u^{n+1}_{i+\frac{1}{2}j} - u^{*}_{i+\frac{1}{2}j}}{\Delta t} + \frac{u^{*}_{i+1j}u^{n+1}_{i+\frac{1}{2}j} - u^{*}_{ij}u^{n+1}_{i-\frac{1}{2}j}}{\Delta r}$$

$$= \nu\frac{u^{n+1}_{i+\frac{3}{2}j} - 2u^{n+1}_{i+\frac{1}{2}j} + u^{n+1}_{i-\frac{1}{2}j}}{\Delta r^{2}} - \frac{1}{2}\frac{\partial P}{\partial r} - \frac{1}{2}RX_{i+\frac{1}{2}j}u^{*}_{i+\frac{1}{2}j}u^{n+1}_{i+\frac{1}{2}j} \tag{B.3}$$

$$\frac{w^{n+1}_{ij+\frac{1}{2}} - w^{*}_{ij+\frac{1}{2}}}{\Delta t} + \frac{w^{*}_{ij+1}w^{n+1}_{ij+\frac{1}{2}} - w^{*}_{ij}w^{n+1}_{ij-\frac{1}{2}}}{\Delta z}$$

$$= \nu\frac{w^{n+1}_{ij+\frac{3}{2}} - 2w^{n+1}_{ij+\frac{1}{2}} + w^{n+1}_{ij-\frac{1}{2}}}{\Delta z^2} - \frac{1}{2}\frac{\partial P}{\partial z} + \frac{\rho-\rho_0}{\rho_0}g_z - \frac{1}{2}RZ_{ij+\frac{1}{2}}w^{*}_{ij+\frac{1}{2}}w^{n+1}_{ij+\frac{1}{2}} \tag{B.4}$$

Equations B.1, B.2, B.3, and B.4 have given almost identical results with the explicit scheme for a time step size below the Courant limit.

APPENDIX C

COMPUTER PROGRAMS

The files, 'prog1 fortran', 'prog2 fortran' and 'prog3 fortran', are the computer programs for calculating the numerical values of the analytical solution in the problem geometries, Fig. 5.3(A), Fig. 5.3(B) and Fig. 5.8.

The file, 'difprg fortran', is the program for testing the calculational logic of the mesh interface implementation of the corrective scheme in section 4.3.4.2. There are two different cases treated separately. When there are inflow and outflow, or all inflows in x, y and z direction mesh interfaces, the cross-flow diffusion constants can be calculated in a simple way as in the first part of the program. When there are two outflows in any of the x, y and z directions, a flow split occurs as shown in Fig. 4.8. In the second part of the program the flow split is considered such that every outflow velocity is partitioned into four components in a three dimensional case in proportion to the velocities of the four neighboring surfaces in contact with the surface under consideration. All the inflow velocities are assumed to be zero. The component velocities are used to calculate the cross-flow diffusion constants for eight subspaces in a three dimensional coordinate space. Then four cross-flow diffusion constants at every interface are summed up to give a total cross-flow diffusion constant because one axis direction, the positive x direction, has four neighboring subspaces. The total cross-flow diffusion constant can be calculated in the same way for every mesh interface.

The subroutine 'tdm' solves tridiagonal matrix problems by forward and backward sweeps. It is used to solve a one dimensional implicit finite difference equation in the ADI scheme.

A portion of the VARR program is introduced to show how the ADI scheme is implemented in the energy and momentum equations. The ADI scheme for the momentum equation is given in Appendix B.

```
      IMPLICIT REAL*8 (A-H,O-Z)
      DIMENSION  T(10)

      READ(10,11) DX,NX,NY,TH,U,ALP
   11 FORMAT(F7.2,2I5,3F7.2)
      PI = 3.1415926536
      C = U/(2.0*ALP)
      CSQ = C*C
      XO = NX*DX
      YO = NY*DX
      YSQ = PI*PI/(YO*YO)
      CCOFF = 2.0*TH/PI
      HPI = PI/2.0


      DO 10 JJ=1,NY
      SUM = 0.0

      DO 20 IP=1,26
      II = IP - 1
      ALN = DSQRT(CSQ+II*II*YSQ)
      IF (II.EQ.0) GO TO 55
      ALNX = (ALN+C)*DEXP(2.0*ALN*XO)/(ALN-C)
      COF = CCOFF/II
      AAN = -COF*DSIN(II*HPI)/(1.+ALNX)
      ATOT = AAN*2.0*ALN*DEXP(ALN*XO)/(ALN-C)
      GO TO 44
   55 ATOT = TH*DEXP(-ALN*XO)/2.0
   44 YY = II*PI*(JJ-0.5)/NY
      ADD = ATOT*DCOS(YY)
      SUM = SUM + ADD
   20 CONTINUE
      T(JJ) = SUM * DEXP(C*XO)
   10 CONTINUE

      WRITE(6,100) (T(I),I=1,NY)
  100 FORMAT(10X,5F11.3)

      STOP
      END
```

```
      IMPLICIT  REAL*8 (A-H,O-Z)
      DIMENSION  TH(10), TL(10), GH(10), GL(10), TC(10)
C
      READ(10,11) DX, NX, NY, THH, U, ALP
   11 FORMAT(F7.2,2I5,3F7.2)
      PI = 3.1415926536
      C = U/(2.0*ALP)
      CSQ = C*C
      XO = DX*NX
      YO = DX*NY
      YSQ = PI*PI/(YO*YO)
      CCOFF = 2.0*THH/PI
      HPI = PI/2.0
      NY2 = NY/2.0
      XXX = 2.0
      RTO = DSQRT(XXX)
C
      DO 10 JJ=1,NY2
      SUMO = 0.0
      SUM1 = 0.0
      SUM2 = 0.0
      SUM3X   0.0
      SUM3Y = 0.0
      SUM4X = 0.0
      SUM4Y = 0.0
      X = (JJ-0.5)*DX
      XN = X + XO/2.0
      YC = (JJ*2-1)*DX
      Y1 = X + YO/2.0
      Y2 = YO/2.0 - X
      Y3 = 1.5*YO - XN
      Y4 = XN - 0.5*YO
C
      DO 20 IP=1,21
      II = IP - 1
      ALN = DSQRT(CSQ + II*II*YSQ)
      EXALO = DEXP(ALN*XO*0.5)
      XALO = DEXP(-ALN*XO*0.5)
      EXAL = DEXP(ALN*X)
      XAL = DEXP(-ALN*X)
      EXALN = DEXP(ALN*XN)
      XALN = DEXP(-ALN*XN)
      IF(II.EQ.0)  GO TO 55
      ALNX = (ALN+C)*DEXP(2.0*ALN*XO)/(ALN-C)
      COF = CCOFF/II
      AAN = -COF*DSIN(II*HPI)/(1.+ALNX)
      BEN = II*PI/YO
      YOO = DCOS(BEN*YC)
      Y11 = DCOS(BEN*Y1)
      Y22 = DCOS(BEN*Y2)
      Y3C = DCOS(BEN*Y3)
      Y3S = DSIN(BEN*Y3)
      Y4C = DCOS(BEN*Y4)
      Y4S = DSIN(BEN*Y4)
      ADDO = AAN*(EXALO + ALNX*XALO)*YOO
```

```
      ADD1 = AAN*(EXAL+ALNX*XAL)*Y11
      ADD2 = AAN*(EXAL+ALNX*XAL)*Y22
      ADD3X = AAN*((C+ALN)*EXALN + ALNX*(C-ALN)*XALN)*Y3C
      ADD3Y = BEN*AAN*(EXALN + ALNX*XALN)*Y3S
      ADD4X = AAN*((C+ALN)*EXALN + ALNX*(C-ALN)*XALN)*Y4C
      ADD4Y = -BEN*AAN*(EXALN + ALNX*XALN)*Y4S
      GO TO 77
   55 ADD1 = THH*XAL*0.5
      ADD0 = THH*XAL0*0.5
      ADD2 = THH*XAL*0.5
      ADD3X = 0.0
      ADD3Y = 0.0
      ADD4X = 0.0
      ADD4Y = 0.0
   77 SUM1 = SUM1 + ADD1
      SUM0 = SUM0 + ADD0
      SUM2 = SUM2 + ADD2
      SUM3X = SUM3X + ADD3X
      SUM3Y = SUM3Y + ADD3Y
      SUM4X = SUM4X + ADD4X
      SUM4Y = SUM4Y + ADD4Y
   20 CONTINUE
C
      TC(JJ) = SUM0*DEXP(C*X0*0.5)
      TH(JJ) = SUM1*DEXP(C*X)
      TL(JJ) = SUM2*DEXP(C*X)
      GH(JJ) = (SUM3X+SUM3Y)*DEXP(C*XN)/RTO
      GL(JJ) = (SUM4X+SUM4Y)*DEXP(C*XN)/RTO
   10 CONTINUE
C
      WRITE(6,100) (TC(I),I=1,NY2)
      WRITE(6,100) (TH(I),I=1,NY2)
      WRITE(6,100) (TL(I),I=1,NY2)
      WRITE(6,100) (GH(I),I=1,NY2)
      WRITE(6,100) (GL(I),I=1,NY2)
  100 FORMAT(10X,5F11.3)

      STOP
      END
```

```
      IMPLICIT  REAL*8 (A-H,O-Z)
      DIMENSION  TH(10), TL(10), GH(10), GL(10), TC(10)
C
      READ(10,11) DX, NX, NY, THH, U, ALP
   11 FORMAT(F7.2,2I5,3F7.2)
      PI = 3.1415926536
      C = U/(2.0*ALP)
      CSQ = C*C
      XO = DX*NX
      YO = DX*NY
      YSQ = PI*PI/(YO*YO)
      CCOFF = 2.0*THH/PI
      HPI = PI/2.0
      NY2 = NY/2.0
      RTO = SQRT(2.0)
      RT3 = SQRT(3.0)
C
      DO 10 JJ=1,NY2
      SUMO = 0.0
      SUM1 = 0.0
      SUM2 = 0.0
      SUM3X = 0.0
      SUM3Y = 0.0
      SUM4X = 0.0
      SUM4Y = 0.0
      XC=YO/(2.0*RT3)+(JJ-0.5)*(XO-YO/RT3)/NY2
      YC=(JJ-0.5)*(YO/3.0+XO/RT3)/NY2
      X1=(JJ-0.5)*(XO-YO/(2.0*RT3))/NY2
      Y1=YO/2.0+(JJ-0.5)*(XO/RT3-YO/6.0)/NY2
      X2=(JJ-0.5)*YO/(2.0*RT3*NY2)
      Y2=YO/2.0-(JJ-0.5)*YO/(2.0*NY2)
      X3=YO/(2.0*RT3)+(JJ-0.5)*(XO-YO/(2.0*RT3))/NY2
      Y3=(JJ-0.5)*(XO/RT3-YO/6.0)/NY2
      X4=XO-YO/(2.0*RT3)+(JJ-0.5)*YO/(2.0*RT3*NY2)
      Y4=YO/3.0+XO/RT3-(JJ-0.5)*YO/(2.0*NY2)
C
      DO 20 IP=1,22
      II = IP - 1
      ALN = DSQRT(CSQ + II*II*YSQ)
      IF(II.EQ.0)  GO TO 55
      ALNX = (ALN+C)*DEXP(2.0*ALN*XO)/(ALN-C)
      COF = CCOFF/II
      AAN = -COF*DSIN(II*HPI)/(1.+ALNX)
      BEN = II*PI/YO
      YOO = DCOS(BEN*YC)
      Y11 = DCOS(BEN*Y1)
      Y22 = DCOS(BEN*Y2)
      Y3C = DCOS(BEN*Y3)
      Y3S = DSIN(BEN*Y3)
      Y4C = DCOS(BEN*Y4)
      Y4S = DSIN(BEN*Y4)
      ADDO=AAN*(DEXP(ALN*XC)+ALNX*DEXP(-ALN*XC))*YOO
      ADD1=AAN*(DEXP(ALN*X1)+ALNX*DEXP(-ALN*X1))*Y11
      ADD2=AAN*(DEXP(ALN*X2)+ALNX*DEXP(-ALN*X2))*Y22
      ADD3X=AAN*((C+ALN)*DEXP(ALN*X3)+ALNX*(C-ALN)*DEXP(-ALN*X3))*Y3C
```

```
      ADD3Y=BEN*AAN*(DEXP(ALN*X3)+ALNX*DEXP(-ALN*X3))*Y3S
      ADD4X=AAN*((C+ALN)*DEXP(ALN*X4)+ALNX*(C-ALN)*DEXP(-ALN*X4))*Y4C
      ADD4Y=-BEN*AAN*(DEXP(ALN*X4)+ALNX*DEXP(-ALN*X4))*Y4S
      GO TO 77
   55 ADDO=THH*DEXP(-ALN*XC)*0.5
      ADD1=THH*DEXP(-ALN*X1)*0.5
      ADD2=THH*DEXP(-ALN*X2)*0.5
      ADD3X = 0.0
      ADD3Y = 0.0
      ADD4X = 0.0
      ADD4Y = 0.0
   77 SUM1 = SUM1 + ADD1
      SUMO = SUMO + ADDO
      SUM2 = SUM2 + ADD2
      SUM3X = SUM3X + ADD3X
      SUM3Y = SUM3Y + ADD3Y
      SUM4X = SUM4X + ADD4X
      SUM4Y = SUM4Y + ADD4Y
   20 CONTINUE
C
      TC(JJ)=SUMO*DEXP(C*XC)
      TH(JJ)=SUM1*DEXP(C*X1)
      TL(JJ)=SUM2*DEXP(C*X2)
      GL(JJ)=(SUM3X*0.5+SUM3Y*0.5*RT3)*DEXP(C*X3)
      GH(JJ)=(SUM4X*0.5*RT3+SUM4Y*0.5)*DEXP(C*X4)
   10 CONTINUE
C
      WRITE(6,100) (TC(I),I=1,NY2)
      WRITE(6,100) (TH(I),I=1,NY2)
      WRITE(6,100) (TL(I),I=1,NY2)
      WRITE(6,100) (GH(I),I=1,NY2)
      WRITE(6,100) (GL(I),I=1,NY2)
  100 FORMAT(10X,5F11.3)

      STOP
      END
```

```
      DIMENSION VELX(8),VELZ(8),VELT(8),DIFRA(8),DIFZA(8),DIFTA(8)
C
      READ(10,5) DELR,DELZ,DELTH,UM,UP,VM,VP,WM,WP
C
      IS1 = 0
      IS2 = 0
      IS3 = 0
      IS4 = 0
      IS5 = 0
      IS6 = 0
C
      RFGR1 = 0.0
      RFGR = 0.0
      RFGT1 = 0.0
      RFGT = 0.0
      QMT1 = 0.0
      QMT = 0.0
C
      IF(UM.LT.0.0)  IS1 = 1
      IF(UP.GT.0.0)  IS2 = 1
      IF(VM.LT.0.0)  IS3 = 1
      IF(VP.GT.0.0)  IS4 = 1
      IF(WM.LT.0.0)  IS5 = 1
      IF(WP.GT.0.0)  IS6 = 1
C
      ISA = IS1 + IS2
      ISB = IS3 + IS4
      ISC = IS5 + IS6
C
      U1 = -0.5*( UM - ABS(UM) )
      U2 =  0.5*( UP + ABS(UP) )
      V1 = -0.5*( VM - ABS(VM) )
      V2 =  0.5*( VP + ABS(VP) )
      W1 = -0.5*( WM - ABS(WM) )
      W2 =  0.5*( WP + ABS(WP) )
C
      IF( ISA.EQ.2.OR.ISB.EQ.2.OR.ISC.EQ.2)  GO TO 80
      UU = U1 + U2
      VV = V1 + V2
      WW = W1 + W2
      PPX = UU/DELR
      PPZ = VV/DELZ
      PPT = WW/DELTH
      PSUM = PPX + PPZ + PPT
      IF( PSUM.EQ.0.0 )  GO TO 500
C
      DIFR = UU*DELR*( PPZ + PPT )/PSUM
      DIFZ = VV*DELZ*( PPX + PPT )/PSUM
      DIFT = WW*DELTH*( PPX + PPZ )/PSUM
C
      RFGR1 = DIFR*IS1
      RFGR  = DIFR*IS2
      RFGT1 = DIFZ*IS3
      RFGT  = DIFZ*IS4
```

```
      OMT   = DIFT*ISG
      GO TO 999
C
   80 PFX = 0.0
      PFZ = 0.0
      PFT = 0.0
      IF( (U1+U2).NE.0.0 )  PFX = U1/(U1+U2)
      IF( (V1+V2).NE.0.0 )  PFZ = V1/(V1+V2)
      IF( (W1+W2).NE.0.0 )  PFT = W1/(W1+W2)
C
      VELX(1) = U1*PFZ*PFT
      VELX(2) = U1*(1.0-PFZ)*PFT
      VELX(3) = U1*(1.0-PFZ)*(1.0-PFT)
      VELX(4) = U1*PFZ*(1.0-PFT)
      VELX(5) = U2*PFZ*PFT
      VELX(6) = U2*(1.0-PFZ)*PFT
      VELX(7) = U2*(1.0-PFZ)*(1.0-PFT)
      VELX(8) = U2*PFZ*(1.0-PFT)
C
      VELZ(1) = V1*PFX*PFT
      VELZ(2) = V2*PFX*PFT
      VELZ(3) = V2*PFX*(1.0-PFT)
      VELZ(4) = V1*PFX*(1.0-PFT)
      VELZ(5) = V1*(1.0-PFX)*PFT
      VELZ(6) = V2*(1.0-PFX)*PFT
      VELZ(7) = V2*(1.0-PFX)*(1.0-PFT)
      VELZ(8) = V1*(1.0-PFX)*(1.0-PFT)
C
      VELT(1) = W1*PFX*PFZ
      VELT(2) = W1*PFX*(1.0-PFZ)
      VELT(3) = W2*PFX*(1.0-PFZ)
      VELT(4) = W2*PFX*PFZ
      VELT(5) = W1*(1.0-PFX)*PFZ
      VELT(6) = W1*(1.0-PFX)*(1.0-PFZ)
      VELT(7) = W2*(1.0-PFX)*(1.0-PFZ)
      VELT(8) = W2*(1.0-PFX)*PFZ
C
      DO 30 I=1,8
      PPX = VELX(I)/DELR
      PPZ = VELZ(I)/DELZ
      PPT = VELT(I)/DELTH
      PSUM = PPX + PPZ + PPT
      IF( PSUM.EQ.0.0 )  GO TO 600
      DIFRA(I) = VELX(I)*DELR*( PPZ + PPT )/PSUM
      DIFZA(I) = VELZ(I)*DELZ*( PPX + PPT )/PSUM
      DIFTA(I) = VELT(I)*DELTH*( PPX + PPZ )/PSUM
      GO TO 30
  600 DIFRA(I) = 0.0
      DIFZA(I) = 0.0
      DIFTA(I) = 0.0
   30 CONTINUE
C
      RFGR1 = DIFRA(5) + DIFRA(6) + DIFRA(7) + DIFRA(8)
      RFGR  = DIFRA(1) + DIFRA(2) + DIFRA(3) + DIFRA(4)
      RFGT1 = DIFZA(2) + DIFZA(3) + DIFZA(6) + DIFZA(7)
```

```
      REGT   = DIFZA(1) + DIFZA(4) + DIFZA(5) + DIFZA(8)                DIFO1110
      QMT1   = DIFTA(3) + DIFTA(4) + DIFTA(7) + DIFTA(8)                DIFO1120
      QMT    = DIFTA(1) + DIFTA(2) + DIFTA(5) + DIFTA(6)                DIFO1130
C                                                                       DIFO1140
  999 WRITE(6,6)  REGR1,REGR,REGT1,REGT,QMT1,QMT                        DIFO1150
      GO TO 200                                                         DIFO1160
  500 WRITE(6,7)                                                        DIFO1170
    5 FORMAT(9F5.2)                                                     DIFO1180
    6 FORMAT(1H ,2X,6F5.2)                                              DIFO1190
    7 FORMAT(1H ,20X,5HSORRY)                                           DIFO1200
  200 STOP                                                              DIFO1210
      END                                                               DIFO1220
```

```
      SUBROUTINE TDM(A,B,C,D,X,N)
      IMPLICIT REAL*8 (A-H,O-Z)
      DIMENSION A(N),B(N),C(N),D(N),X(N),P(400),Q(400)
C
      X(1) = D(1)
      Q(1) = B(1)
      NM1 = N - 1
      DO 2 I=1,NM1
      P(I+1) = A(I+1)/Q(I)
      Q(I+1) = B(I+1) - P(I+1)*C(I)
    2 X(I+1) = D(I+1) - P(I+1)*X(I)
C
      X(N) = X(N)/Q(N)
      DO 3 I=1,NM1
      K = N - I
    3 X(K) = (X(K) - X(K+1)*C(K))/Q(K)
      RETURN
      END
```

```
C NOTE. U AND W TILDE VELOCITY EQUATIONS SECTION .
C
      IF(ICALI.EQ.1) GO TO 49998
C    ADI SOLUTION FOR SIE, ICONV=3,4
C
C   1ST SWEEP IN X-DIRECTION
      IKBR = IBR*KBR
      I1 = 2
      I2 = IEP1
      K1 = 2
      K2 = KBP1
C CROSS-FLOW DIFFUSION CONSTANT CALCULATION
      DO 40000 I=1,IBP2
      DO 40000 K=1,KBP2
      IK = 1 + (I-1)*K2NC + (K-1)*NWPC
      IKXX = IK - K2NC
      IKZZ = IK - NWPC
      IF(K.EQ.1.OR.I.EQ.1) GO TO 40001
      IF(K.EQ.KBP2.OR.I.EQ.IBP2) GO TO 40002
      AUG = ABS(0.5*(U(IK)+U(IKXX)))
      AWG = ABS(0.5*(W(IK)+W(IKZZ)))
      GO TO 40005
40001 AUG = ABS( U(IK) )
      AWG = ABS( W(IK) )
      GO TO 40005
40002 AUG = ABS( U(IKXX) )
      AWG = ABS( W(IKZZ) )
40005 PM = 1.E-10
      IF(AUG.LT.PM.AND.AWG.LT.PM) GO TO 40010
      DNFFX(I,K) = AUG*DX*AWG*RDZ/(AUG*RDX+AWG*RDZ)*XMX
      DNFFZ(I,K) = AWG*DZ*AUG*RDX/(AUG*RDX+AWG*RDZ)*XMX
      GO TO 40000
40010 DNFFX(I,K) = 0.0
      DNFFZ(I,K) = 0.0
40000 CONTINUE
C
```

```
C                                                                       VAR18340
49999 RHDX = 0.5*RDX                                                    VAR18350
      RDXD = RDX*RDX                                                    VAR18360
      RDZD = RDZ*RDZ                                                    VAR18370
C                                                                       VAR18380
      IF(IMOM.EQ.1.OR.ICALI.EQ.2) GO TO 89999                           VAR18390
      IKBR = IBR*(KBR-1)                                                VAR18400
      SIGMA = NU                                                        VAR18410
      BUOY = ALPO*EXP( - TIMET/TADD )                                   VAR18420
C                                                                       VAR18430
      IF(IMOM.EQ.3) GO TO 80205                                         VAR18440
C                                                                       VAR18450
      DO 80100 I=2,IBR                                                  VAR18460
      DO 80100 K=2,KBP1                                                 VAR18470
      IK = 1 + (I-1)*K2NC + (K-1)*NWPC                                  VAR18480
      IKL = 1 + (I-1)*K2NCL + (K-1)*NWPCL                               VAR18490
      IPK = IK + K2NC                                                   VAR18500
      IKMS = IK - NWPC                                                  VAR18510
      IMKS = IK - K2NC                                                  VAR18520
      IKP = IK + NWPC                                                   VAR18530
C                                                                       VAR18540
      UC = UD(IK)                                                       VAR18550
      UL = UD(IMKS)                                                     VAR18560
      UR = UD(IPK)                                                      VAR18570
      UT = UD(IKP)                                                      VAR18580
      UB = UD(IKMS)                                                     VAR18590
      DCR = DIFFCD(IKL)                                                 VAR18600
      DCT = DIFFCD(IKL+1)                                               VAR18610
      DCL = DIFFCD(IKL+2)                                               VAR18620
      DCB = DIFFCD(IKL+3)                                               VAR18630
C                                                                       VAR18640
      WRT = ( WD(IK) + WD(IPK) )*0.5                                    VAR18650
      WRB = ( WD(IKMS) + WD(IPK-NWPC) )*0.5                             VAR18660
      URH = ( UD(IK) + UD(IPK) )*0.5                                    VAR18670
      ULH = ( UD(IK) + UD(IMKS) )*0.5                                   VAR18680
C                                                                       VAR18690
      CONX = ( URH*(UC+UR) + ABS(URH)*(UC-UR) - ULH*(UL+UC)             VAR18700
```

```
     1                - ABS(ULH)*(UL-UC) )*0.5*RDX
      CONZ = ( WRT*(UC+UT) + ABS(WRT)*(UC-UT) - WRB*(UB+UC)
     1                - ABS(WRB)*(UB-UC) )*0.5*RDZ
      DIFX = SIGMA*RDXD*( (UR-UC)*DCR - (UC-UL)*DCL )
      DIFZ = SIGMA*RDZD*( (UT-UC)*DCT - (UC-UB)*DCB )
C
      U(IK) = UD(IK) + DT*( -( P(IPK)-P(IK) )*RDX - CONX - CONZ
     1                + DIFX + DIFZ )
80100 CONTINUE
C
      DO 80200 I=2,IBP1
      DO 80200 K=2,KBR
      BUOYN = 0.0
      IF(I.EQ.IDG.AND.K.EQ.KDG) BUOYN=BUOY
      IK = 1 + (I-1)*K2NC + (K-1)*NWPC
      IKL = 1 + (I-1)*K2NCL + (K-1)*NWPCL
      IPK = IK + K2NC
      IKMS = IK - NWPC
      IMKS = IK - K2NC
      IKP = IK + NWPC
C
      WC = WD(IK)
      WL = WD(IMKS)
      WR = WD(IPK)
      WT = WD(IKP)
      WB = WD(IKMS)
      DCR = DIFFCD(IKL)
      DCT = DIFFCD(IKL+1)
      DCL = DIFFCD(IKL+2)
      DCB = DIFFCD(IKL+3)
C
      URT = 0.5*( UD(IK) + UD(IKP) )
      ULT = 0.5*( UD(IMKS) + UD(IMKS+NWPC) )
      WTH = 0.5*( WD(IK) + WD(IKP) )
      WBH = 0.5*( WD(IK) + WD(IKMS) )
C
      CONX = ( URT*(WC+WR) + ABS(URT)*(WC-WR) - ULT*(WL+WC)
     1                - ABS(ULT)*(WL-WC) )*0.5*RDX
      CONZ = ( WTH*(WC+WT) + ABS(WTH)*(WC-WT) - WBH*(WB+WC)
     1                - ABS(WBH)*(WB-WC) )*0.5*RDZ
      DIFX = SIGMA*RDXD*( (WR-WC)*DCR - (WC-WL)*DCL )
      DIFZ = SIGMA*RDZD*( (WT-WC)*DCT - (WC-WB)*DCB )
C
      W(IK) = WD(IK) + DT*( -( P(IKP)-P(IK) )*RDZ - CONX - CONZ
     1                + DIFX + DIFZ + BUOYN )
80200 CONTINUE
      GO TO 89999
80205 CONTINUE
      DO 81000 I=2,IBR
      DO 81000 K=2,KBP1
      J = (I-2)*KBR + K - 1
      IK = 1 + (I-1)*K2NC + (K-1)*NWPC
      IKL = 1 + (I-1)*K2NCL + (K-1)*NWPCL
```

```
      IMKS = IK - K2NC
      IKMS = IK - NWPC
C
      DCT = DIFFCD(IKL+1)
      DCB = DIFFCD(IKL+3)
      WRT = (W(IK) + W(IPK))*0.5
      WRB = (W(IKMS) + W(IPK-NWPC))*0.5
C
      A1(J) = 0.5*RDZ*( -WRB - ABS(WRB)) - SIGMA*RDZD*DCB
      B1(J) = RDT + 0.5*RDZ*( WRT + ABS(WRT) - WRB + ABS(WRB) )
     1                 + SIGMA*RDZD*( DCT + DCB )
      C1(J) = 0.5*RDZ*( WRT - ABS(WRT) ) - SIGMA*RDZD*DCT
      D1(J) = U(IK)*RDT
81000 CONTINUE
C
      CALL TDM(A1,B1,C1,D1,X,IKBR)
C
      DO 81100 I=2,IBR
      DO 81100 K=2,KBP1
      IK = 1 + (I-1)*K2NC + (K-1)*NWPC
      IX = (I-2)*KBR + K - 1
81100 U(IK) = X(IX)
C
      DO 82000 K=2,KBR
      DO 82000 I=2,IBP1
      J = (K-2)*IBR + I - 1
      IK = 1 + (I-1)*K2NC + (K-1)*NWPC
      IKL = 1 + (I-1)*K2NCL + (K-1)*NWPCL
C
      IPK = IK + K2NC
      IKP = IK + NWPC
      IMKS = IK - K2NC
      IKMS = IK - NWPC
C
      DCR = DIFFCD(IKL)
      DCL = DIFFCD(IKL+2)
      URT = 0.5*( U(IK) + U(IKP) )
      ULT = 0.5*( U(IMKS) + U(IMKS+NWPC) )
C
      A1(J) = 0.5*RDX*( -ULT - ABS(ULT) ) - SIGMA*RDXD*DCL
      B1(J) = RDT + 0.5*RDX*( URT + ABS(URT) - ULT + ABS(ULT) )
     1                 + SIGMA*RDXD*( DCL + DCR )
      C1(J) = 0.5*RDX*( URT - ABS(URT) ) - SIGMA*RDXD*DCR
      D1(J) = W(IK)*RDT
82000 CONTINUE
C
      CALL TDM(A1,B1,C1,D1,X,IKBR)
C
      DO 82100 K=2,KBR
      DO 82100 I=2,IBP1
      IK = 1 + (I-1)*K2NC + (K-1)*NWPC
      IX = (K-2)*IBR + I - 1
82100 W(IK) = X(IX)
C
      DO 83000 K=2,KBP1
```

```
      DO 83000 I=2,IBR
      J = (K-2)*(IBR-1) + I - 1
      IK = 1 + (I-1)*K2NC + (K-1)*NWPC
      IKL = 1 + (I-1)*K2NCL + (K-1)*NWPCL
C
      IPK = IK + K2NC
      IKP = IK + NWPC
      IMKS = IK - K2NC
      IKMS = IK - NWPC
C
      DCR = DIFFCO(IKL)
      DCL = DIFFCO(IKL+2)
      URH = 0.5*( U(IK) + U(IPK) )
      ULH = 0.5*( U(IK) + U(IMKS) )
C
      A1(J) = 0.5*RDX*( -ULH - ABS(ULH) ) - SIGMA*RDXD*DCL
      B1(J) = RDT + 0.5*RDX*( URH + ABS(URH) - ULH + ABS(ULH) )
     1              + SIGMA*RDXD*( DCR + DCL )
      C1(J) = 0.5*RDX*( URH - ABS(URH) ) - SIGMA*RDXD*DCR
      D1(J) = U(IK)*RDT - RDX*( P(IPK) - P(IK) )
83000 CONTINUE
C
      CALL TDM(A1,B1,C1,D1,X,IKBR)
C
      DO 83100 K=2,KBP1
      DO 83100 I=2,IBR
      IK = 1 + (I-1)*K2NC + (K-1)*NWPC
      IX = (K-2)*(IBR-1) + I - 1
83100 U(IK) = X(IX)
C
      DO 84000 I=2,IBP1
      DO 84000 K=2,KBR
      BUOYN = 0.0
      IF(I.EQ.IDG.AND.K.EQ.KDG) BUOYN=BUOY
      J = (I-2)*(KBR-1) + K - 1
      IK = 1 + (I-1)*K2NC + (K-1)*NWPC
      IKL = 1 + (I-1)*K2NCL + (K-1)*NWPCL
C
      IPK = IK + K2NC
      IKP = IK + NWPC
      IMKS = IK - K2NC
      IKMS = IK - NWPC
C
      DCT = DIFFCO(IKL+1)
      DCB = DIFFCO(IKL+3)
      WTH = 0.5*( W(IK) + W(IKP) )
      WBH = 0.5*( W(IK) + W(IKMS) )
C
      A1(J) = 0.5*RDZ*( -WBH - ABS(WBH) ) - SIGMA*RDZD*DCB
      B1(J) = RDT + 0.5*RDZ*( WTH + ABS(WTH) - WBH + ABS(WBH) )
     1              + SIGMA*RDZD*( DCT + DCB )
      C1(J) = 0.5*RDZ*( WTH - ABS(WTH) ) - SIGMA*RDZD*DCT
      D1(J) = W(IK)*RDT - RDZ*( P(IKP) - P(IK) ) + BUOYN
84000 CONTINUE
C
```

```
      CALL TDM(A1,B1,C1,D1,X,IKBR)
C
      DO 84100 I=2,IBP1
      DO 84100 K=2,KBR
      IK = 1 + (I-1)*K2NC + (K-1)*NWPC
      IX = (I-2)*(KBR-1) + K - 1
84100 W(IK) = X(IX)
C
89999 CONTINUE
      IF(ICONV.LE.2.OR.ICALI.EQ.1) GO TO 2040
C
      ISEQ = ISEQ + 1
      IF(ISEQ.EQ.NSEQ)  ISEQ = 0
33333 CONTINUE
C
      DO 60000 K=K1,K2
      DO 60000 I=I1,I2
      J = IBR*(K-2) + I - 1
      IK = 1 + (I-1)*K2NC + (K-1)*NWPC
      IKL = 1 + (I-1)*K2NCL + (K-1)*NWPCL
      RC = FLOAT(I-1)*DX - HDX
      RRC = 1.0/RC
      CR = CYL*0.25*RRC
      CYRX = CYL*0.5*RRC*RDX
C
      CFC = CF(IK)
      IF (CFC.NE.1)  GO TO 55000
      DCR = DIFFCD(IKL)
      DCT = DIFFCD(IKL+1)
      DCL = DIFFCD(IKL+2)
      DCB = DIFFCD(IKL+3)
      IPK = IK + K2NC
      IKP = IK + NWPC
      IMKS = IK - K2NC
      IKMS = IK - NWPC
C
      CFR = CF(IPK)
      CFL = CF(IMKS)
      UC = U(IK)
      WC = W(IK)
      UL = U(IMKS)
      WB = W(IKMS)
      AUC = DABS(UC)
      AUL = DABS(UL)
      AWC = DABS(WC)
      AWB = DABS(WB)
      SIEC= SIE(IK)
      SIER = SIE(IPK)
      SIEL = SIE(IMKS)
      SIET = SIE(IKP)
      SIEB = SIE(IKMS)
      SIECO = SIEO(IK)
C
      TSRA = 0.5*(TS(IK)+TS(IPK))
      TSLA = 0.5*(TS(IK)+TS(IMKS))
```

```
      TSTA = 0.5*(TS(IK)+TS(IKP))                                       VAR20910
      TSBA = 0.5*(TS(IK)+TS(IKMS))                                      VAR20920
C                                                                       VAR20930
      GAMT = TGAM                                                       VAR20940
      IF (TS(IK).LE.NU)  GAMT=RPRAN                                     VAR20950
      DIFFR = GAMT*TSRA - 0.5*(DNFFX(I,K)+DNFFX(I+1,K))                 VAR20960
      DIFFL = GAMT*TSLA - 0.5*(DNFFX(I,K)+DNFFX(I-1,K))                 VAR20970
      DIFFT = GAMT*TSTA - 0.5*(DNFFZ(I,K)+DNFFZ(I,K+1))                 VAR20980
      DIFFB = GAMT*TSBA - 0.5*(DNFFZ(I,K)+DNFFZ(I,K-1))                 VAR20990
C                                                                       VAR21000
C                                                                       VAR21010
      A1(J) = (-RHDX+OR)*(UL+AUL) + DIFFL*DCL*(CYRX-RDXD)               VAR21020
      B1(J) = RDT + DIFFR*DCR*(CYRX+RDXD) - DIFFL*DCL*(CYRX-RDXD)       VAR21030
     1              + (RHDX+OR)*(UC+AUC) + (-RHDX+OR)*(UL-AUL)          VAR21040
      C1(J) = (RHDX+OR)*(UC-AUC) - DIFFR*DCR*(CYRX+RDXD)                VAR21050
      D1(J) = SIEC*RDT - CO(IK)*0.5                                     VAR21060
C                                                                       VAR21070
      IF(CFL.EQ.1) GO TO 59950                                          VAR21080
      D1(J) = D1(J) - A1(J)*SIEL                                        VAR21090
      A1(J) = 0.0                                                       VAR21100
59950 IF(CFR.EQ.1) GO TO 60000                                          VAR21110
      IF(CFR.EQ.11.AND.NNOPR.EQ.1) GO TO 55500                          VAR21120
      D1(J) = D1(J) - C1(J)*SIER                                        VAR21130
      C1(J) = 0.0                                                       VAR21140
      GO TO 60000                                                       VAR21150
55500 B1(J) = B1(J) - DIFFR*DCR*( CYRX + RDXD )                         VAR21160
      C1(J) = 0.0                                                       VAR21170
      D1(J) = D1(J) + DIFFR*DCR*( CYRX + RDXD )*DX                      VAR21180
      GO TO 60000                                                       VAR21190
55000 D1(J) = SIECO                                                     VAR21200
      A1(J) = 0.0                                                       VAR21210
      B1(J) = 1.0                                                       VAR21220
      C1(J) = 0.0                                                       VAR21230
60000 CONTINUE                                                          VAR21240
C                                                                       VAR21250
60001 CALL TDM(A1,B1,C1,D1,X,IKBR)                                      VAR21260
C                                                                       VAR21270
      DO 61000 K=K1,K2                                                  VAR21280
      DO 61000 I=I1,I2                                                  VAR21290
      IX = IBR*(K-2) + I - 1                                            VAR21300
      IK = 1 + (I-1)*K2NC + (K-1)*NWPC                                  VAR21310
61000 SIE(IK) = X(IX)                                                   VAR21320
C                                                                       VAR21330
      IF(KIRK.EQ.1)  GO TO 33337                                        VAR21340
33334 CONTINUE                                                          VAR21350
C                                                                       VAR21360
C   2ND SWEEP IN Z-DIRECTION                                            VAR21370
C                                                                       VAR21380
      DO 70000 I=I1,I2                                                  VAR21390
      DO 70000 K=K1,K2                                                  VAR21400
      J = KBR*(I-2) + K - 1                                             VAR21410
      JINV = IBR*(K-2) + I - 1                                          VAR21420
      IK = 1 + (I-1)*K2NC + (K-1)*NWPC                                  VAR21430
      IKL = 1 + (I-1)*K2NCL + (K-1)*NWPCL                               VAR21440
      CFC = CF(IK)                                                      VAR21450
```

```
      IF ( CFC.NE.1)  GO TO 65000
C
      DCR = DIFFCO(IKL)
      DCT = DIFFCO(IKL+1)
      DCL = DIFFCO(IKL+2)
      DCB = DIFFCO(IKL+3)
C
      IPK = IK + K2NC
      IKP = IK + NWPC
      IMKS = IK - K2NC
      IKMS = IK - NWPC
C
      CFT = CF(IKP)
      CFB = CF(IKMS)
      WB = W(IKMS)
      WC = W(IK)
      AWB = DABS(WB)
      AWC = DABS(WC)
      TSTA = 0.5*(TS(IK)+TS(IKP))
      TSBA = 0.5*(TS(IK)+TS(IKMS))
C
      GAMT = TGAM
      IF(TS(IK).LE.NU) GAMT = RPRAN
      DIFFT = GAMT*TSTA - 0.5*(DNFFZ(I,K)+DNFFZ(I,K+1))*XMX
      DIFFB = GAMT*TSBA - 0.5*(DNFFZ(I,K)+DNFFZ(I,K-1))*XMX
C
C
      D1(J) = RDT*SIE(IK) - CO(IK)*0.5
      A2(J) = -0.5*(WB+AWB)*RDZ - DIFFB*DCB*RDZD
      B2(J) = RDT + (DIFFT*DCT+DIFFB*DCB)*RDZD
     1                  + 0.5*(WC+AWC-WB+AWB)*RDZ
      C2(J) = 0.5*(WC-AWC)*RDZ - DIFFT*DCT*RDZD
      IF(CFB.EQ.1) GO TO 69950
      D1(J) = D1(J) - A2(J)*SIE(IKMS)
      A2(J) = 0.0
69950 IF(CFT.EQ.1) GO TO 70000
      IF(CFT.EQ.11.AND.NNOPT.EQ.1) GO TO 65500
      D1(J) = D1(J) - C2(J)*SIE(IKP)
      C2(J) = 0.0
      GO TO 70000
65500 B2(J) = B2(J) - DIFFT*DCT*RDZD
      C2(J) = 0.0
      D1(J) = D1(J) + DIFFT*DCT*RDZ
      GO TO 70000
65000 D1(J) = SIE(IK)
      A2(J) = 0.0
      B2(J) = 1.0
      C2(J) = 0.0
70000 CONTINUE
C
      CALL TDM(A2,B2,C2,D1,X,IKBR)
C
      DO 71000 I=I1,I2
      DO 71000 K=K1,K2
      IX = KBR*(I-2) + K - 1
```

```
      IK = 1 + (I-1)*K2NC + (K-1)*NWPC
71000 SIE(IK) = X(IX)
C
      IF(KIRK.EQ.1)  GO TO 33333
      IF(ISEQ.NE.0)  GO TO 33339
      DO 33335 I=I1,I2
      DO 33335 K=K1,K2
      IK = 1 + (I-1)*K2NC + (K-1)*NWPC
      STOR(I,K) = SIE(IK)
33335 SIE(IK) = SIEO(IK)
      KIRK = 1
      GO TO 33334
33337 CONTINUE
      DO 33338 I=I1,I2
      DO 33338 K=K1,K2
      IK = 1 + (I-1)*K2NC + (K-1)*NWPC
33338 SIE(IK) = 0.5*( SIE(IK) + STOR(I,K) )
      KIRK = 0
33339 CONTINUE
C
C NOTE. TRANSFERS VELOCITIES TO STORAGE ARRAY( AT TIME=N ) .
 2040 K1=1
      K2=KBP2
      LWPC=1 - NWPC
      DO 2109 K=K1,K2
      LWPC=LWPC+NWPC
      IK=LWPC
      IKS=I2K2 + IK
      SIE(IKS)=SIE(IK)
      U(IKS)=U(IK)
      W(IKS)=W(IK)
      TO(IKS)=TO(IK)
      TS(IKS)=TS(IK)
 2109 CONTINUE
      I1=2
      I2=IBP1
      K1=2
      K2=KBP2
      KK=0
      KKL = 0
      DO 2989 I=I1,I2
      KK=KK+K2NC
      KKL = KKL + K2NCL
      LWPCL = 1
      LWPC=1
      IKMS=I2K2 + 1
      SIE(1)=SIE(IKMS)
      U(1)=U(IKMS)
      W(1)=W(IKMS)
      TO(1)=TO(IKMS)
      TS(1)=TS(IKMS)
      SIE(IKMS)=SIE(KK+1)
      U(IKMS)=U(KK+1)
      W(IKMS)=W(KK+1)
      TO(IKMS)=TO(KK+1)
```

TYPICAL INPUT FILES

The file, 'input mom', is the input to test the stability of the ADI scheme for momentum equation. The file, 'inputn dat', is for calculating the natural convection flow field in a Cartesian closed compartment. The output results are in Fig. 5.1 and Fig. 5.2. The files, 'inputd 3' and 'inputd 7', are for calculating the numerical solution by donor cell scheme in the problem geometry, Fig. 4.3(B). The output results are in Fig. 5.6 and Fig. 5.7. The files, 'inputd HUH' and 'inputd DM', are for comparing Huh's and De Vahl Davis and Mallinson's correction formulas in the problem geometry, Fig. 5.8.

```
       4          4          0          1        0.5          0       0
 ADI STABILITY TEST FOR MOMENTUM
     1.0      2.0    1.+20    1.+20      6.0 8 2 1 3 0  2  2
0
0
    10.0     10.0      0.0      0.0      1.0      1.0      0.0      1.7     1.-4    10.0
1 1 1 1       1.0   0.045      1.5     10.0     0.75     1.-4 0.09375   0.013
    2.44      4.9     0.01    0.01 0      0.0      0.0      0.0      0.0      0.0
     0.0      0.0      0.2      1.0      0.0 1 3
     1.0     10.0     10.0      0.0 4  1 16
     0.0      1.0     -1.0      0.0     -1.0      0.0      1.0      1.0      0.0
     0.0      0.0      0.0      0.0      0.0      0.0      1.0
       2         2         2         0         0         0       .  0
     0.0      0.0     60.0      0.0
     0.0      0.0     60.0      0.0
     0.0      0.0     60.0      0.0
     0
     0
     0
     0
     0
     0
     0
    2    5    2    5 1
    10.0     1.-4     1.-4      0.0      0.0
    0
```

```
          5         10         0          1        0.0          0       0
 NATURAL CONVECTION IN A CARTESIAN CLOSED COMPARTMENT
      1.0     10.0    1.+20    1.+20     60.0 8 2 1 3 1  3  3
 0
 0
     1.67      2.0      0.0    -32.2      1.0       1.0     0.0      1.7     1.-5    1.0
 1 1 1 1       1.0    0.045      1.5      1.0     0.751.2179-5    1.-20    1.-20
     2.44     4.90     0.01     0.01
      0.0      0.0      1.0
      1.0     68.0     68.0      0.5 5 1 43
                                                                    1.0      1.0      0.0
                                                                    1.0
          1         1         1         0         0         0          1
      1.0      0.0
      1.0      0.0
      1.0      0.0
    677.4
      0
      0
      0
      0
      0
      0
      0
    2     6     2    11 1
     0.0    1.-20    1.-20     0.0      0.0
    6     6     2    830
    58.0    1.-20    1.-20     0.0      0.0
0
```

```
       10        10        0          1        0.0          0       0
NUMERICAL DIFFUSION - CASE 3
   0.02      2.0     1.120    1.+20      2.0 8 2 1 3 0  7  6
1  0.000  0.002  0.014  0.063  0.204  0.497  0.948  1.457  1.861  2.207
1  0.000 -0.002 -0.014 -0.063 -0.204 -0.497 -0.948 -1.457 -1.861 -2.207
0.70711 0.70711     0.0      0.0       1.0      1.0      0.0      1.5     1.-47.07107
2 4 2 4       1.0   0.045      1.5       1.0    0.75      1.0 0.09375   0.013
   2.44     4.9    0.01     0.01 0       0.0      0.0       0.0      0.0
    0.0     0.0     0.0     -1.5     1.-3 1 1
    1.0     5.0     5.0      0.0 4 1 36
    0.0     1.0    -1.0      0.0     -1.0      0.0      1.0      1.0      0.0
    0.0     0.0     0.0      0.0      0.0      0.0      1.0
         2        2        2
    0.05.000024     60.05.000024
    0.0     1.0     60.0     1.0
    0.0     0.0     60.0     0.0
    1       1.0    1.511
    2       1.0    0.249
    3       1.0    0.089
    4       1.0    0.026
    5       1.0    0.009
    6       1.0    0.003
    7       1.0    0.001
    8       1.0    0.000
    9       1.0    0.000
   10       1.0    0.000
    0
    0
    0
    1       1.0    8.489
    2       1.0    9.751
    3       1.0    9.911
    4       1.0    9.974
    5       1.0    9.991
    6       1.0    9.997
    7       1.0    9.999
    8       1.0   10.000
    9       1.0   10.000
   10       1.0   10.000
    0
    0
    0
    0
  2    11      2   .11 1
   0.0      1.0      1.0 7.07107 7.07107
  2    11      1      113
   5.0      1.0      1.0      0.0 7.07107
  1     1      2     1113
   5.0      1.0      1.0 7.07107      0.0
  2    11     12     1211
   5.0      1.0      1.0      0.0 7.07107
 12    12      2     1111
   5.0      1.0      1.0 7.07107      0.0
  0
```

```
        6         6         0         1         0.0         0         1
 NUMERICAL DIFFUSION - CASE 7
     0.01      2.4     1.+20    1.+20     2.4 8 2 1 3 0  2  2
 1   0.001  0.014  0.143  0.633  1.457  2.003
 1 -0.001 -0.014 -0.143 -0.633 -1.457 -2.003
1.17851 1.17851     0.0      0.0      1.0      1.0      0.0      1.5     1.-47.07107
2 4 2 4      1.0    0.045     1.5      1.0     0.75    -2.0 0.09375   0.013
    2.44     4.9     0.01     0.01 0     0.0      0.0      0.0      0.0     0.0
     0.0     0.0      0.0   -3.167    1.-3 1 1
     1.0     5.0      5.0     0.0 4 1 36
     0.0     1.0     -1.0     0.0     -1.0      0.0      1.0      1.0      0.0
     0.0     0.0      0.0     0.0      0.0      0.0      1.0
         2         2         2
     0.08.333327     60.08.333327
     0.0     1.0     60.0     1.0
     0.0     0.0     60.0     0.0
     1       1.0    0.626
     2       1.0    0.089
     3       1.0    0.013
     4       1.0    0.002
     5       1.0    0.000
     6       1.0    0.000
     0
     0
     0
     1       1.0    9.374
     2       1.0    9.911
     3       1.0    9.987
     4       1.0    9.998
     5       1.0   10.000
     6       1.0   10.000
     0
     0
     0
     0
   2    7    2    7 1
    5.0      1.0      1.0 7.07107 7.07107
   2    7    1    113
    5.0      1.0      1.0     0.0 7.07107
   1    1    2    713
    5.0      1.0      1.0 7.07107     0.0
   2    7    8    811
    5.0      1.0      1.0     0.0 7.07107
   8    8    2    711
    5.0      1.0      1.0 7.07107     0.0
   0
```

```
      24          8        0        1       0         0      0
NUMERICAL DIFFUSION - HUH
   0.02     2.0   1.+20   1.+20    2.0 8 2 1 3 0  7  6
1  0.009 -0.079 -0.225 -0.415 -0.610 -0.797 -0.937 -1.044
1  0.016  0.053  0.090  0.126  0.166  0.207  0.248  0.291  0.334  0.377
 0.419  0.459  0.499  0.536  0.568  0.601  0.625  0.648  0.664  0.674
 0.682  0.675  0.660  0.661
 0.2406  1.0267    0.0      0.0      1.0      1.0      0.0      1.5     1.-4   10.0
2 4 2 4      1.0   0.045     1.5      1.0     0.75      1.0 0.09375   0.013
   2.44     4.9    0.01    0.01 0     0.0      0.0      0.0      0.0
    0.0     0.0     0.0     1.5     1.-3
    1.0     5.0     5.0     0.4 4  1 36
    0.0     1.0    -1.0     0.0    -1.0      0.0      1.0      1.0      0.0
    0.0     0.0     0.0     0.0     0.0      0.0      1.0
       2         2         2
    0.02.083668    60.02.083668
    0.0     1.0    60.0     1.0
    0.0     0.0    60.0     0.0
     1      1.0   1.808
     2      1.0   1.491
     3      1.0   1.175
     4      1.0   0.859
     5      1.0   0.726
     6      1.0   0.614
     7      1.0   0.522
     8      1.0   0.449
     9      1.0   0.378
    10      1.0   0.329
    11      1.0   0.281
    12      1.0   0.243
    13      1.0   0.209
    14      1.0   0.179
    15      1.0   0.157
    16      1.0   0.135
    17      1.0   0.120
    18      1.0   0.104
    19      1.0   0.093
    20      1.0   0.085
    21      1.0   0.077
    22      1.0   0.075
    23      1.0   0.074
    24      1.0   0.072
   0
   0
   0
   1  2.463684   7.102
   2  2.463684   7.857
   3  2.463684   8.306
   4  2.463684   8.637
   5  2.463684   8.885
   6  2.463684   9.069
   7  2.463684   9.199
```

```
  0
  0
 2   25    2    9 1
  0.0   1.-20   1.-20     5.0  8.6603
 2   25    1    113
  5.0   1.-20   1.-20     0.0  8.6603
 1    1    2    913
  5.0   1.-20   1.-20     5.0     0.0
 2   25   10   1011
  5.0   1.-20   1.-20     0.0  8.6603
26   26    2    911
  5.0   1.-20   1.-20     5.0     0.0
 0
```

```
       24         0         0          1        0.0          0       0
NUMERICAL DIFFUSION - DM
   0.02     2.0    1.120    1.120     2.0 0 2 1 3 0  7  6
1 -0.002 -0.026 -0.099 -0.260 -0.522 -0.840 -1.144 -1.309
1  0.034  0.061  0.080  0.115  0.156  0.197  0.246  0.302  0.360  0.420
 0.496  0.566  0.636  0.705  0.767  0.830  0.876  0.920  0.951  0.969
 0.983  0.966  0.949  0.932
 0.2406  1.0267    0.0      0.0      1.0      1.0      0.0      1.5      1.-4  10.0
2 4 2 4      1.0    0.045     1.5      1.0     0.75      1.0 0.09375    0.013
   2.44      4.9    0.01     0.01 0     0.0      0.0      0.0      0.0
    0.0      0.0     0.0      1.5     1.-3
    1.0      5.0     5.0      0.4 4 1 36
    0.0      1.0    -1.0      0.0     -1.0      0.0      1.0      1.0      0.0
    0.0      0.0     0.0      0.0      0.0      0.0      1.0
        2        2        2
    0.02.003660     60.02.003660
    0.0      1.0    60.0      1.0
    0.0      0.0    60.0      0.0
    1        1.0    1.606
    2        1.0    1.223
    3        1.0    0.841
    4        1.0    0.460
    5        1.0    0.336
    6        1.0    0.242
    7        1.0    0.174
    8        1.0    0.133
    9        1.0    0.093
   10        1.0    0.072
   11        1.0    0.051
   12        1.0    0.038
   13        1.0    0.029
   14        1.0    0.021
   15        1.0    0.016
   16        1.0    0.011
   17        1.0    0.009
   18        1.0    0.007
   19        1.0    0.005
   20        1.0    0.003
   21        1.0    0.003
   22        1.0    0.003
   23        1.0    0.002
   24        1.0    0.002
    0
    0
    0
    1  2.463684   7.461
    2  2.463684   8.526
    3  2.463684   9.044
    4  2.463684   9.365
    5  2.463684   9.567
    6  2.463784   9.700
```

```
    0
    0
  2   25     2     9 1
   0.0   1.-20   1.-20     5.0  0.6603
  2   25     1     113
   5.0   1.-20   1.-20     0.0  0.6603
  1    1     2     913
   5.0   1.-20   1.-20     5.0     0.0
  2   25    10    1011
   5.0   1.-20   1.-20     0.0  0.6603
 26   26     2     911
   5.0   1.-20   1.-20     5.0     0.0
  0
```